Generic neuromorphic principles of cognition and attention for ants, humans and real world artefacts:

a comparative computational approach.

Zenon Mathews

TESI DOCTORAL UPF / ANY 2010

DIRECTOR DE LA TESI
Paul F.M.J. Verschure
Departament Tecnologies de la Informació i les Comunicacions

This dissertation is dedicated to Amma for being what she is to me.

Acknowledgments

This doctoral thesis has been carried out at the Universitat Pompeu Fabra (UPF) in Barcelona, in the research group SPECS lead by Prof. Paul F.M.J. Verschure. My first and earnest thanks goes to Prof. Verschure, whose encouragement, supervision and constant support from the preliminary to the final level enabled me to develop and connect research ideas.

My deepest gratitude also to Dr. Sergi Bermúdez i Badia for the constructive discussions, reviews and the abundant guidance over the many years that contributed crucially to my thesis. A semester project under the supervision of Sergi Bermúdez i Badia and Paul Verschure at the ETH in Zürich nearly five years ago started me on the path I traveled at UPF in Barcelona.

I would like to extend my special thanks to all SPECS members for the many useful feedbacks on my thesis and the great team work during several years. I have acquired invaluable scientific and social skills through the constant interaction with the SPECS group members.

I am heartily thankful to my parents and my brother for always being there when I needed them most, despite my negligence to visit them often enough. They deserve far more credit than I could ever offer.

My final, and most heartfelt, acknowledgment goes to Arantxa for her painstaking and successful work to show me the world outside the university campus and the beauty and hospitality of Spain. Her wit, support, patience, companionship and courage has turned my journey through graduate school into a pleasure.

Abstract

Biological cognition is thought to employ mechanisms like prediction, anticipation and attention for solving complex tasks. These mechanisms are suggested to be materialized through inter-layer cortical interactions in mammals, whereas their manifestation in relatively simpler brains, like the invertebrate brain, remains unclear. In artificial cognition, the nature and interplay of the above mechanisms remain largely unquantified. Here we propose a phylogenic, model-based approach to answer how these cognitive mechanisms interplay. We start with a simple model of the insect brain and demonstrate the necessity of the so-called forward models to account for insect behavior in dynamic scenarios. We then propose the PASAR framework to integrate and quantify the interplay of the above components of cognition. We validate PASAR in robotic tasks and in a human psychophysical experiment, proving PASAR as a valuable tool to model and evaluate biological cognition and to construct artificial cognitive systems.

Resum

Es considera que la cognició biològica fa servir mecanismes com la predicció, l'anticipació i l'atenció per resoldre tasques complexes. S'ha suggerit que aquests mecanismes es materialitzen en els mamífers a través d'interaccions entre les capes corticals, mentre que la seva manifestació en cervells relativament més simples, como el dels invertebrats, és encara poc clara. En la cognició artificial, la naturalesa i la interacció dels mecanismes mencionats roman, en gran mesura, no quantificada. Aquí proposem un enfoc filogènic i basat en models per descobrir com interactuen aquests mecanismes cognitius. Comencem amb el model simple del cervell d'un insecte i demostrem la necessitat dels anomenats forward models per explicar el comportament d'un insecte a escenaris dinàmics. Llavors proposem el marc PASAR per integrar i quantificar la interacció dels mencionats components de la cognició. Validem el PASAR en tasques robòtiques i en un experiment psicofísic humà, demostrant que el PASAR és una eina valuosa per modelar i avaluar la cognició biològica i per construir sistemes cognitius artificials.

Summary

List of Figures

List of Tables

Chapter 1

INTRODUCTION

More than a decade ago, Allen Newell argued that a model of a cognitive system should be capable of explaining how intelligent organisms flexibly react to stimuli from the environment, how they predict future events, how they exhibit goal-directed rational behavior, how they represent knowledge, and how they learn [81]. Newell also defines the term cognition to include perception and motor control. Despite intense research in cognitive sciences, it still remains unclear how these specific mechanisms such as prediction, anticipation, sensation, attention, memory or behavior contribute to the general process of cognition and how they interplay in autonomous systems acting in dynamic uncertain environments [129]. On the one hand this question has been the starting point for several behavioral and neuroscientific studies, with the goal of understanding the biological brain. On the other hand, this question has also been of immense interest to roboticists building artificial cognitive systems acting in real-world environments. This is because even *simpler* biological systems, such as insects, far outperform the most advanced robotic systems in solving real-world cognitive tasks. Modeling and constructing artificial cognitive systems, besides being a source of inspiration to roboticists, enables better understanding of the capabilities and limitations of biological cognition. In the scope of this dissertation we address the problem of cognition from a biological perspective rather than from

that of traditional artificial intelligence point of view. We model the minimal components of cognition, aiming to capture the key ingredients of cognition and their interplay.

1.1 The minimal components of biological cognition

We first address the question of what minimal set of mechanisms are necessary for a cognitive system. Unveiling these minimal components serves as the starting point of our investigation about the interplay among them. One such mechanism, namely the one that predicts the future state of a system given the current state and the control signals, is increasingly thought to play an important role in neuroscientific explanations of motor control, goal oriented behavior and cognition [128]. The existence of such a mechanism, known conventionally as the *forward model*, means that biological systems should be able to predict the sensory consequences of their actions in order to have robust adaptive behavior. In this context, the distinction between vertebrate and invertebrate nervous systems becomes crucial as the cognitive capabilities of animals from the two animal groups largely vary. In vertebrate neuroscience, there is substantial interest in interpreting the function of various brain areas in these terms (e.g. the cerebellum [76]). Besides, several authors have suggested that forward modeling could be a unifying framework for understanding the brain circuitry that underlies cognition [27, 11, 31]. The components of a forward model not only include sensory input, sensory processing, motor command and motor output, but also a prediction mechanism of future stimuli [120, 60]. In this context, the notions of *top-down* and *bottom-up* information flows are commonly used. Top-down information flows are modulatory inputs from higher-level cognitive areas to lower-level sensory areas. This supports the notion of a forward model as they are used to modulate bottom-up sensory information to fit expectations based on past events [60]. Also, growing evidence from physiology suggests that higher cortical areas of the brain are involved in a top-down and bottom-

up dialogue with lower areas (midbrain and superior colliculus) to solve low-level tasks like multisensory integration [101]. In the context of this dissertation we take a phylogenic approach to model a modular cognitive system, starting with a simple model and then incorporating forward models to account for observed insect navigational behavior in dynamic scenarios. We then generalize and test our model in complex real-world and simulated robotic tasks and in human visual processing.

1.2 Do biological cognitive systems use forward-models?

Despite the fact that many authors suggest the use of forward models for a unifying framework for understanding brain circuitry, the question whether all biological cognitive systems use forward models is still relevant [120]. The distinction between the vertebrate and the invertebrate brain is of special interest in this discussion. It can be argued that the vertebrate brain employs higher level cognitive mechanisms like prediction and anticipation which require the brain to possess forward models [60]. The question if the invertebrate brain possesses such capabilities is subject of ongoing debate [120]. We restrict the present work to ants as a prototypical invertebrate insect and to humans as a prototype of mammalian vertebrates. Most behaviors observed in insects and other invertebrates can be accounted for using the specialized layout and peripheral processing characters of invertebrate sensors and simple bottom-up models without the use of explicit forward models [121]. Nevertheless, some studies suggest the existence of forward models even in insect cognition (see [120] for review). At the same time, it can be argued that the mammalian brain needs to possess higher level mechanisms like prediction and anticipation as the action space of mammals are much larger that the action space of invertebrates, given that the difference in the available sensory space is not that large [36]. Besides that, the mammalian cerebral cortex is widely considered to be the seat of higher level cognitive capabilities like prediction, symbolic processing, attention etc. [95]. Nevertheless, it

is not evident that the invertebrate kingdom does not posses such capabilities, e.g. insects have brain structures called the mushroom bodies, which might have comparable functions [53]. Evolution is yet another argument that speaks for unique higher cognitive capabilities in higher animals, as adapting to more complex habitats should have given rise to more complex cognitive capabilities [36]. At the anatomical level, the difference in cognitive capabilities is remarkable, materialized in the number of neurons and synapses and in the complexity of brain layer structuring [106]. In summary, there is a general consensus that higher animals like mammals use forward mechanisms like prediction or anticipation to achieve adaptive behavior in uncertain environments. Nevertheless, the question whether invertebrates do the same or if their task solving behavior can be explained with relatively simpler models, without explicit use of forward models, is still subject of debate.

1.3 The stepwise refinement approach for modeling cognition

To contribute to the above discussion, in this dissertation we model the key components of cognition with the aim of understanding their interplay while solving complex tasks in uncertain environments. We base our model on a wide range of behavioral and neuroscientific studies in mammals that suggest the existence of cognitive mechanisms like attention, prediction and anticipation (in the scope of this dissertation we consider only these three higher level brain mechanisms) and strong vertical interactions between different hierarchichal layers of the brain during tasks such as sensory data processing, object recognition, navigation, memory acquisition and recall etc. [27, 11, 31, 101]. Thereby our approach is twofold: 1) we conduct experiments in biological systems (adhering to other relevant literature in the field) and intend to model the minimal cognitive framework that should be at work to account for the observed behavior, 2) we test our model in real-world artefacts in solving similar cognitive tasks and quantify the strengths and weaknesses of the model.

We follow the principle of stepwise refinement in modeling the key cognitive components. We start with the relatively *simpler* nervous system of the ant and investigate the behavior of the ant in navigation tasks and we finish with a model that integrates prediction, anticipation, sensation, attention and motor response.

1.4 The cognitive system as a largely feedforward mechanism: strengths and limits of an insect model

It is unclear if insect task solving skills require a high-level forward-model or they can be explained using low-level properties of the insect brain [120, 49]. We first consider that the rather *simple* insect brain does not posses any of the higher level cognitive mechanisms like attention, prediction and anticipation (no forward model for predicting future stimuli). We investigate this hypothesis in the context of navigation (foraging) tasks by comparing real ant behavior to our basic model. We show how our model can explain ant behavior in static environments and we also replicate those results on an indoor mobile robot for mapless landmark navigation. Nevertheless, the navigational behavior of the ant in dynamic environments seem to show some evidence for the existence of a forward-model, that predicts the positions of known landmarks. We find that our simple model, without explicit usage of forward models, soon reaches its limits to account for behavior in dynamic environments even in the case of the ant. We therefore incorporate forward models and replicate ant foraging behavior in highly dynamic environments on a simulated robot. Our approach thereby proposes a biologically plausible alternative to the solution of the SLAM problem in robotic navigation [99]. The crucial difference to the conventional SLAM solution is the replacement of a map with graph structures and the reformulation of localization as a question of relative distances and directions to landmarks.

1.5 Accommodating the forward-model for complex robotic tasks

We update our model to accommodate higher-level cognitive mechanisms like prediction, anticipation and attention and test the refined model for solving complex robotic tasks. Our model is inspired by the immense efforts invested over the past two decades in discovering the brain mechanisms involved in the interplay between prediction, anticipation, perception, memory and action [66]. Scrutinizing the highly hierarchichal structure of the brain has been a starting point for various studies investigating these subcomponents of cognition. The interdisciplinary research of cognitive brain and robotics research has profited from the above findings about the key hierarchical and vertical mechanisms involved in biological cognition.

Based on the above mentioned empirical (anatomical, physiological and behavioral) evidence that supports the notion of layered hierarchichal control systems, many interesting theories have been proposed until today. These theories propose a multi-layered framework of the brain, that has strong top-down and bottom-up information flows (see [91] for review). Furthermore, many of those models have been also designed with the aim of building novel artificial systems. Among others, the Distributed Adaptive Control (DAC) framework has been proposed to accommodate perceptual and behavioral learning in artificial systems in a single framework [113] (see [66] for review). Although most of the current proposals have been highly influential in cognitive sciences and robotics research, none of them has a framework that integrates prediction, anticipation, sensation, attention and response. We believe that such a framework is necessary to test the interplay between the different subcomponents and the contribution of each subcomponent to the whole artificial system in realistic tasks such as the ones performed by biological systems. In this context we propose PASAR, a concise and modular framework for integrating prediction, anticipation, sensation, attention and response. PASAR builds on the DAC architecture to structure perceptual and behavioral learning in three layers of control: reactive, adaptive and con-

textual [113]. In our simulation and real-world robotic experiments, we address the question of how each sub-component of PASAR contributes to the overall performance in the given task and what insights we can gain about robotic control and cognitive mechanisms in general. By performing these experiments we want to gain deeper insights into the interplay of the different cognitive subsystems involved in solving complex tasks. In order to test the hypothesis posed by our model about the specific interplay of attention, prediction and anticipation, we perform a psychophysical experiment with humans, thereby validating the model in biological cognition.

1.6 Signature and model of anticipatory biases in human visual processing

Besides the evaluation of our model to solve robotic tasks, we also test our model in a psychophysical experiment in humans to investigate the existence of the hypothesized forward models in PASAR. We thereby propose a psychophysical experimental paradigm to measure the interplay of top down, bottom up processes and the generation of saccades. In addition, we formulate a probabilistic computational model of data association in predictable dynamic scenarios. Our model integrates top down, bottom up processes and saccade generation, and proposes the existence of an anticipatory field that predicts and anticipates future stimuli in a spatiotemporally constrained fashion, and suggests the violation of anticipations as a trigger for attention. Our psychophysical results support the notion of top down prediction of visual stimuli revealing the existence of an anticipatory field. We find that humans rely more on predictions when working under higher cognitive loads. Our results clearly suggest the existence of a forward model mechanism in human visual processing involving prediction, anticipation and attention mechanisms. Moreover, we propose a concrete signature and model for anticipatory biases in human visual processing. Many earlier studies have addressed the so-called prediction hypothesis in human visual processing [94, 119, 61]. Also,

some studies support the prediction hypothesis in multiple object tracking [110, 119, 61], but others doubt its validity [61]. Here we not only provide a signature of an anticipatory gate, supporting the existence of predictive mechanisms, in human visual processing, but also propose a model for the same.

Chapter 2

AN INSECT-BASED MODEL OF KNOWLEDGE REPRESENTATION AND EXPLOITATION

The question of knowledge representation and exploitation is a key element for cognitive systems and is crucial for solving the specific problem of autonomous navigation in a priori unknown and dynamic environments [13]. This problem of autonomous navigation, despite massive advances in computing power and classical branches of robotics, remains a challenge especially when not using global positioning information and heavy sensory and computational resources [6, 97]. Insects like ants, despite having relatively limited cognitive and sensory resources, display remarkable navigational skills over hundreds of meters in very dynamic environments [122]. It is therefore interesting to the robotics community to understand the parsimonious navigational strategies employed by small-brained insects like ants. Also, navigation (among other phenomena) serves as reflection of the cognitive capabilities of the ant [29, 124]. In this chapter we therefore investigate and model the behavior of ants when solving visual landmark navigation tasks. Thereby, we use land-

mark navigation as a benchmark task to understand the basic cognitive principles employed by ants.

Ants have been investigated widely for their remarkable navigational capabilites. Ants, like a wide range of other animals, are foragers and robust navigation skills are crucial to survival for foraging successfully in unknown environments [103, 122, 127, 29]. Some remarkable behaviors such as landmark navigation, homing, path integration (PI) and learning are in many occasions required to perform successful foraging. Many ant species, like the desert ant (*Cataglyphis Fortis*), are known to forage successfully in very dynamic environments and find their way back to the nest, speaking for their robust navigational skills in changing environmental conditions. Also, ants are a particularly interesting preparation since the navigation of ants in dynamic environments can be tested in a controlled manner in indoor ant arenas. We design a minimal cognitive model that can capture ant behavior and implement it in a real-world robotic platform to navigate using the same model.

This initial minimal cognitive model does not contain any forward models but finds strong support in earlier ant navigational studies that try to explain ant navigation using vector-like memory representations of landmark to landmark routes [123, 124]. In the first section, we argue that knowledge representation and exploitation in static environments in the context of landmark navigation does not require higher level cognitive mechanisms like attention or prediction. We also propose and implement a model of mapless landmark navigation on an indoor robotic platform based on ant navigational behavior. In the second section we extend the navigation problem to include dynamic landmarks. There we test real ants in landmark manipulation tasks to understand and model their behavior. We test our model on a simulated robot to navigate in highly dynamic environments, demonstrating the feasibility of our model for robotic navigation . Our results suggest the necessity of a forward model for solving the landmark navigation task in highly dynamic environments.

2.1 Basic model and robot implementation for static environments

Our initial navigational model is inspired by the discussion about the presence or absence of a cognitive map in the insect brain. The concept of *cognitive map* for navigation, carried out mainly by Tolman [105], was fuelled by the discovery of the so-called place cells in the hippocampus of the rat and has widely increased our understanding of cognitive navigation mechanisms [84, 85]. It spawned early research on navigational strategies in cognitive neuroscience based on hippocampal representations of space [86, 22, 77]. While mammals are assumed to learn a place/map-like representation for foraging [84, 85], this does not seem the case in insects.

Insect navigation has been studied for more than a century [117, 28, 122, 98]. Interestingly, a wide range of findings suggests that insects do not rely on a map for solving foraging tasks [123, 28]. Recent studies suggest that rather than using map-like representations, insects make optimal use of proprioception, landmark recognition and memory to navigate [29]. In particular, desert ants use sun position and visual panorama for heading direction computation [122, 4]. Complex allocentric navigational behaviors using mainly ego-centric cues can be seen both in mammals like rodents but also in insects like ants and bees, which have considerably lower computational resources with only hundreds of thousands of neurons. Therefore, insect navigation studies are useful in that they reveal essential components for an efficient mapless navigation strategy. This is especially relevant for robotic implementations of autonomous systems and artificial foragers.

Despite massive advances in computing power and classical branches of robotics [13, 6, 97], robotic autonomous navigation, even with the use of global positioning information, remains a challenge. Until today a number of neurobiologically plausible models of navigation paradigms have been proposed for mobile robots [42, 7]. In the wake of neurobiological studies of place-cells, biomimetic robotic models of map-based navigation have recently seen great interest [7, 45]. The above mentioned models explain navigation from place to place only in very restricted fa-

miliar environments like mazes and small enclosures [64]. Navigators using such map based models of navigation are required to learn those place representations [50, 131]. Moreover, only a few of those models have been tested with real robots [46, 45].

As map based navigation strategies suffered from an inability to traverse unvisited regions of space, newer theories have incorporated path integration and head direction signals [107]. Even more recent versions also include cortical grid cells but still concentrate on the self-localization aspect of navigation rather than navigation between places [51, 75]. At the same time, the parsimonious navigation strategies of insects offer a guideline for computationally cheaper and eventually simpler navigation methods for mobile robots. A number of models exploit and reproduce some of the capabilities required during foraging [15, 16, 93]. However, many are biologically unrealistic and only deal with a very limited foraging task.

This section describes a comprehensive mapless biologically based model, including chemical search, PI and landmark navigation, of insect navigation strategies that is implemented in the framework of the Distributed Adaptive Control (DAC) architecture [113, 111]. The organization of behavior and optimal use of landmark recognition, proprioceptive information, heading direction information and memory usage is controlled by DAC and tested on an artificial foraging ant robot. Our results show a successful integration of a number of biologically based models and behaviors that give rise to realistic foraging. Moreover, our model explains the generalization process as a probabilistic use of memory, which generates allothetic behavior from a limited set of idiothetic cues in static environments.

This initial model serves as a novel biomimetic approach to mapless autonomous navigation based on insect neuroethology. Our model unifies different aspects of insect navigation and foraging including landmark recognition, chemical search, path integration and optimal memory usage. We test our model using a mobile robot performing a foraging task. While foraging for chemical sources in a wind tunnel, the robot memorizes the followed trajectories, using information from landmarks and

heading direction accumulators. After foraging, landmark navigation is tested with the odor source turned off. Our results show stability against robot *kidnapping* and generalization of homing behavior to stable mapless landmark navigation. This demonstrates that allocentric and efficient goal-oriented navigation strategies can be generated by relying on purely local information. Furthermore, we argue that ant brain does not need to possess any forward model to achieve stable landmark navigation in static environments. Consistent with recent findings the model supports navigation using heading direction information, thus precluding the use of global information [123, 124].

2.1.1 Experimental setup

The experimental scenario consists of a robot forager called *SyntheticAnt*, which is tested in a controlled indoor environment (figure 2.1). The test environment consists of a wind tunnel used by *SyntheticAnt* to localize the feeder tracking an odor plume. The wind tunnel floor contains a set of visual cues (landmarks) for *SyntheticAnt* to learn its way through the environment. A vision based overhead tracking system (AnTS) is used to localize the robot and compute its heading direction within the test arena, allowing for an analysis of the behavior of the robot.

2.1.2 Task

The task of the *SyntheticAnt* is to perform foraging using chemical sensing to localize food (odor source), and vision to learn to navigate through the environment, followed by successful homing. *SyntheticAnt* leaves its nest (marked by a unique visual cue) embarking on a foraging task to find a food source by following an odor plume up to its source (marked by another visual cue). On this outgoing route, the robot detects visual cues placed on the floor while performing foraging. Meanwhile collision avoidance has to be performed using proximity sensors. Upon feeder detection, it has to return to the nest using path integration information and restart foraging again. After foraging, landmark memorization is tested by

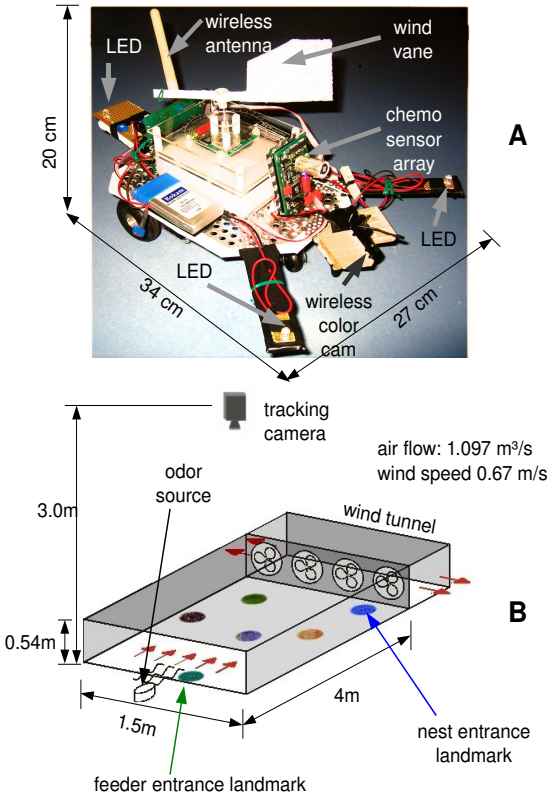

Figure 2.1: **(A) The artificial forager *SyntheticAnt*.** The robot is equipped with a wireless color camera for visual cue recognition, a chemosensor array for odor detection, a wind sensor for wind direction computation and three LEDs for head direction computation using an overhead tracking system. The camera image is transmitted using a 2.4 GHz analogue wireless link. The exchange of motor commands and sensor readings with the robot are realized via a serial port over Bluetooth. **(B) Wind tunnel arena.** At the back of the wind tunnel there are exhaust ventilators that create a controlled wind flow inside the tunnel. Visual cues are placed on the floor and an overhead vision based tracking system (AnTS) is used to reconstruct the position and heading direction of the robot.

placing the robot in an arbitrary location in the absence of the odor plume. Hence, in order to achieve this, *SyntheticAnt* has to recall the memorized landmarks and be able to navigate to other landmarks, including the nest and the feeder.

In figure 2.2**A)**, each HD accumulator cell stores the value $d \times cos\theta$ where d is the distance indicated by the movement arrow and θ the deviation angle of the movement from the preferred angle of the accumulator cell. The slope of activation falls as a sinusoidal function of angular deviation from the actuated direction, being 0 at 90°. In figure 2.2**C)**, Individual paths from landmark to landmark are indicated by numbers 1..4. In figure 2.2**E)**, after several foraging runs, the LTM contains several segment sequences (a segment is defined as a combined representation containing the landmark features of one landmark and a HDA set) of different lengths since in each foraging run only a subset of available landmarks are visited. In figure 2.2**C)**, Note that the recalled segment and the goal segment can be on different LTM sequences, in which case the segments from the current landmark to the nest on one sequence, and the nest to the goal landmark on the other have to be combined.

2.1.3 Simple model for mapless landmark navigation in static environments

SyntheticAnt is based on the Distributed Adaptive Control (DAC) architecture [113, 112] for the integration of a number of biologically based models and behaviors that give rise to a realistic foraging behavior. DAC consists of three, tightly coupled, layers for behavioral control; the reactive, adaptive and contextual layers (figure2.3). The reactive control layer provides the behaving system with a pre-wired repertoire of reflexes such as collision avoidance, chemosearch, homing etc. The adaptive layer provides the mechanisms for the processing and classification of sensory events. The sensor and motor representations formed at the level of the adaptive layer provide the input to the contextual layer, which acquires, retains, and expresses sequential representations by means of short-term and long-term memories. These representations are used to plan ongoing

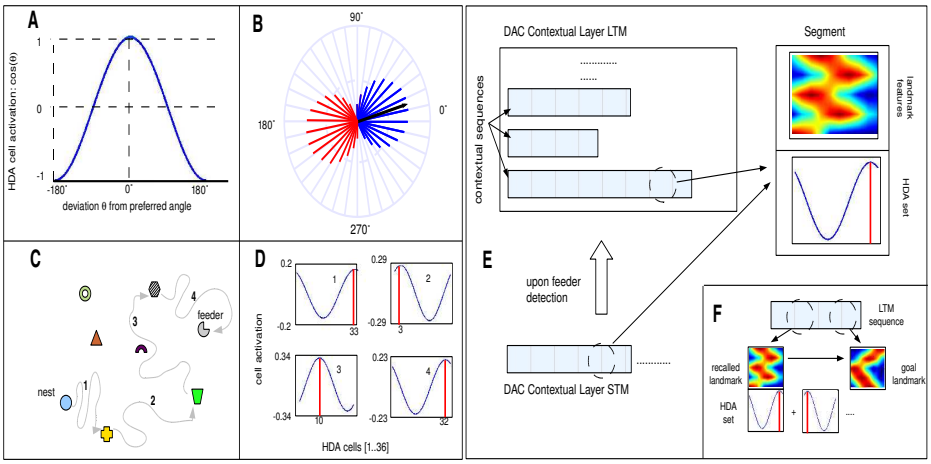

Figure 2.2: **Contextual learning of landmarks:(A)** Activation of HDA cells as a sinusoidal function of the angular difference from the cell's preferred angle. **(B)** HDA-set activation for a group of 36 HDA cells (of 10° resolution each) for a movement indicated by the arrow. Blue and red lines represent positive and negative activations respectively. **(C)** An example of a foraging run from nest to feeder traversing some landmarks indicated by the colored shapes. **(D)** HDA cell activities at the end of each landmark to landmark path. Y axis represents the cell activity and correlates with the distance traveled in the preferred angle of each cell, i.e. distance coded as firing rate. The X axis stands for the accumulator cells 1 to 36. The red vertical line with the corresponding number at the X axis shows the accumulator cell with the highest activity. **(E)** During the foraging runs from the nest to the feeder, the encountered landmarks are chained in the DAC contextual layer short-term memory (STM) together with the HDA set. Upon feeder detection, the contents of the STM are transferred into the LTM and the HDA-set is reset. **(F)** During the recall phase, the HDA-sets starting from the recalled segment to the goal segment are combined to compute the optimal route to the feeder.

behavior, and have been shown to be compatible with formal Bayesian models of decision making [112]. All computations are implemented using the neural simulation tool IQR [17].

2.1.4 Reactive behaviors

The reactive layer of *SyntheticAnt* implements a set of reactive behaviors including:

• *Chemical search: SyntheticAnt* implements a model based on the best studied case of chemotactic behavior, moth chemotaxis (as in [93]). It consists of an upwind movement (surge) whenever the animal perceives the odor stimulus and otherwise an oscillatory crosswind search (cast) until the odor plume is found again. The implementation of this behavior was done using the IQR neural simulator [17].
• *Collision avoidance:* Virtual proximity sensors, derived from the tracking system (figure 2.1), are used to avoid immediate collisions.
• *Feeder detection:* After finding the feeder (odor source) *SyntheticAnt* returns to the nest using a computed home vector by means of path integration, further referred to as *homing*.
In the absence of the odor plume *SyntheticAnt*'s surge-and-cast reactive behavior simplifies to a simple cast, which enables *SyntheticAnt* to explore the environment until a memorized landmark is encountered. In the absence of the odor plume a stochastic behavior is employed to avoid getting stuck.

2.1.5 Landmark recognition

Landmark recognition is implemented using a neural network that extracts prominent hue and edge features of visited landmarks using a neural network for extracting salient landmark features from the camera image using the neural simulation tool IQR [17]. See table 2.1 for the neural network parameters.

2.1.6 Heading direction accumulation

Path integration (PI) uses self-motion cues to compute the vector between the navigator's current position and the starting point, i.e. home base. In our model we make use of heading direction and proprioceptive information to acquire PI. We propose the use of head direction accumulators (HDA), as postulated in [64]. A HDA is a neuron that fires only when the navigator heads in a particular direction. Furthermore, the firing rate of such a neuron correlates with the distance covered in that direction (figure 2.2, B). HDAs are assumed to integrate sensory information such as optic flow, polarized photoreceptors, sun position and proprioceptive information until reset [64]. Hence, a group of HDA neurons each of which is tuned to a different angle at equal intervals covering 0 to 360 degrees encodes the direction and distance from the previous position at which the HDA-set was reset. The activation of an HDA-set is governed by a cosine function as shown in figure 2.2. The slope of the activation rate is highest when the navigator moves in the HDA cell's preferred direction and falls according to the cosine function with angular deviation, consistent with [64] [100]. During foraging, whenever *SyntheticAnt* encounters a landmark, the set of detected landmark features and the current HDA information is passed to the STM of the contextual layer of DAC, as discussed in the next subsection. After that, the HDA-set is reset and the foraging continues.

2.1.7 Short and long term memories

The contextual layer supports the formation of more complex representations of perception and events (processed by the adaptive layer) expressing their relationship in time. In the case of the *SyntheticAnt*, pairs of visual cues and HDA information form basic memory elements, called memory segments. During the acquisition phase (foraging) salient events (cue detections) are first stored in short-term memory (STM) together with the current HDA. When the goal state is reached, the content of the STM is stored in the long-term memory (LTM) as a sequence (figure 2.3). During the recall phase (landmark navigation), the LTM is matched

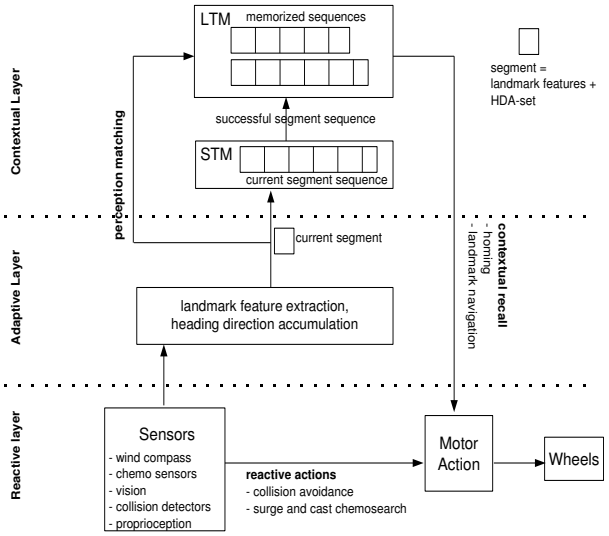

Figure 2.3: ***SyntheticAnt* Foraging Model:** The reactive layer performs reflex actions like collision avoidance, chemical search, homing, etc. During foraging, the adaptive layer performs landmark recognition, feature extraction, HDA computation and constructs memory segments for each observed landmark. A segment, as shown on the top right, contains the extracted landmark features and an HDA-set. These segments are sequenced temporarily in the short-term memory (STM) of the contextual layer until feeder detection, when the contents of the STM are transferred into the long-term-memory (LTM). During the recall phase (homing, landmark navigation), the LTM is matched against the current sensory events and an optimal trajectory is computed from recalled LTM segments.

against the current sensory events. Goal cue is defined as a the feature set characterizing a specific landmark. Matching LTM sequences containing both current sensory perception and goal cues are recalled to compute the optimal route from the current position to the goal landmark. Matching is accomplished by the following distance function:

$$d(a,b) = \frac{1}{K}\sum_i |\frac{a_i}{max(a)} - \frac{b_i}{max(b)}| \tag{2.1}$$

a where a and b are vectors in $\mathbb{R}^K$ and a is the current activity of the cue information and b is the stored cue information. A segment is selected when the distance $1 - d(a,b)$ is higher than a predefined threshold. The selected segment and segments stored in the same sequence together contain the accumulated PI information (HDA) to the goal.

To compute the optimal route from the currently perceived landmark to an arbitrary landmark, we consider the scenario where the currently selected segment (landmark) and the goal segment (landmark) are on different LTM sequences. To do this, we first compute the homing vector by summing and inverting the sequence of HDA-sets stored in all segments from the currently selected segment until nest on the first sequence. To this we add the sum of the HDA-s from nest to the goal segment (landmark) on the second sequence. This allows computing optimal routes between any two landmarks represented in arbitrary segments in the whole LTM.

After multiple foraging runs, *SyntheticAnt* might encounter landmarks, that had been seen in different foraging runs. This fact will select segments of different sequences in the LTM during recall. In this case, each selected segment will return a homing vector, which have to be merged optimally. This generalizes from homing to landmark navigation if the goal landmark is not the nest. In general we refer to the decoded heading direction and distance as *action* (or action HDA-set). Assuming a white noise error, this decoded heading direction and distance to the goal can be formulated as a 2D Gaussian probability distribution:

$$\bar{\boldsymbol{X}} \sim \boldsymbol{N}(\bar{\boldsymbol{\mu}}, \boldsymbol{\sigma^2}) \tag{2.2}$$

where $\bar{X} = [\alpha, \delta]^T$. α is the angle and δ the distance coded by the action HDA-set. The action HDA-set, $\bar{X}$, can be formulated as a Gaussian distribution with mean $\bar{\mu}$ and variance σ^2. The variance σ^2 grows with the total distance $dist$ covered during the heading direction accumulation. This can generally formulated as a function: $\sigma^2 = f(dist)$. Given this Gaussian distribution for each recalled segment action, we use Bayesian inference to compute the best action. If n actions are recalled, the best action a is the action with the highest conditional probability: $P(a|\bar{X}_1, \bar{X}_2, ..., \bar{X}_n)$. And using Bayes theorem., the probability of the optimal action is computed:

$$P(a|\bar{X}_1, \bar{X}_2, ..., \bar{X}_n) = \frac{P(a)P(\bar{X}_1, \bar{X}_2, ..., \bar{X}_n|a)}{P(\bar{X}_1, \bar{X}_2, ..., \bar{X}_n)} \tag{2.3}$$

where the numerator $P(a)P(\bar{X}_1, \bar{X}_2, ..., \bar{X}_n|a)$ is the joint distribution $P(a, \bar{X}_1, \bar{X}_2, ..., \bar{X}_n)$ and the denominator $P(\bar{X}_1, \bar{X}_2, ..., \bar{X}_n)$ is a constant without effect.

Using conditional independence of memory sequences, the above equation can be reformulated as:

$$P(a|\bar{X}_1, \bar{X}_2, ..., \bar{X}_n) \propto P(a) \prod_i^n P(\bar{X}_i|a) \tag{2.4}$$

$P(a)$ is uniformly distributed in an a priori unknown environment. Therefore, the computation of $P(a)$ in equation 2.4 can be reduced to the product of Gaussians $\bar{X}_1, \bar{X}_2, ..., \bar{X}_n$. The resulting action with the highest probability is optimal in the Bayesian sense.

SyntheticAnt runs on an Intel(R) Core(TM)2 Duo CPU 2.66GHz machine with GNU/Linux Suse10.3 operating system at about 35 Hz. The parameters of the neural simulation using the IQR toolkit [17] is summarized in table 2.1.

2.1.8 Results

SyntheticAnt was exposed to a number of tests in the arena shown in figure 2.1, where it had to forage starting from the nest and to find the feeder

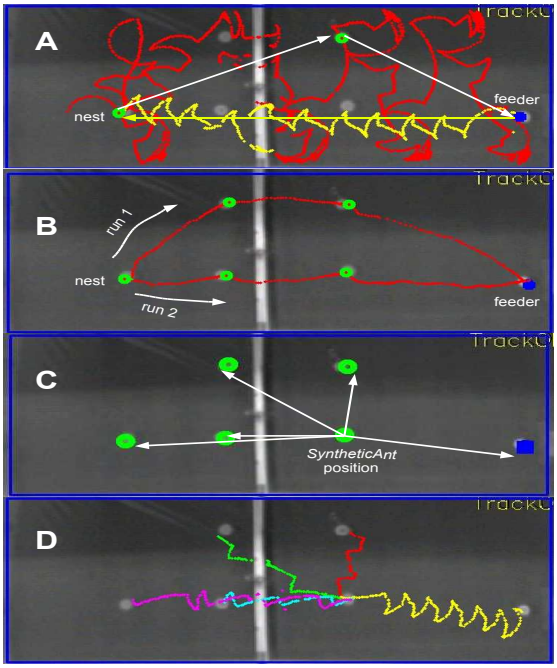

Figure 2.4: **Foraging to landmark navigation:** All plots are superimposed on the tracking camera image. The vertical bar in the middle of the image belongs to the wooden structure of the wind tunnel and does not interfere with the movement freedom of *SyntheticAnt*. **(A) Foraging and homing.** The red dots indicate robot positions during foraging from nest to feeder. The green circles indicate encountered landmarks. The white arrows indicate the corresponding HDA sets from the DAC contextual layer. The blue square on the right is the feeder. The yellow arrow corresponds to the computed homing HDA. The yellow track shows the homing behavior of the robot after feeder detection. **(B) Nest to feeder trajectories.** *SyntheticAnt* is guided through two different trajectories from nest to feeder (indicated as run 1 and run 2, leading through available landmarks. **(C) Generalization of homing.** After the runs shown in B, *SyntheticAnt* is kidnapped and placed in an arbitrary position in the arena. Upon landmark detection *SyntheticAnt* recalls all possible straight routes to other landmarks including the nest and feeder, indicated by the white arrows. **(D) Route execution.** After recall, *SyntheticAnt* traverses recalled routes.

# total neurons	62771
# total neuron groups # integrate and fire # linear threshold # random spike	252 29 202 21
# total synapses	103872
# cells in HDA set	72
# cells in landmark features	2×4
processes	16

Table 2.1: Neural simulation parameters

placed at the upwind end of the wind tunnel. Upon feeder detection it had to compute the homing vector and return to nest. After foraging runs, the chemical cue was switched off and *SyntheticAnt* was kidnapped and placed in an arbitrary position in the arena. At this point, it had to find a landmark and reach other landmarks and the feeder by generating optimal routes.

An overhead camera is used to track the position of the robot for data analysis, together with the logged data from the neural simulation of the model. Figure 2.4 A, shows a foraging run through landmarks and homing behavior on a straight line to the nest from the feeder. Encountered landmarks during the foraging run are shown as green circles in figure 2.4, A. The nest is indicated by the blue rectangle. After a foraging run, when the feeder is found, the homing vector is recalled automatically and the DAC reactive layer of *SyntheticAnt* initiates the homing behavior. *SyntheticAnt* is also able to generalize homing to landmark navigation and can traverse unknown paths to go from a given landmark to another landmark encountered during a different foraging run (figure 2.4 B,C,D). The homing path shows a zig-zag movement as the robot tries to correct its current heading direction using the difference between the accumulated HDA starting at the feeder and the contextual memory response HDA. Such a correction is equivalent of the general proportional controller

Memorized and computed HDA sets are direction vectors leading from

one landmark to another (shown as arrows in figure 2.4). Decoding of an HDA neuron group into the direction α is done as following:

$$\alpha = \frac{360}{N} * I$$

where N is the number of neurons in the HDA set and I the index of the neuron with highest activity in the set. The distance D is coded directly by the activity rate of the neuron I. See also figure 2.2 A,B,C,D for HDA coding.

Figure 2.5 is the density plot of tracking data and summarizes the typical behavior of *SyntheticAnt* during 5 foraging runs. The landmark regions get very high density as landmark recognition stops the robot for some time to ensure precise feature extraction of the landmark. The robot stops to avoid collisions when at the periphery of the field and this results in some high density spots along the periphery.

The use of overhead tracking for the computation of the heading direction and proprioception of the *SyntheticAnt* gives highly precise HDA-sets. This is very useful for testing the feasibility of our insect model and also to conduct tests inside a wind tunnel. However, in real world experiments these computations will be erroneous due to sensor errors. Therefore in future work the overhead tracking will be replaced by odometry sensors (e.g. using optic flow) and heading direction sensors (e.g. using solar compass). This means that the precision of HDA computation will fall since such sensors have intrinsic errors. While error in heading direction and path integration accumulates with the distance traveled, the precision of the computed HDA falls. To evaluate the performance of our system when using such imperfect information, we conducted the following experiment. From three foraging runs of *SyntheticAnt* going through different landmarks, we evaluated the error in the computation of the homing vector when using one, two or three recalled DAC LTM sequences. Noise in the HDA sets for each path-segment in each sequence (from one landmark to the next), was modeled as linearly correlated with the distance traveled. Specifically a white noise of mean zero and a vari-

able variance (SNR) proportional to the distance traveled was induced on each HDA set. After this, the homing vector was computed in three different ways: using each of the three sequences individually, by combining just two of the three and by combining all three together. The fusion of different sequences was done using the DAC Bayesian fusion algorithm described earlier (equation 2.4). We assessed the robustness of the system by measuring the error when varying the signal to noise ratio (SNR) from 0.1 to 100. Results show that the error falls with the number of sequences used to compute the homing vector (number of runs/experience of the forager) for all ranges of the SNR values of sensors, see figure 2.6. This not only justifies the Bayesian merging of LTM responses but also, it indicates the validity of the proposed insect-model also when using real odometry and heading direction sensors. The error in homing vector computation (or in landmark to landmark route recall in general) is negatively correlated with the SNR of the HDA computation. For low SNRs (i.e. low precision sensors) the error rises drastically whereas for high SNRs (high precision sensors) it falls, see figure 2.6.

A remarkable property of the three coupled control layers of DAC is the emergence of useful behavioral properties. One of them is maneuvering in a dynamically changing world. To test this behavior we placed obstacles in the arena as *SyntheticAnt* was performing landmark navigation or homing. The collision avoidance reactive behavior then had to compete with the previously active behavior mode (e.g. homing or surge-and-cast) to maneuver around the obstacle. Thereby the desired heading direction has to be corrected for the movement of the robot. A typical example of such a maneuver is shown in figure 2.7.

We note that our results were achieved in static environments with just the use of a memory sequencing mechanism and recall. There was no explicit forward model at use. Our model provides a concise explanation to the supposedly mapless landmark navigation mechanism employed by insects like ants. Next we investigate how the model can be extended to solve the problem of landmark navigation in highly dynamic environments.

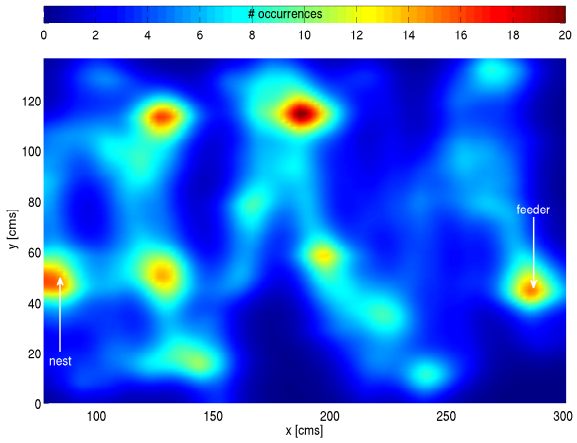

Figure 2.5: **Foraging behavior as density plot:** Position data from five foraging runs of *SyntheticAnt* were used. The high density areas are near landmarks, the nest (leftmost high density circle) and feeder (rightmost high density circle). Also some peripheral areas have relatively high densities due to the fact that *SyntheticAnt* stops to avoid collisions. The plot illustrates the typical behavior of the robot during foraging. The colorbar indicates the number of occurrences of the robot at a given position. A numerical interpolation was applied to smoothen the tracked position data.

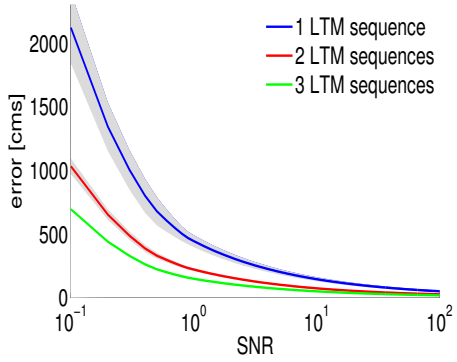

Figure 2.6: **Bayesian merging of LTM sequences:** The error in homing vector computation (or in landmark to landmark route recall in general) as a function of the SNR of the HDA computation. The errors when using one, two or three LTM sequences in combination are shown. The colored lines are mean values and the patches signify standard deviation.

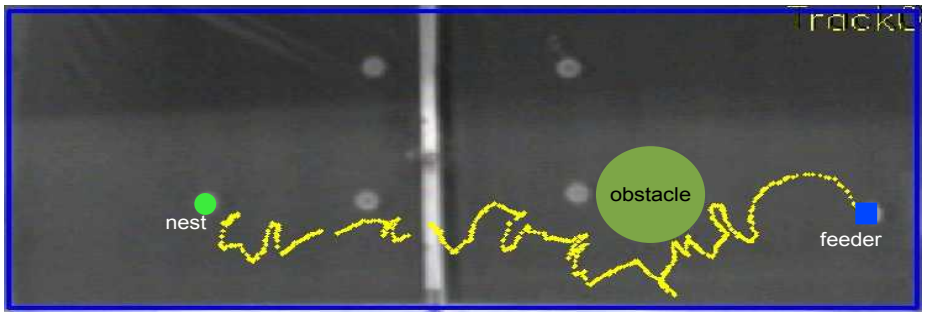

Figure 2.7: **Acting in a dynamic world:** *SyntheticAnt* was exposed to virtual obstacles (filled circle) placed on its route during homing or landmark navigation. The tracked positions of the robot are indicated by the yellow dots.

2.2 Extended model and comparison with the biological system in dynamic environments

In the previous section we described a comprehensive mapless model, including chemical search, PI and landmark navigation, of insect navigation strategies [74]. That navigational strategy was based on the so called heading direction accumulation mechanism, which was recently hypothesized to be used by insects for navigational purposes [64]. However, the problem of information gathering, representation and usage was not addressed in the context of dynamic environments. This becomes highly relevant as the autonomous navigator has to act in a dynamic world with non-static landmarks, where previously acquired knowledge has to be exploited and adapted at the same time. We address here the question whether insects like ants use forward models to do the address the above problem for landmark navigation in dynamic environments. We analyze navigational behavior of the *Formica Cunicularia*[1] ant species in controlled landmark manipulation experiments and we observe that ants do use expectations about the relative direction and distance of landmarks from other landmarks and they adapt their expectations to match their current perceptions, speaking for the existence of a forward model. We enhance our simple model to accommodate for the more complex behavior.

To this end we propose an autonomous navigation method in dynamic environments based on recent views from cognitive psychology [79] and insect neuroethology and physiology, which suggest that insects expect future events based on past experiences [44]. We propose an *expectation reinforcement* paradigm to adapt the confidence of the artificial forager in encountered landmarks. We also propose a variant of an insect-like probabilistic search strategy suggested earlier to be used by insects upon expectation violation [116, 96]. As the initial simpler model, our current model is also based on the Distributed Adaptive Control (DAC) framework that organizes behavior in three levels of adaptive control [113, 111]. We im-

[1] a mining ant of the *Formica fusca* group, commonly seen in southern England

plement the model using the large-scale neural simulator IQR [17] and test it in a simulated robot. In our experiments we first evaluate the capability of our model to solve a complex navigational task in an unknown dynamic environment. We further carry our experiments with real ants to compare their behavior with the robot model in the same navigational task. Our results show a successful autonomous navigation strategy in dynamic unknown environments and striking similarity to insect behavior. Moreover, our model explains autonomous navigation as a dynamic process of memory reconsolidation, which harnesses expectations that are readily available from past explorations.

2.2.1 Navigational task and the test environment

Task

Both the real ant and the artificial forager called *SyntheticAnt* are made to forage for the feeder (food location) in an initially unknown environment starting from its nest. The environment contains many visual landmarks which could be used by the forager for navigation. After many foraging runs, some landmarks are displaced or removed. The forager is then made to forage in this manipulated environment. In the next foraging runs, the original landmark constellation is restored. This task allows to study and compare three key issues of autonomous navigation:
• learning landmark navigation in a dynamic environment
• behavior upon detection of landmark manipulation
• confidence adaptation depending on the reliability of the landmarks after restoration.

See figure 2.9 for an illustration.

Real ant experiments in dynamic environments

We perform real ant foraging experiments as described above using the desert ant *(genus Cataglyphis)*. Landmark manipulation tasks are performed using several colored ants and the ant trajectories of the foraging runs are recorded using the AnTS overhead camera tracking system. It

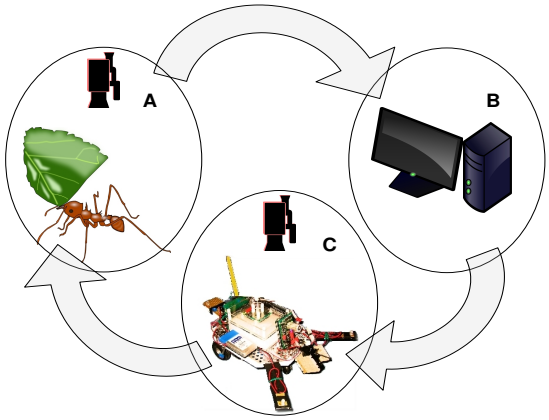

Figure 2.8: **Insect behavioral analysis, modeling and testing on robots: A)** Real-world ant experimental studies are performed and the behavior of the ant is recorded using a tracking camera. Controlled manipulations of visual landmarks in the ant arena are made in order to analyze the ant behavior. **B)** We first model the ant behavior based on the understanding of the underlying neural principles. The ant experimental data is analyzed and fed into the *SyntheticAnt* simulation of the navigational model. This simulation is used to tune the parameters of our navigational model on a simulated robot. **C)** The real-world robot *SyntheticAnt* is tested with analogous manipulations of visual landmarks in the arena, allowing direct comparisons of the behaviors of real ant and the robot. The results of this is again used to design new ant experiments.

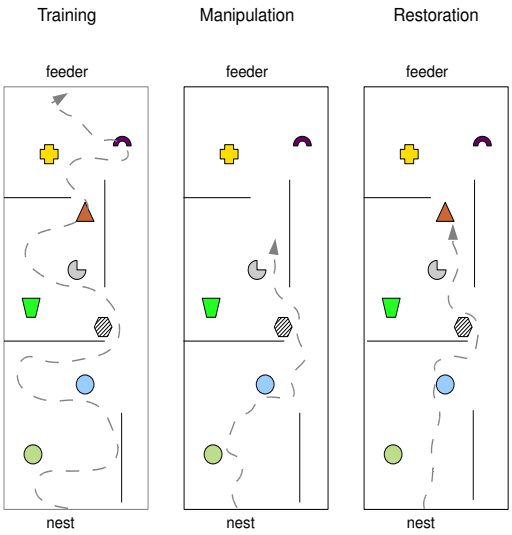

Figure 2.9: **Autonomous Navigation Task: Left)** In the training session (also called foraging) the navigator leaves its nest to forage for food, traversing an arena with visual landmarks. These visual cues are used by the navigator to memorize its routes. **Middle)** After several foraging runs, a manipulation is made in the arena (i.e. a landmark is displaced or removed as the red triangle in the figure), and the behavior of the navigator observed. **Right)** The original constellation of the landmarks is restored and the behavior of the navigator is observed.

is important to note that in the real ant navigation experiments, the paper on the floor of the arena was replaced after each foraging run, in order to avoid the use of chemical cues by the ants.

Modeling and simulation environment

The modeling environment allows the input of the real ant trajectory for the simulated ant called the *SyntheticAnt*, allowing it to have the same perceptual input during foraging. Also free foraging behavior is available. The simulation replicates the real arena and the robot. It allows testing navigational paradigms before they are tested on the real robot. In this work we only consider the simulated robot.

We test the proposed navigational model on the simulated robot. As the neural implementation of the model is the very same for the simulated and the real *SyntheticAnts*, the transition from simulation to real world is readily manageable. More details of the experimental setup and the real robot version of the *SyntheticAnt* are discussed in [74].

2.2.2 The extended model for mapless landmark navigation in dynamic environments

Here we discuss how we adapt the Distributed Adaptive Control (DAC) architecture we used in the previous section to model the behavior of ants in dynamic environments [74]. The Distributed Adaptive Control (DAC) architecture has been shown earlier to be capable of optimizing behavior using behavioral and perceptual learning in robots [113, 112]. DAC consists of three, tightly coupled layers for behavioral control; the reactive, adaptive and contextual layers. The reactive control layer provides the behaving system with a pre-wired repertoire of reflexes such as collision avoidance, chemosearch, homing etc. The adaptive layer provides the mechanisms for the processing and classification of sensory events. The contextual layer acquires, retains, and expresses sequential representations by means of short-term and long-term memories, figure 2.10, A. (In this section, as we are concerned with information representation and

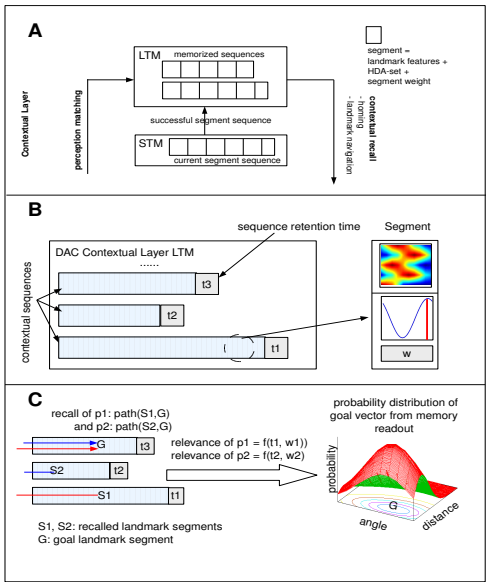

Figure 2.10: **(A) DAC Contextual Layer** A segment contains the extracted landmark features, an HDA-set and the segment weight. Segments are sequenced temporarily in the short-term memory (STM) whenever a landmark is encountered. Upon feeder detection, the contents of the STM are transferred into the long-term-memory (LTM). During recall phase (homing, landmark navigation), the LTM is matched against the current sensory events and an optimal trajectory is computed from recalled LTM segments. **(B) Sequencing:** During the foraging runs from the nest to the feeder, encountered landmarks are chained in the DAC contextual layer short-term memory (STM) together with the HDA set. Each LTM sequence has a retention time t owing to the *transiency* of memory and each segment has a weight w. **(C) Recall:** During the recall phase, the HDA-sets starting from the recalled segment to the goal segment are combined to compute the optimal homing vector. When the recalled segment and the goal segment are on different LTM sequences, the segments from the recalled segment to the nest on one sequence, and the nest to the goal segment on the other are combined (such a combination is called *path*). *Paths* are weighted according to the retention time of the sequence and the mean relevance weights of the segments of the recalled LTM sequence.

using it as a forward model, we only deal with the contextual layer.) These representations are used to plan ongoing behavior, and have been shown to be compatible with formal Bayesian models of decision making [112]. We use the DAC contextual layer to learn sequences of landmarks together with their Heading Direction Accumulator (HDA) set. Using this the navigator can memorize several trajectories from the nest to feeder, leading through different landmarks. The DAC contextual layer recall mechanism is used when in the test scenario, a particular landmark is encountered, to recall the vectors to other landmarks. The details of this mapless navigational strategy is discussed in the previous section [74]. In this section, we consider the use of DAC contextual layer and its recall mechanism as a forward model for learning to navigate in unknown and dynamic environments.

2.2.3 Dynamic memory consolidation using expectations

Cognitive psychology has recently begun to embrace a new position recognizing memory as a highly dynamic process [79]. In this new view, remembering and forgetting are not merely transient processes; moreover they are achieved through a highly dynamic (re)consolidation process. Strong support for such a dynamic memory comes from animal neuroscience studies as reviewed in [79].

At the same time, insects have also been shown to expect events using memories acquired in the past, speaking clearly for the existence of a forward model [44, 43]. Building upon these two recent advances in neuroscience and cognitive psychology, we propose a dynamic memory model for insect-like mapless navigation in uncertain environments, which uses expectations to consolidate or forget already acquired memories, figure 2.11. We propose a dynamic contextual layer LTM of Distributed Adaptive Control for mapless navigation using heading direction accumulation cells. Therefore we consider memory transiency (to account for dynamics of the memory), adaptive confidence in landmarks and an expectation mechanism (to account for a forward model) as the necessary enhancements of our simple model to account for the complex ant behavior in

highly dynamic environments.

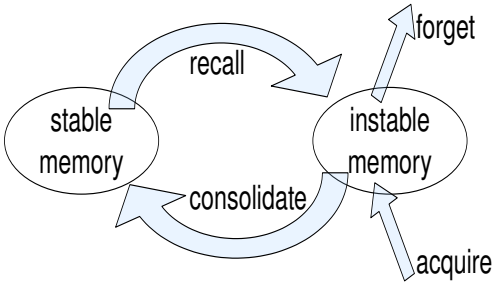

Figure 2.11: **Dynamic Memory Reconsolidation Schema:** As a memory is acquired it enters the instable state and then is consolidated into the stable state. Nevertheless, memories in the stable state can reenter the instable state upon recall. Reconsolidation again stabilizes this memory that otherwise gets forgotten [79].

Transiency and confidence in memory sequences

We elaborate how transiency and confidence in memory traces are formulated for mapless navigation in uncertain environments. First we consider the situation, where the *SyntheticAnt* is kidnapped after many foraging runs and placed at an arbitrary visual landmark. The details of the memory recall using the DAC contextual layer for mapless navigation can be consulted in section 2.1.7 [74]. Memory recall of the DAC contextual layer is used to compute an optimal path to another given landmark; we further refer to this as the *memory answer*. We define a vector $\vec{V}$ as a two dimensional vector indicating the angle γ and distance ψ of a given memory answer: $\vec{V} = [\gamma, \psi]^T$. Assuming that n LTM sequences were recalled, we are interested in computing the probability distribution:

$$P(\vec{V}|t, \vec{V}_1^t, t_1^{ret}, r_1^{seg} \cdots \vec{V}_n^t, t_n^{ret}, r_n^{seg}) \tag{2.5}$$

where $\vec{V}$ is the vector indicating the goal, t is time, $\vec{V}_i^t$ is the vector suggested by LTM sequence i, t_i^{ret} is *retention time* of LTM sequence i and r_i^{seg} is the segment relevance of the recalled segment of LTM sequence i.

We look at the contribution of one LTM sequence i to the overall memory answer:

$$P(\gamma\psi|t, \vec{V}_i^t, t_i^{ret}, r_i^{seg}) \tag{2.6}$$

First, we consider equation 2.6 without the retention times:

$$P(\gamma\psi|t, \vec{V}_i^t, r_i^{seg}) \tag{2.7}$$

Using conditional independence of angle and distance we get

$$\begin{aligned} P(\gamma\psi|t, \vec{V}_i^t, r_i^{seg}) &= P(\gamma|t, \vec{V}_i^t, r_i^{seg}) \\ &\quad \cdot P(\psi|t, \vec{V}_i^t, r_i^{seg}) \\ &\quad \cdot P(t, \vec{V}_i^t, r_i^{seg}) \end{aligned} \tag{2.8}$$

where $\vec{V}_i^t = [\gamma_i^t, \psi_i^t]^T$. We formulate $P(\gamma|t, \vec{V}_i^t, r_i^{seg})$ and $P(\psi|t, \vec{V}_i^t, r_i^{seg})$ as Gaussian distributions centered around the means γ_i and ψ_i respectively with time dependent variances, signifying that higher weight segments have a higher influence on the total memory answer as they have a smaller variance. This dynamically adapting variance is used to weight successful segments more and unsuccessful ones less.

$$P(\gamma|t, \vec{V}_i^t, r_i^{seg}) = \mathcal{N}(\gamma_i, f_1(r_i^{seg})) \tag{2.9}$$

$$P(\psi|t, \vec{V}_i^t, r_i^{seg}) = \mathcal{N}(\psi_i, f_2(r_i^{seg})) \tag{2.10}$$

where f_1 and f_2 are exponential growth functions of variance:

$$f_1(x) = a_1 e^{k_1(x)} \tag{2.11}$$

$$f_2(x) = a_2 e^{k_2(x)} \tag{2.12}$$

As all memory answers should be seen as equally probable and no correlations of distance, angle and retention-times of LTM sequences are known, we assume the uniform distribution:

$$P(t, \vec{V}_i^t, r_i^{seg}) = \mathcal{U} \tag{2.13}$$

Now we consider the contributions of all selected LTM sequences weighted by segment retention times t_i^{ret}:

$$P(\vec{V}|t, \vec{V}_1^t, t_1^{ret}, r_1^{seg} \cdots \vec{V}_n^t, t_n^{ret}, r_n^{seg}) = \sum_i \frac{t_i^{ret}}{t_{tot}} P(\gamma|t, \vec{V}_i^t, r_i^{seg}) P(\psi|t, \vec{V}_i^t, r_i^{seg}) P(t, \vec{V}_i^t, r_i^{seg}) \tag{2.14}$$

where $t_{tot} = \sum_i t_i^{ret}$. Equation 2.14 signifies that the sequence retention times are used to weight the shares of LTM sequences to the final memory answer. In other words, sequences are weighted so that memory acquired further back in the past is weighted less than more recent memory.

Building up confidence in uncertain environments

When a landmark (or feeder) at a known location ceases to be available or its position is manipulated, insects have been shown to exhibit search patterns that optimize rediscovery of the landmark (or feeder) [116]. We further refer to landmark manipulations of all kinds as *manipulation*. It has also been proposed that such search patterns in insects could be modeled using Lévy walks [96]. Lévy walks are characterized by a distribution function

$$P(l_j) \sim l_j^{-\mu} \tag{2.15}$$

with $1 \leq \mu \leq 3$, where l_j is the walk length. The direction of the walk is drawn from a uniform distribution. The natural parameter μ has been shown to be optimal at the value 2 for modeling insect *manipulation* behavior, yielding an inverse square power-law distribution [116].

Here we propose a modified version of Lévy walk, to model the *confidence building behavior* exhibited by ants upon *manipulation*. By *confidence building behavior* we mean the specific behavior exhibited by the animal once it detects the manipulation of a known landmark, namely the environment resampling strategy that seems to serve the purpose of *rebuilding the confidence* about the route to the feeder. The key idea is to propagate the initialization point of the Lévy walk towards the nest, so that the probability of encountering known landmarks is increased. Thus, the forager can slowly build up *confidence* about the distance and direction to the navigational goal. The proposed version of Lévy walk is summarized in the pseudo-algorithm below:

while $|con| \leq \epsilon$ **do**
  $t \leftarrow 0$
  while $t \leq \theta$ **do**
    $perform\ Lévy\ walk\ from\ i$
    $upon\ landmark\ detection : update\ con$
  end while
  if $i = nest$ **then**
    $reset\ i\ to\ manipulation\ point$
  else
    $propagate\ i\ towards\ nest$
  end if
end while

where con is the mean confidence about the goal direction and distance, i the current position at which the Lévy walk is initialized, and θ and ϵ two appropriate thresholds. The artificial forager is made to switch to the above described search mode, when either an expected landmark is not encountered or when a landmark with a very low confidence is found. The duration of the Lévy walk is much higher in the first case and linearly decreases with the confidence in the landmark, controlled by setting the above parameters ϵ and θ. Our new proposal of the Lévy walk helps the reinforcement of expectations as it lets the autonomous navigator validate its expectations by going back to known terrain, instead of searching ran-

domly in the whole arena. This is strongly suggested by observed ant behavior in similar situations and is evaluated in our experiments.

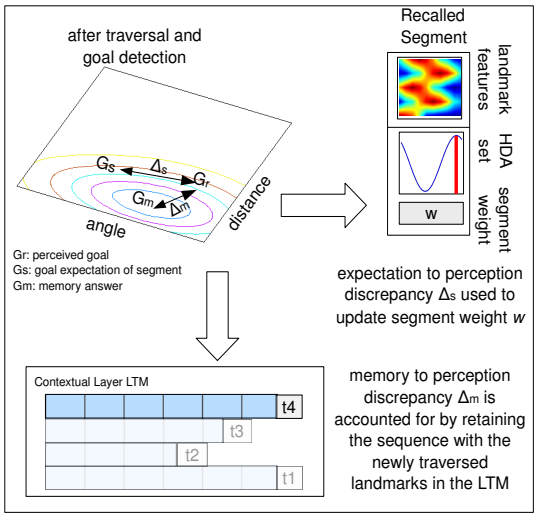

Figure 2.12: **Expectation reinforcement for memory consolidation:** Discrepancy between expected paths and computed paths are used to consolidate memory by means of setting LTM segment weights and writing new LTM sequences.

Adapting landmark reliability measure using expectations

The forager's belief about the reliability of individual landmarks should be updated each time a landmark is encountered. For this we use an expectation reinforcement mechanism, which gives rise to a dynamic memory reconsolidation process [79]. Expectations for positions of individual landmarks can be read out from the DAC contextual layer memory. The discrepancy between perceived position of a landmark and the expected position is used to update the reliability of the landmark, i.e. the weight of a DAC contextual layer segment, as shown in figure 2.12.

To update the DAC LTM segment weight using the discrepancy, we use the exponential decay function

$$r_{t+1}^{seg} = r_t^{seg} \mathrm{e}^{-\lambda d} \tag{2.16}$$

where d is the discrepancy and t is time step. This causes the segment weight to fall exponentially from its current value if the discrepancy is high. Discrepancies are normalized ($0 \leq d \leq 1$) so that $d = 1$ for the highest possible discrepancy (the length of the diagonal of the arena). The natural parameter λ was shown to optimally fit observed insect behavior at the value 2 [116]. The above decay is applied only if the discrepancy is above a fixed threshold. Otherwise, the segment weight is allowed to grow according to a linear function. In the following, we use the terms landmark *reliability* and *confidence* interchangeably.

2.2.4 Results

First we test the ability of the proposed model to learn the reliability of landmarks. For this purpose we test the simulated *SyntheticAnt* in an arena with 10 visual landmarks. During the foraging no landmark manipulation were carried out. After that, during the test 9 of the 10 visual landmarks were displaced randomly in each run, i.e. there was only a single stable landmark. After the foraging runs, we test the feeder direction and angle from the nest, computed as discussed earlier, using each of the 10 landmarks. Note that for this the distance and angle to the feeder from an arbitrary landmark is computed first using DAC contextual recall (as in [74]), which is then added to the vector leading from the nest to this landmark. This allows to visualize the belief of the forager in the reliability of each landmark as a probability distribution, as plotted in figure 2.13. The *SyntheticAnt* learns through expectation reinforcement that only landmark number 10 is stable. The evolution of the confidence in the landmarks are shown in figure 2.13 A (before the test runs), B (after 5 test runs) and C (after 10 test runs).

Note that a single simulation trial approximately runs for the same time as an ant foraging run and we perform qualitatively the same kind

of landmark manipulations in the real ant experiment and in the simulation. We also use similar landmarks in the simulation as used in the ant experiments. Nevertheless, for simplicity we do not consider complex landmarks such as shadows, light direction etc. known to be used by real ants in the simulation. Our simulations run at about 30Hz on an Intel(R) Core(TM)2 Duo CPU 2.66GHz machine under openSUSE 10.3.

Table 2.2 shows the learned parameters of confidence in the individual landmarks, which corresponds to figure 2.13, C. The growing skewness of the distributions from left to right shows growing asymmetry in the distribution, indicating that the navigator increases confidence in some landmarks and decreases in some others.

Table 2.2: **Landmark stability learning experiment:** the table shows the ten landmarks available in memory, the angle and distance from each landmark to feeder, the segment relevance of the segment containing the landmark (r^{seg}) and the retention time (t^{ret}) of the memory sequence from which this landmark recalled.

Landmark	Distance	Angle	r^{seg}	t^{ret}
1	5.1	181.5	0.019569	10
2	2.5	220.3	0.09090	5
3	3.3	94.6	0.03333	3
4	1.1	144.4	0.04	4
5	2.4	124.6	0.06666	5
6	3.5	91.0	0.04348	6
7	3.5	55.9	0.05263	7
8	4.2	64.1	0.04762	1
9	5.7	44.1	0.05263	3
10	9.1	35.2	0.9	9

The segment retention time t^{ret} is the number of the latest foraging run in which the corresponding landmark was encountered, i.e. giving a high value to recent runs. The segment weight r^{seg} is initialized to 1. Note that landmark 1 was seen more recently than landmark 10, but as

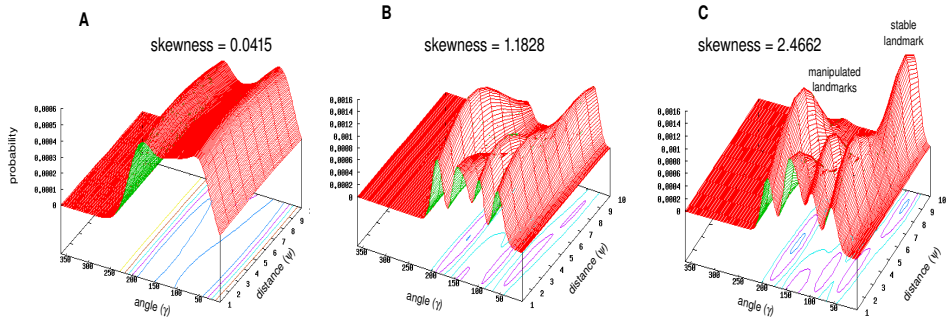

Figure 2.13: **Expectation reinforcement for learning stable landmarks: A)** Before the test runs (but after several foraging runs) *SyntheticAnt* has encountered all 10 landmarks, but has the same confidence in all of them. The observed variance is due to different LTM sequence acquisition times. **B)** After 5 test runs, during which 9 out of 10 landmarks were displaced, the probability distribution for the confidence changes. *C)* The confidence probability distribution after 10 test runs. The plot shows the computed home distances and angles (as a probability distribution) using individual landmarks using memory recall for each landmark. The indicated skewness values are the third central moments of sample values, divided by the cube of their standard deviations. The growing skewness from left to right indicates growing asymmetry in the distribution.

the segment weight of landmark 1 is very low it has low influence on the overall answer. As shown in figure 2.13, the confidence for stable landmarks is reinforced and is higher than instable landmarks; i.e. the forager learns the stability of the landmarks. In short, higher frequency of landmark position manipulations lead to lower segment weights, meaning lower confidence represented by higher covariances of Gaussians. The stable landmark has a greater influence than instable ones on the overall memory readout (higher probability). The forager thus learns the stability of the individual landmarks. Therefore higher frequency manipulations of landmarks are reflected directly in the joint probability distribution with lower probabilities. In short, the higher the search intensity the lower the confidence.

Given the above result, we now investigate how the *SyntheticAnt* can regain its confidence, once its expectation is violated. Expectation is violated when an expected landmark is missing or if a low confidence landmark is encountered. As described before, the *SyntheticAnt* falls into the Lévy search mode and the intensity of the search is higher if the landmark is missing. We evaluate how confidence is regained with time and how the search intensity influences (figure 2.14). The θ value indicates the search intensity ($\theta_3 > \theta_2 > \theta_1$). The results show that the confidence is regained with time, where high intensity searches allow to reach a higher confidence threshold in a shorter amount of time.

In figure 2.15**B)** the animal finds high discrepancy between its expectation and perception. This results in very low confidence and it performs correction maneuvers by going back towards the nest. The norms of the position density matrix, reflecting the task resolution times, for the real ant and the robot are shown in figure 2.16.

Given the above results, we predict that our model should behaviorally be similar to a real ant. This prediction is tested using real ants in the same landmark manipulation and restoration task. To perform the same landmark manipulation task, we first test the real ant and feed the recorded trajectory to the *SyntheticAnt*, so that both navigators have the same perceptual input. In further analysis, we define the *confidence* of the real ant or the *SyntheticAnt* in a landmark as inversely correlated with the com-

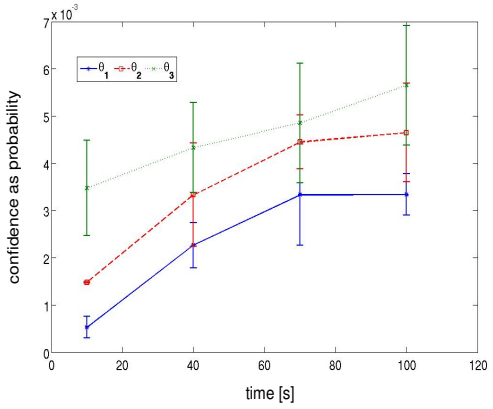

Figure 2.14: **Confidence recovery and search intensities:** The recovery of confidence with time (after initialization of the Lévy search) is indicated. High intensity searches (indicated by the θ values) reach a certain confidence threshold quicker. A high intensity Lévy search is initialized when a landmark is missing and a low intensity one is launched when a low confidence landmark is encountered ($\theta_3 > \theta_2 > \theta_1$).

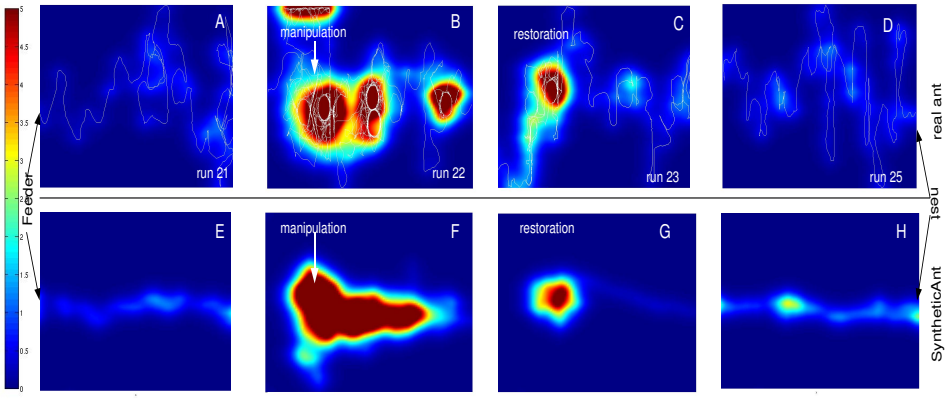

Figure 2.15: **Real ant benchmark:** The upper panel and lower panels show real and *Synthetic* ant data in the same landmark manipulation task. The ant performs 25 foraging runs from nest (located at the right end the arena) to the feeder (at the left end of the arena). The arena contains displaceable visual landmarks and also non-displaceable obstacles, both of which the ant cannot walk over. Trajectories are indicated by white lines. The density maps are computed from the trajectories; we define here density as inversely proportional to the *confidence* in the landmarks. **A)** Ant trajectory in the 21st foraging run. **B)** Ant trajectory in the 22nd run, where some landmarks were manipulated at the indicated positions. **C)** In the next run (23) all the visual landmarks are again placed in the positions as in runs 1 to 21. **D)** The density plot of trajectory after landmark restoration. The lower panel shows the performance of the *SyntheticAnt* in the same experiment. **E)** Before the manipulation, the *SyntheticAnt* has the same high confidence value in all landmarks and therefore does the traversal on almost a straight line. **F)** Upon manipulation, a high intensity Lévy search is initiated and propagated back home. **G)** Upon restoration, a low intensity search at the low confidence landmark is performed, as captured by the density plot. **H)** The confidence in the manipulated landmark recovers slowly as indicated by the density plot.

puted trajectory density. The ant is let to forage from feeder to nest for 21 runs, during which no landmark manipulations are made. The trajectory after several foraging runs shows low densities all over the arena, indicating high confidence of the animal in the visual landmarks. In the 22nd run, two landmarks are removed at the indicated position (figure 2.15B). The ant does a high intensity search and tracks back almost to its nest. The density plots indicate that the ant does not trust the landmarks in the area that violated its expectations in the the past (figure 2.15C). In the next run, the landmarks are again restored in the original constellation. Nevertheless, the ant does not *trust* these manipulated landmarks in the following runs, as indicated by the high densities around these landmarks. But after subsequent foraging runs in the restored arena the confidence of the animal in the landmarks increases again through expectation reinforcement, as indicated by the low densities throughout the arena , figure 2.15 D. Such behavior was prototypical of all four ants as shown in figure 2.16. In the following we discuss how this behavior of the ants can be explained by the proposed variant of the Lévy walk.

We compare the behavior of the real ant, with the behavior of the *SyntheticAnt* in the same task as above. The artificial forager switches to the above described random search using Lévy walk, when an expected landmark is not encountered (figure 2.15, F) or when a landmark with a very low confidence is encountered (figure 2.15, G). Our results show striking similarity in the behavior of the real and the *SyntheticAnt* in similar situations of landmark manipulation tasks. The task resolution time before and after manipulation shows the time taken by the forager to reach the feeder. This task resolution time is reflected in the norm of the position density plots. This is plotted in figure 2.16, the data of which was obtained from position tracking of 4 ants in landmark manipulation tasks. Both the real ants and the *SyntheticAnt* follow the same trend in the norm of the position density matrices, therefore also in the task resolution times. The norm rises in both cases when a landmark is manipulated, and falls again upon restoration of the landmark constellation. Baseline density before manipulation slowly reached as relearning progresses. We observed that ants track back to known terrain upon expectation violation. This behav-

ior is captured by our model using the proposed new variant of the Lévy walk. This new mechanism fits the context of expectation reinforcement, as it allows the navigator to track back to known terrain to test the validity of its expectations, while at the same time exploring new terrain.

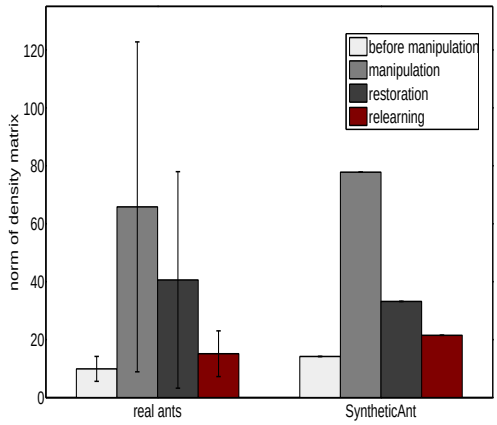

Figure 2.16: **Position density norms reflecting task resolution times:** Bars represent the norm of the position density matrices before, at and after manipulation of the landmarks (errors bars indicate standard deviation of norms). Data obtained from 4 ants in the described landmark manipulation tasks and from the SyntheticAnt simulation. 2.15.

2.3 On the necessity of top-down cognitive influence on perception

Our experiments with real ants [2] and our modeling work suggest that ants use forward models to solve complex tasks in dynamic unknown environments under limited resources constraints. Our initial simple navigational

[2] we thank Dr. Markus Knaden from the Max Planck Institute for Chemical Ecology in Jena, Germany for generously sharing the ant landmark manipulation experiment data

paradigm without a forward model had to be extended to be able to capture more complex ant behavior in dynamic environments. Our findings about the necessity of forward models for acting in dynamic environments are supported by numerous other earlier studies (see [120] for review). For example cockroaches executing a very rapid escape response need to know the current position of their legs in order to send the correct motor commands [24]. It has been suggested that proprioceptive feedback, even though very fast in invertebrates in general, might be too slow to realize such rapid reactions as the leg positions are very dynamic, suggesting the maintenance of predictions of the current limb positions based on previous motor output [24]. Moreover flying insects need to be very fast at distinguishing self-induced changes in the visual input (e.g. head movement) from externally imposed stimulation (e.g. movement induced by wind) in order to stabilize flight, suggesting the necessity of the existence of forward models to predict expected visual input from executed motor commands especially when acting in dynamic/turbulent environments [118]. Moving on from insects to higher order animals like mammals, the difference in brain size suggests the existence of higher order cognitive mechanisms, as they become highly necessary given the increased richness in the sensory and action spaces [106]. This inspired the phrasing of PASAR as an integrated bottom-up and top-down cognitive model for cognitive agents acting in highly dynamic environments, which allows us to study the different components of such an integrated cognitive mechanism.

Chapter 3

PASAR: AN INTEGRATED BOTTOM-UP AND TOP-DOWN MODEL FOR ACTING IN DYNAMIC UNCERTAIN ENVIRONMENTS

In the previous chapter we discussed the necessity of the existence of a forward model in a cognitive system for solving complex tasks in dynamic environments under limited resources constraints. In this chapter we elaborate our model which integrates bottom-up sensory input with high-level cognitive mechanisms and top-down influences on perception. Furthermore, we address the question of how the different subcomponents of such a cognitive system interplay to solve a given task.

After more than 50 years of robotics and cognitive sciences research, artificial systems have not yet achieved performance comparable to their biological counterparts, especially in complex tasks in dynamic environments. For this reason, the interest in understanding biological systems

for designing new generations of artificial sensori-motor systems has steadily been growing over the last decades. Nevertheless, even the basic notion of persistent knowledge representation, which is arguably at the very core of understanding human intelligence, is until today subject of heated debate [20, 21, 129]. Besides persistent knowledge representation, the biological brain (both in insects and mammals) employs many additional mechanisms like prediction, anticipation, sensation, attention and motor response to survive in dynamic and partially known environments [63, 40, 82]. In this context, building artificial sensori-motor systems has been the only benchmarkable way to test biologically based cognitive models and has played a key role in identifying the minimal and key mechanisms of cognition [91]. However, despite the fact that many cognitive architectures have been proposed over the past three decades, none of them account for the interplay between the key ingredients of cognition [65, 5, 67, 32, 33]. In other words, the individual quantitative contributions of some subcomponents of cognition - perception, anticipation, sensation and attention - to behavior in artificial and biological cognitive systems is largely unknown. For this reason we propose *Prediction-Anticipation-Sensation-Attention-Response (PASAR)*, a model of knowledge acquisition, representation and action selection for artificial autonomous systems. PASAR makes use of automated reasoning procedures involving anticipation of future stimuli and fusion of bottom-up and top-down information streams. The modular formulation of the PASAR architecture allows the dissection and evaluation of the contribution of its individual components. We demonstrate that PASAR can solve complex real-world and simulated robotic tasks. Our experimental results testing PASAR have strong implications on how prediction, anticipation, attention, sensation and motor response interplay. We show that a combined attentive, predictive and anticipatory system is clearly preferable to systems without those mechanisms when acting in dynamic environments under limited resources constraints. Nevertheless, we also find that attention, prediction and anticipation are only useful if the memory is transient (i.e. contains a forgetting mechanism). Beyond providing a framework to investigate the interplay of the subcomponents of cognition. Thus, PASAR

reveals itself as a very valuable tool for a systematic evaluation of the interplay between the above mentioned subcomponents of cognition in both biological and artificial cognitive systems.

3.1 Related Work

Immense efforts have been invested over the past two decades in discovering the brain mechanisms involved in the interplay between prediction, anticipation, sensation, attention and motor response [66]. Scrutinizing the highly hierarchichal structure of the brain has been a starting point for various studies investigating these subcomponents of cognition [108, 130]. Growing evidence from physiological research suggests that higher cortical areas of the brain are involved in a dialogue with lower areas (midbrain and superior colliculus) to solve low-level tasks, like the integration of multisensory information [101]. Recent neuroscientific and behavioral evidence also suggests that higher cortical areas of the brain modulates the incoming sensory data to fit expectations by actively searching for relevant information [82]. Some researchers even argue that the higher cortical areas are involved in predicting future stimuli based on past experience and subsequently anticipating sensory events in time and space when solving complex sensori-motor tasks [40]. In this context, bottom-up and top-down mechanisms are highly relevant and have long been demonstrated to be at work in biological cognitive systems [57, 87, 26]. In the domain of attention, influential bottom-up processing models [57] and more recently top-down models [87, 108] have been proposed. At the same time, some theories propose the emergence of attention from knowledge representation itself, suggesting the interplay between subsystems at different hierarchichal levels of the brain [19]. The potential neural correlates of the sub-systems responsible for multi-sensory integration and attention generation have been subject of extensive research in psychology and cognitive neuroscience [47, 89, 52]. The interdisciplinary research of cognitive brain and robotics research has profited hugely from the above findings about the the key hierarchical and

vertical mechanisms involved in biological cognition [125].

Based on such empirical (anatomical, physiological and behavioral) evidence that supports the notion of layered hierarchichal control systems, many interesting theories have been proposed until today to model a multi-layered framework of the brain, that has strong top-down and bottom-up information flows (see [91] for a review). Furthermore, many of those models have been also designed with the aim of building novel artificial systems. R.Brooks introduced the subsumption architecture as a distributed architecture for building autonomous systems capable of sustained activity in real-world environments [20]. The SOAR architecture is another example that has been under development since the 70s and that aims at explaining biological reasoning [65]. ACT-R is yet another family of cognitive architectures, concerned primarily with modeling human behavior [5]. Other approaches such as ICARUS use notions of hierarchical relationship between objects to achieve problem-solving behavior [67]. Others have proposed biologically based hierarchical cognitive architectures emphasizing the notion of embodied cognition and linguistic interaction [33] or action imitation based on hierarchical representations of perception and action [32]. Also in this context, the Distributed Adaptive Control (DAC) framework has been proposed to accommodate perceptual and behavioral learning in artificial systems in a single framework [113] (see [66] for a review). Nevertheless, to our knowledge none of the above (and other) cognitive models address the issue of investigating and quantifying the interplay of the minimal ingredients of cognition.

3.2 Research Question

We propose PASAR, a concise and modular framework for integrating prediction, anticipation, sensation, attention and response. PASAR builds on the DAC architecture for structuring perceptual and behavioral learning in three layers of control: reactive, adaptive and contextual [113, 111, 72] (see fig. 3.1). In our experiments in simulations and complex real-world robotic tasks, we address the question of how each sub-component

of PASAR contributes to the overall performance in the given task and what insights we can gain about robotic control and cognitive mechanisms in general. More concretely we investigate if a complete sensorimotor system with attentional, anticipatory and predictive mechanisms perform better than combinations of subsystems in complex tasks. Also we question the use of a memory decay mechanism (forgetting) and the use of higher level knowledge for modulating bottom-up sensory information, as observed in biological systems [102]. Furthermore, we want to gain deeper insights into the interplay of the different cognitive subsystems involved in solving complex tasks. We thereby also aim to provide new hypothesis about the functional organization of biological cognition and also invitations to perform specific physiological and psychophysical experiments to support our findings in biological systems.

3.3 The model and the components

The proposed PASAR model is embedded in the DAC framework and comprises of three layers of control: reactive, adaptive and contextual (see fig.3.1). This layered hierarchy of control has been shown earlier to be optimal for solving diverse robotic sequence learning tasks [113, 72]. The arrows in fig.3.1 indicate information flows. Data perception and the bottom-up saliency computation are indicated by the red arrow, all of which are contained in the reactive layer. The adaptive layer contains the data alignment and the data association mechanisms. Also, the bottom-up and top-down attentional saliencies are integrated in the adaptive layer. The contextual layer accomplishes higher-level knowledge acquisition in the world-model, the top-down attentional modulation of action generation (green arrow) and the anticipatory bias in data association (blue arrow). The individual components are elaborated in the following subsections.

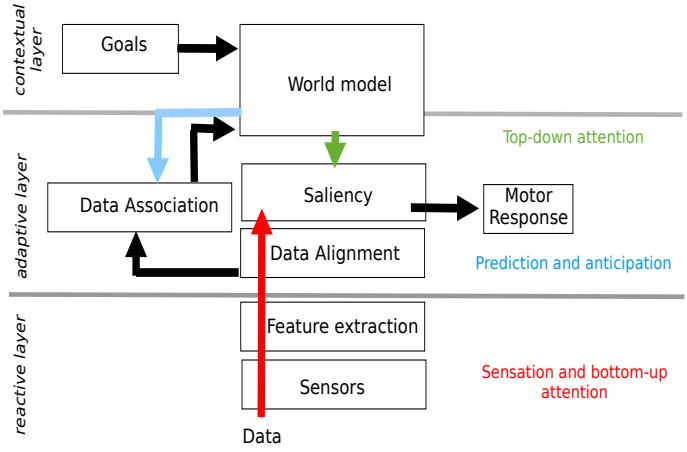

Figure 3.1: **PASAR** proposes a three-layered distributed architecture: reactive, adaptive and contextual (as in [113]). The reactive layer contains the physical *sensors* and the *feature extraction* mechanisms. The adaptive layer contains the *data alignment*, the *data association* and *saliency* computation mechanisms. The contextual layer contains the *world-model* and the *goals* of the system. The arrows indicate information flow, and the colored arrows indicate sensation and bottom-up attention (red), prediction and anticipation (blue) and top-down attention (green). The *motor response* is a result of the integration of the bottom-up and top-down saliency maps.

3.3.1 World Model

The *world-model* of the contextual layer contains all the high-level knowledge about the external world, acting as a memory mechanism (fig.3.1). This memory is organized in terms of individual memory items, further referred to as *concepts*. *Concepts* are defined as vectors in a high dimensional space, where the artificial sensori-motor system acts in a complex world using multimodal sensors for perception. The *world-model* is seen as a mechanism for acquiring and maintaining knowledge about different *concepts* either provided by bottom-up multimodal sensory signals or even by long-term-memory retrieval. The covariances of concepts represent the spatio-temporal precision of the acquired knowledge, which is computed from the prediction errors of the model for the *concepts*. On the one hand, *concepts* are *transient* as they are forgotten with the passage of time, where we define *forgetting* as a linear growth function of the covariance of the *concepts*. On the other hand the covariance of the *concepts* vary, depending on the spatial (in)congruence (spatially congruent stimuli simply means stimuli perceived at the same position in space) of the incoming sensory data and the predictions of the same, representing the spatial certainty of the *concepts*. A schema of perception/sensation of the world and the representation of the *concepts* with their covariances are depicted in figure 3.2. The generation of attention from such a world-model is discussed in the forthcoming subsections.

3.3.2 Prediction, Anticipation and Sensation

Given the above *world-model* with *concepts* and their covariances, we discuss here how predictions of future stimuli and anticipations are computed. *Prediction* refers to the mechanism of prognosing future stimuli based on recently perceived stimuli related to a *concept*. Harnessing such predictions, sensory stimuli *associated* to *concepts* can be *anticipated* in a spatio-temporally constrained region. In this sense, multimodal perception/sensation therefore involves prediction, subsequent anticipation and finally data association. To model these processes we use the Joint Probabilistic Data Association (JPDA) method [10]. JPDA is a powerful tool

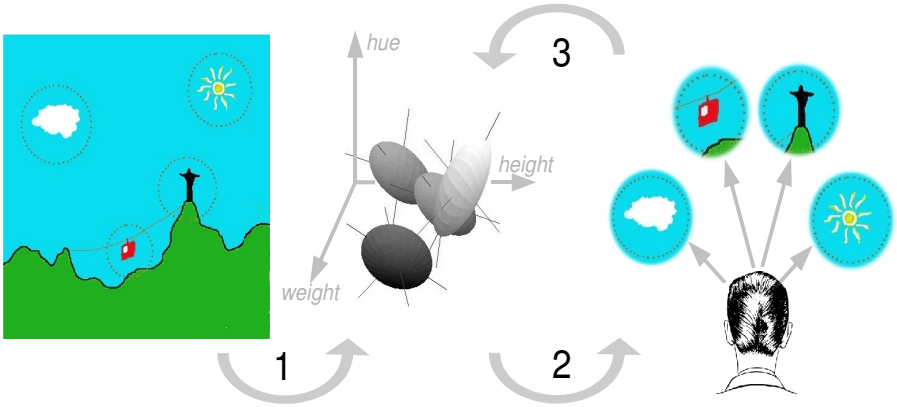

Figure 3.2: Schematic of *world-model* and selective attention generation for a dynamic scenario. **Left panel:** A dynamic scene as perceived by an autonomous system. Four encircled objects are perceived as closed entities by the autonomous system. **Middle Panel:** Four *concepts* (memory representation of real-world objects) in $n = 3$ feature space with *hue*, *weight* and *height* as example features. The ellipsoids represent the covariance of the *concepts*. **Right Panel:** The top-down attention mechanism initiates an action that might have an immediate effect on the world model (arrow 3) as the sensory input is changed by the performed action.

for solving data association problems, which arise in many applications such as computer vision, surveillance, mobile robotics etc. The JPDA algorithm uses the notion of a validation gate to restrict the association of data to targets. JPDA is applicable to non-linear filters and our results can be easily generalized [10]. In the following, each *concept* is a well defined multidimensional vector of sensory data in a high dimensional space, that depends on the type of the multimodal sensory input of the system. Let $\mathcal{K}$ be the number of *concepts* in memory. The state dynamics of *concept* k (x^k) is modeled as

$$x_{t+1}^k = A_t^k x_t^k + \psi_t^p \tag{3.1}$$

for $t = 1, 2, ...$ where $x_t^k \in \mathbb{R}^{n_x}$ is the state of *concept* k at time t. ψ_t^p is process noise with covariance matrix Q. A_t^k is the state transition matrix of *concept* k at time t. Let $y_t^j \in \mathbb{R}^{n_y}$ be the j-th observation at time t for $j = 1, ..., n_t$. The measurement model is

$$y_t^j = H x_t^j + \phi_m \tag{3.2}$$

where ϕ_m is a white Gaussian measurement error with covariance R_k and H the measurement matrix. Given this Gaussian noise model and assuming linear dynamic and measurement models, we use a Kalman filter for state approximation of *concepts* [59]. In this sense, the Kalman filter is an iterative mechanism that allows us to make predictions of future sensory input as well as to use the sensory input to correct the state of the world-model.

Using a priori knowledge about the world (e.g. state transition matrix, process noise and measurement matrix in the case of the Kalman filter) and the current state of the world-model, a prediction is made for each *concept*. At timestep t, for each *concept* k, we compute the state prediction $\tilde{x}_t^k$, its covariance $\tilde{P}_t^k$ and the measurement prediction $\tilde{y}_t^k$ as follows

$$\tilde{x}_t^k = A\hat{x}_{t-1}^k \tag{3.3}$$

$$\tilde{P}_t^k = A\hat{P}_{t-1}^k A^T + Q_{t-1}^k \tag{3.4}$$

$$\tilde{y}_t^k = H\tilde{x}_t^k \tag{3.5}$$

Anticipation refers to harnessing the prediction to expect stimuli in a spatio-temporally constrained region of the feature space for the given *concepts*. Given the computed measurement prediction for *concept* k, we now compute an anticipatory field (validation gate) for the same *concept*. For each observation j the Kalman innovation (i.e. the prediction error computed as the difference between the prediction and the actual stimulus) and its covariance (for details see [59]) with respect to a *concept* k are:

$$v_{jk} = y_t^j - \hat{y}_t^k \tag{3.6}$$

$$S_{jk} = H\tilde{P}_t^k H^T + R_k \tag{3.7}$$

An anticipatory field, or validation gate, is defined for each *concept* as follows:

$$v_{jk}^T S_{jk}^{-1} v_{jk} < \epsilon \tag{3.8}$$

Since the weighted norm of the innovation that defines the validation gate is chi-square distributed with the number of degrees of freedom equal to the dimensionality of the measurement, the threshold ϵ is obtained from the tables of a chi-square distribution, as described in [10]. The size of the obtained anticipatory field can be modulated by higher-level mechanisms by varying this threshold. A validation gate for each *concept* dimension is computed earlier using the Kalman innovation of new observations as in [10].

We define *sensation* as the state estimation of *concept* k, using the given sensory input, prediction and anticipation. Given multiple *concepts* and multiple stimuli the problem of data association (see figure 3.1) naturally arises [10]. For each *concept*, only observations inside its validation gate are associated to it. The JPDA algorithm enumerates all possible associations between observations and *concepts* at each time step. The association probability β_{jk} stands for the probability that the j-th observation originated from the k-th *concept*. The *concept* state is estimated by Kalman filter and this conditional expectation of the state is weighted by

the association probability. Let x_t^k indicate the state of *concept* k at time step t, ω_{jk} the association event where the observation j is associated to *concept* k and $Y_{1:t}$ stands for all the observations from time step 1 to time step t. Then the state of the *concept* can be estimated as

$$E(x_t^k|Y_{1:t}) = \sum_{\omega} E(x_t^k|\omega, Y_{1:t})P(\omega|Y_{1:t}) \tag{3.9}$$

$$= \sum_{j} E(x_t^k|\omega_{jk}, Y_{1:t})P(\omega_{jk}|Y_{1:t}) \tag{3.10}$$

where ω_{jk} denotes the association event when the observation j is associated to *concept* k and ω_{0k} denotes the event that no observation is associated to *concept* k. Therefore the event association probability β_{jk} is

$$\beta_{jk} = P(\omega_{jk}|Y_{1:t}) \tag{3.11}$$

The computation of β_{jk} requires a summation over the posteriors and its exact calculation is NP-hard [30]. We implemented a Markov Chain Monte Carlo (MCMC) method to compute β_{jk} in polynomial time similar to the proposal in [83][1].

Time dependent forgetting is achieved by linearly growing the covariance of the represented concepts with the passage of time. This allows to remove the representation of concepts in memory if they are not updated by associations to novel stimuli, similar to the rehearsal-decay paradigm for memory [8]. In short, the *world-model* acts as a memory mechanism containing *concepts*. The *prediction*, *anticipation* and *sensation* mechanisms act on *concepts* in the *world-model*. Next we discuss the integration of top-down and bottom-up *attention* into the same framework.

3.3.3 Top-Down and Bottom-Up Attention

Having elaborated on the generation of *world-model* containing the *concepts*, the data association, prediction and attention mechanisms, we now

[1] see details of the MCMC implementation in appendix section 7.1

move on to attention. We aim to phrase attention in terms of bottom-up and top-down processes as employed by the brain [57]. Recent psychophysiological research suggests that selective attention is load-dependent [89]. Artificial systems with limited and/or shared resources could benefit from such a load-dependent protocol. Our architecture makes use of a load-dependent push-pull mechanism, by means of a competition between distinct feature saliencies of *concepts*, the winner of which decides which actions or sensory events the system decides to dedicate its resources to. In PASAR, low level feature filters extract relevant features of incoming multimodal stimuli. For vision, a number of feature filters like color, orientation, luminance etc. are implemented. The combination of these filter outputs give rise to a bottom-up saliency map based on the Itti and Koch model [57]. At the same time, top-down attention is triggered by similarity interference, i.e. when similarity between memory *concepts* is the major memory impairing factor of identification, similar to some earlier proposals [80]. Similarity interference between *concepts* is measured using the Mahanalobis distance between the *concepts* [68]. Top-down and bottom-up saliency maps are combined and a winner-take-all (WTA) neural network computes the most salient attentional *spotlight*, which is then used to trigger an action (figure 3.3). See also [71] for more details.

3.3.4 Sensory Data Alignment

As seen in figure 3.1, the adaptive layer also contains the data alignment mechanism. Such aligned maps of multimodal sensors have long been discovered in the superior colliculus of the brain [102]. The superior colliculus, which has top-down connections from higher cortical areas, is considered as the primary domicile of sensory data association and appropriate motor action generation in animals [102]. It has been shown that the superior colliculus contains a *sensory map* for each sensor, on which the whole sensory space is represented on [58]. Biological systems have been shown to be capable of (re)learning such sensory representations using the representation of another sensory modality as the refer-

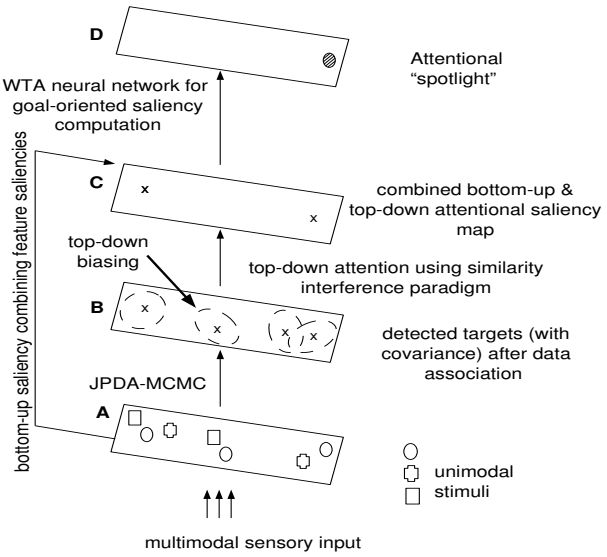

Figure 3.3: **Saliency computation from multimodal sensory input:** The multimodal sensory input **(A)** is associated to existing targets by means of the anticipatory fields of JPDA **(B)**. The top-down biasing of the anticipatory fields using the world-model is applied before data association. The bottom-up and top-down saliency maps are combined using a common neural group onto which both the above saliencies are mapped **(C)**. A winner-take-all WTA neural network computes a single winner from this map **(D)** and an appropriate action is triggered.

ence whenever one of the modalities is perturbed [126, 62]. Analogously the PASAR adaptive layer uses top-down information to learn sensory map alignments as shown in figure 3.1. PASAR is transparent to the specific learning mechanism itself, and we have demonstrated the capability of PASAR using two different learning paradigms, asymmetric Hebbian learning and Levenberg-Marquardt [2], which is an iterative error reduction algorithm.

[2] see appendix section 7.2 for implementation details

3.3.5 Motor Response

Until now, we have discussed the mechanisms of *world-model*, *prediction*, *anticipation*, *sensation* and *attention* in the PASAR framework. However, to act in a dynamic world, the sensori-motor system needs to perform motor responses (fig.3.1). To choose the optimal motor response we consider the general problem of an efficient energy consumption strategy [14]. In this formulation, the artificial autonomous system has to optimize the *utility* of its actions while at the same time minimize its limited energy consumption. As the utilities of future actions are a priori not known, predictions of the same are necessary. Here we formulate this in the context of a Bayesian framework based on transient memory, prediction and attention.

In this framework, the *attentional saliency* of a *concept* is defined as the perceived relevance of the stimuli associated to this *concept*. Note that although this is a simplification that reduces all forms of attention into a single variable, it allows for testing the contribution of attention to overall performance in a well-defined testbed. We assume that the *utility* of an action is predefined for a given task. E.g. in our multi-robot testbed the utility of a *concept* is defined as inversely proportional to the perceived charge of the robot (i.e. high utility for a low charge robot and vice versa). PASAR computes the predicted utility distribution of actions from the individual utilities of single *concepts*. We write Θ_s^t for utility of a certain *concept* s at time t, and for computing the utility distribution, we are interested in the following conditional probability distribution defined as the predicted utility:

$$\text{Predicted utility of concept} = P(\Theta_s^t | F_s^t(\Theta_s^{t-1}) A_t(s)) \tag{3.12}$$

where $F_s^t(\Theta_s^{t-1})$ and $A_t(s)$ are two time-dependent functions that weight the *concept* s. For example, $F_s^t(\Theta_s^{t-1})$ evaluates the temporal weight of the *concept*: if there is at least one stimulus associated to this *concept* currently, it has the highest temporal weight and decays linearly otherwise. Such a mechanism allows for a simple time-dependent forgetting. $A_t(s)$ evaluates the attentional saliency of this *concept* proportional to

the perceived utility of the *concept*. By computing the joint distribution of the predicted utility probabilities for all *concepts*, the system can perform the action with the highest predicted utility.We elaborate the update mechanism of this predicted utility distribution. Lets assume that we can compute predicted utility probabilities of individual *concepts* as shown in eq. 3.12. Given these individual *concept* utilities, we are interested in the total predicted utility distribution:

$$\text{Predicted total utility} = P(\Theta^t | F^t(\Theta^{t-1}) A_t) \tag{3.13}$$

We express this probability as the normalized sum of probabilities of individual utilities:

$$P(\Theta^t | F^t(\Theta^{t-1}) A_t) = \sum_s P(s) P(\Theta^t_s | F^t_s(\Theta^{t-1}_s) A_t(s) S) \tag{3.14}$$

where the random variable $S \in 1...n$, n being the number of *concepts* and $P(s)$ indicates the probability of the utility of this *concept*. Normalization is straightforward as $P(s)$ is uniformly distributed over all *concepts*. PASAR then either selects the action of maximum utility or draws from this distribution, where the former can be seen as *exploitation* of the world-model and the latter as *exploration*. We are therefore interested in the following probability distribution of actions:

$$P(Action | F^t_s(\Theta^{t-1}_s) A^t(s)) \tag{3.15}$$

This probability distribution can be computed using Bayesian inference, given a priori information about the environment PASAR is acting in.

The formalizations in this section allows us to test the contributions of the individual components of PASAR to the overall performance of the system. In summary, we have elaborated on how an optimal motor response is chosen by the system using a prediction, anticipation, sensation, attention and memory decay. In the next section, we define our experimental setup, with which we want to quantify the contribution of each of the above sub-components to the overall system performance.

Chapter 4

TESTING PASAR: CONTROLLING ARTEFACTS IN REAL-WORLD DYNAMIC ENVIRONMENTS

In the above sections we have elaborated on the PASAR model and how the different sub-components (prediction, anticipation, sensation, attention and response) are formalized. Here we discuss a rescue robot simulation and real-world robotic testbeds, which we use to evaluate PASAR's performance and the contribution and interplay of its sub-components. The real-world robotic testbed is a multi-modal multi-person mixed reality space named the eXperience Induction Machine (XIM) that allows extensive testing of PASAR for learning multi-model sensory map alignments, dynamic update of the world-model for solving the multi-person tracking task using bottom-up sensory information and top-down information for controlling active sensors. In the rescue robot simulation testbed we test PASAR's performance in exploiting the world model knowledge to solve a multi-goal task under limited resources constraints in a partially known world.

4.1 eXperience Induction Machine (XIM)

XIM is a physical space, which is part of the Persistent Virtual Community (PVC) where groups of real, remote and synthetic characters interact with each other [18]. XIM comprises a pressure sensitive floor, overhead, infrared and controllable pan-tilt color cameras, moving lights, triplets of microphones for sound recognition and localization, projection screens, and also ambient and spatialized sonification. On the projection screens the virtual world of PVC is made visible to the real visitors of XIM. XIM is about 25 square meters and allows several humans to be active in it simultaneously (fig.4.1). XIM, as an artificial autonomous entity, is a suitable testbed for PASAR as it comprises of multimodal sensors and effectors in a scalable and controlled environment for solving complex collective mixed reality interaction tasks (fig.4.2). The accurate tracking of real objects in the XIM physical space is a requirement for meaningful interaction scenarios among the different types of users. PASAR is tested in XIM for solving this task.

We use the IQR system for distributed large-scale real-time real-world neuronal simulations of the winner-take-all network of the attention system for driving the movable pantilt cameras in XIM [17]. For image processing we used the OpenCV library [1], and for the human torso detection in the mixed reality space testbed we used the OpenCV Haar classifier method [115]. The PASAR implementation for the mixed reality testbed runs 7 applications developed in C++ on 3 Intel(R) Core(TM)2 Duo CPU 2.66GHz machines with the GNU/Linux Suse10.3 operating system, which communicate with each other using UDP sockets.

4.2 Rescue Robot Simulation

In this testbed we consider the following multi-robot scenario: N robots are on a common mission in a given environment. The individual robots move around in a given common field solving a given task (e.g. demining). One of the robots, named PASAR, has the specific task of rescueing expired (out of charge) robots. For this PASAR first has to localize the

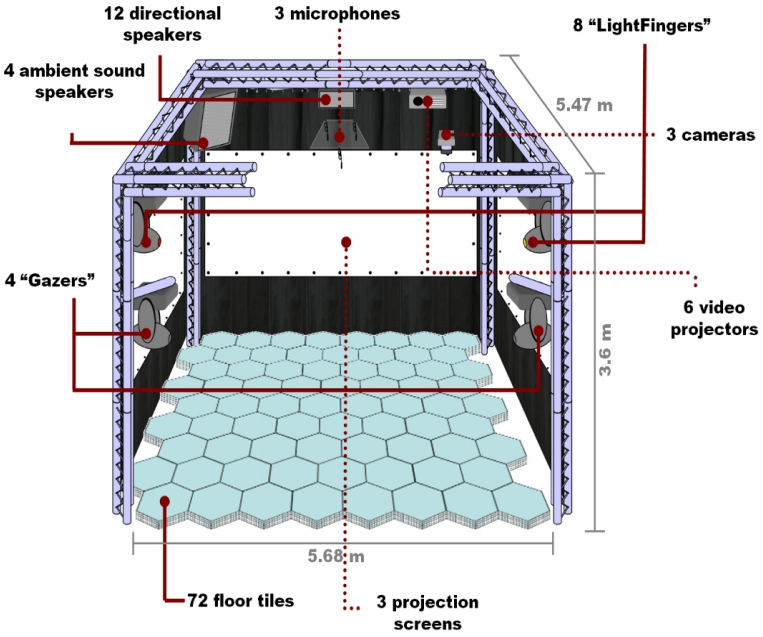

Figure 4.1: **The eXperience Induction Machine (XIM)** can be considered as an artificial organism in the shape of an environment, that has its own goals and expresses its own internal states. It comprises a pressure sensitive floor, overhead and pan-tilt cameras (gazers), movable lights (light-fingers), triplets of microphones for sound recognition and localization, projection screens and ambient and directional sound output (adapted from [70]).

Figure 4.2: **XIM Multiuser Interaction Scenario:** Multiple real users interacting with each other in a mixed reality Pong game, which is one of the scenarios used to evaluated PASAR performance. Also remote users take part in the same interaction by logging in from remote machines into the virtual world and they are represented by avatars on the projection screens (adapted from [55]).

expired robots using its sensors and approach them and recharge them so that they can continue on their missions. PASAR is equipped with a limited number of distance measurement sensors like sonar and laser range scanners, that are used to scan the environment and localize the robots to recharge. We simplify all these sensors in the form of a circular *perceptive field* around PASAR, inside which it perceives its co-robots. From time to time, PASAR has to return to the base station to recharge itself. We implemented this testbed in a simulation with $N = 10$ robots (figure 4.3). *Concepts* in this testbed are the robots involved in the common mission.

4.3 Data Collection

Given the PASAR model and the testbeds, here we discuss the data we collect in the two testbeds. For the Bayesian inference computations we used the ProBT Bayesian library [2]. The simulation runs on a single Intel(R) Core(TM)2 Duo CPU 2.66GHz machine with the GNU/Linux Suse10.3 operating system.

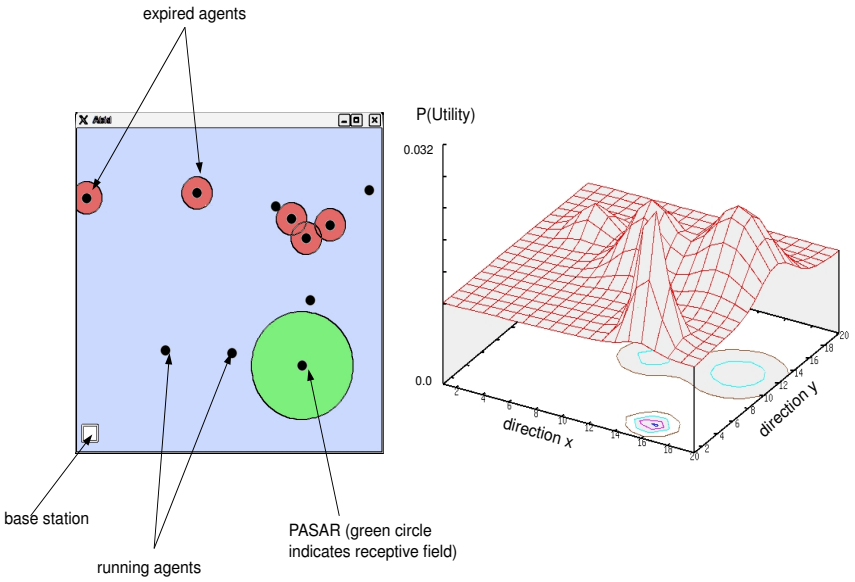

Figure 4.3: **PASAR multi-robot rescue scenario. Left** Snapshot from PASAR Experiment: The bigger circle surrounding PASAR shows sensory range. Everything outside this range is not perceived by PASAR. The smaller circles surrounding some of the agents indicate that the corresponding agents are expired. The base station, where PASAR recharges itself, is indicated by the rectangle on the left bottom. **Right** Example of the predicted total utility as a probability distribution. PASAR either goes to the location with the highest probability (exploitation phase) or draws form this distribution (exploration phase).

4.3.1 XIM

In this testbed, learning sensory map alignment, creation and maintenance of a world-model under limited resources constraints when acting in an unknown environment and attentional mechanisms for active information acquisition are tested. All the above problems are addressed in the context of solving the multi-person tracking problem under limited resources constraints.

The sensory map alignment of the overhead camera and floor modalities are learned online using the sensory input provided by a single person walking in XIM[1]. For evaluating the construction and maintenance of a world-model we look at the problem of multi-person tracking. Tactile floor tiles and overhead infrared cameras are the sensors used for this. A *concept* here is a single human in XIM. We use a 8-dimensional space for the *concepts* containing the x-y positions, x-y velocities, x-y accelerations, hue of the outfit and weight. To test the precision of the world-model during interactions involving different difficulty levels of tracking, a number of experiments are performed[2]. Bottom-up and top-down attention for action generation is tested using the controllable pan-tilt cameras for collecting hue information about tracked persons. Using this active recruitment mechanism we analyze ID maintenence in four different interaction scenarios[3]. To evaluate the scalability of the system, we also implemented a simulation of the XIM environment to test PASAR in the above tasks, for a much higher number of persons than was possible in the real setup.

4.3.2 Rescue Robot Simulation

PASAR is tested in a multi-robot simulation for optimal usage of the acquired world-model for multiple goal decision making. This testbed, in contrast to the previous one, allows for testing how to capitalize on the existence of such a world-model for generating optimal actions in a partially observable world. In particular, we will use this second testbed for evaluating the contributions of the individual components of PASAR to the overall performance.

In this context, the *attentional saliency* of a *concept* is defined as perceived utility of the stimuli associated to this *concept*, where a *concept* is defined as a robot in involved in the scenario. I.e. the *attentional saliency* is defined to be proportional to the detected remaining power of a *concept*,

[1] see appendix section 7.2 for details on sensory map alignment learning

[2] see appendix section 7.4 for details on multi-person tracking experiment in XIM

[3] see appendix section 7.5 for details on attention trigger in XIM

giving a high utility for reapproaching nearly expired *concepts*. PASAR computes the predicted utility distribution of actions from the individual utilities of single *concepts*. Performance is measured by the total expiry time in seconds of the robots. I.e. the lower this value, the better the performance. For each test case 100 trials were performed. Each trial lasted 160 seconds. The expiry time of the normal robots was 30 seconds and that of the PASAR rescue robot was 60 seconds. Solving this multiple goal task involves goal-driven selective attention generation for attending to the most vital subtask at the moment and maintaining a dynamic transient world model, which is used to compute the optimal action in the Bayesian sense. We formulated an optimal Bayesian decision making method for generating actions based on the world-model. PASAR computes the predicted utility distribution of going to a certain point (x, y) from the individual utilities of the *concepts*[4].

In order to evaluate the contributions of prediction, attention and memory decay, we perform the following experiments. First we evaluate the performance of the whole system using the complete PASAR framework for the robot rescue task (*COMPLETE*). Note that for this case we use the optimal memory decay rate, as discussed in section 4.2, and an adaptive exploratory behavior of PASAR. The optimal memory decay rate is set to be the memory decay for which the highest performance was observed for the *COMPLETE* test case (value 13, see figure 4.11). With adaptive exploratory behavior, we mean that PASAR drew from the predicted utility distribution much more often at the beginning of the run, than towards the end. This allowed PASAR to explore the world at the beginning, when the world-model did not contain any *concepts*, and to exploit this acquired knowledge more towards the end of the run. This behavior is achieved simply by making the draw probability a linear function of time, in a negatively correlated fashion. Next we evaluate the performance of the system without the use of attention, i.e. we set the attentional saliency of all perceived *concepts* to be the same (*NO-ATT*). Further we evaluate the performance of the system without memory decay and without

[4]for the elaboration of how the general PASAR equations 3.12, 3.13 and 3.14 are applied to the multi-robot testbed, see appendix section 7.3

attention (*NO-DECAY-NO-ATT*). We also test the case without memory decay, but with attention (*NO-DECAY-ATT*). Finally we evaluate the performance of the system also when not using the utility predictions of the world-model. I.e. the rescue robot randomly wanders around the arena to find and recharge expired robots (*RAND*).

4.4 Data Analysis

For all offline analysis we used Matlab(R) (2007a, The MathWorks). For multiple error comparisons we use Tukey-Cramer multiple comparison method $p < 0.05$. The hue bin comparisons were done using the student's t-test $p < 0.05$. For the Bayesian inference computations and analysis we used the ProBT Bayesian library [2].

4.5 Results

4.5.1 Mixed Reality Space XIM Testbed

In the XIM mixed reality space testbed, we test the online learning of sensory maps, use of high level knowledge for world-model maintenence, the use of attentional resources for triggering motor commands for active information acquisition and the use of the same for correction of the world-model.

First, we consider sensory map learning using PASAR adaptive layer. The tactile floor delivers low resolution but precise position data and therefore is used as the reference for aligning the higher resolution sensory map of the overhead infrared tracking camera placed arbitrarily in XIM. The procedure for this learning consists of a person walking freely in XIM while the tactile floor and the overhead infrared camera tracking data are used by the PASAR adaptive layer. See section 4.3.1 for details of data collection. This procedure drastically reduces the camera perspective and distortive errors (from 75 to 26 cms) in the overhead camera tracking (figure 4.4 A,B, Tukey-Cramer multiple comparison, $p < 0.05$).

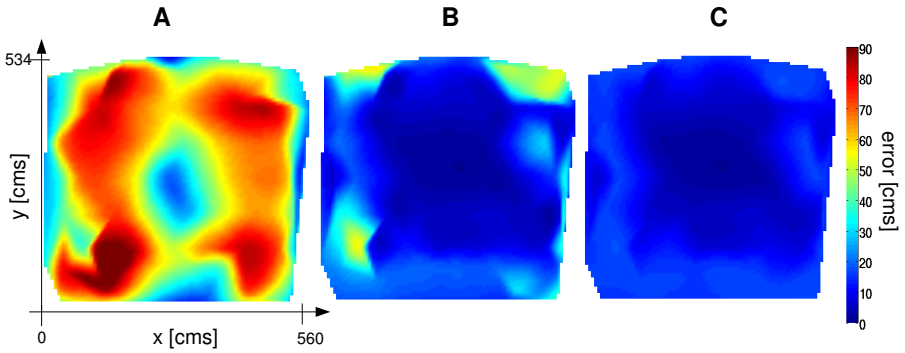

Figure 4.4: **Sensory Map Learning Using PASAR Adaptive Layer: A** shows the error map in [cms] for the overhead infrared camera tracking before learning (mean 75 cms). High errors are due to camera perspective and distortive errors. **B** shows the error after online learning with a single user in XIM (mean 26 cms). **C** The validation gates of the *concepts* (i.e. the tracked persons) for the tactile floor modality are made larger along the periphery of the space. Using this top-down bias in PASAR improves the tracking error significantly (mean 14 cms). The error distributions decrease significantly from A to B to C (Tukey-Cramer multiple comparison, $p < 0.05$)

After this initial learning, the overhead camera tracking still has relatively high error along the periphery of the tracked area (mean error 26 cms, figure 4.4 B). The PASAR contextual layer fuses the multimodal data taking into account prior knowledge such as that the tactile floor data is more reliable along the periphery of the space and uses this to modulate the validation gate of the floor modality accordingly (the larger the validation gate, the more reliable the modality). This gives less than 15cms tracking position error (Tukey-Cramer multiple comparison, $p < 0.05$)(figure 4.4 C). This demonstrates the use of top-down attentional bias using the validation gate thresholds (see equation 3.8).

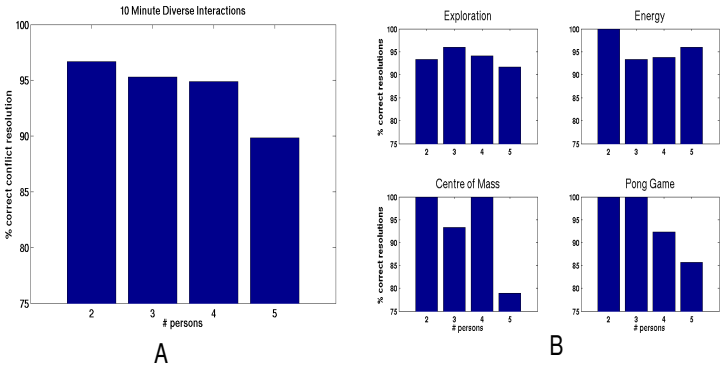

Figure 4.5: **PASAR for multimodal multitarget tracking: A** shows correctness of ID resolution in cluttered situations of tracking with 2 to 5 persons freely interacting in XIM. **B** shows ID resolution accuracy for different interaction scenarios (see text for further details).

We consider the complex problem of multi-person tracking in XIM using the passive and active sensors available in XIM. We evaluate the tracking performance of PASAR under different tracking difficulty levels where multiple persons interact simultaneously in XIM.The PASAR world-model thereby contains the high dimensional information about the tracked humans. To test the precision of the world-model during interactions involving different difficulty levels of tracking, a number of experiments are performed. ID maintenence is analyzed for four different

interaction scenarios: *exploration, energy, center of mass, pong game*. The results in the four different scenarios show high precision of the world-model even for challenging tracking conditions involving occlusions, clutter and high movement speed (about 88% correct ID resolutions in average for 5 persons) (fig.4.5). To evaluate this with a high number of tracked objects, we use a simulation of the XIM persons and use PASAR for tracking. The performance falls with the number of tracked persons as expected for upto 20 persons. For each number of persons, we perform 20 trials. The computed mean and standard deviation are depicted in fig.4.6.

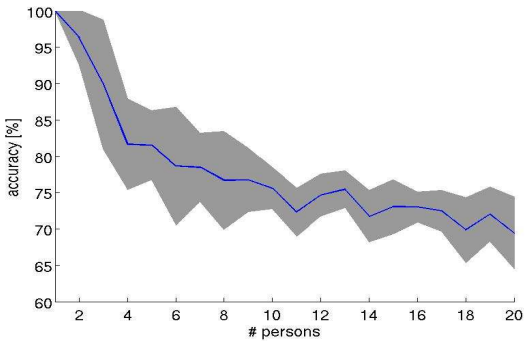

Figure 4.6: **PASAR for multimodal multitarget tracking:** ID resolution performance percentage as a function of the number of objects tracked in XIM simulation.

In the context of multi-person tracking in XIM, we now look at top-down modulation of incoming bottom-up sensory data to achieve a higher tracking performance. The idea of using a priori information is to be able to modulate the association probabilities of sensory data to tracked persons using a priori information about the world. We use the a priori knowledge that spatio-temporal proximity of multimodal sensory data should mean the same origin. Therefore, we give more weight to unimodal data, that is spatio-temporally correlated with data of other modalities. Here the camera data that is proximal to floor data in space and time is weighted more, i.e. the association probabilities of such data *concepts*

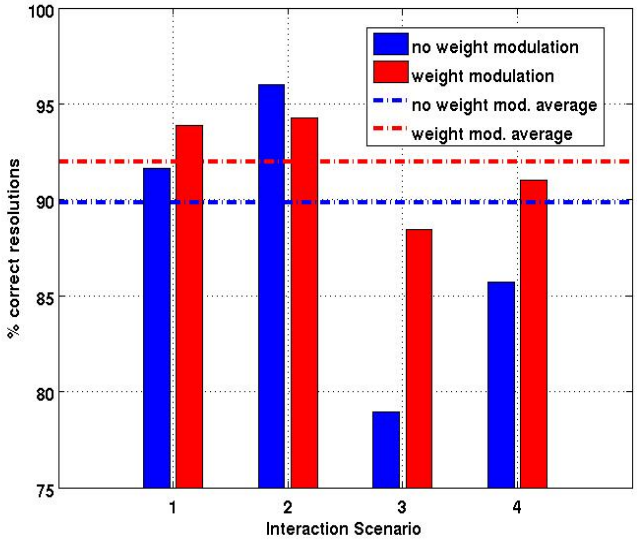

Figure 4.7: **Usage of a priori knowledge: spatiotemporal congruence of multimodal data in XIM** Multimodal data that is proximal to data of another modality in space and time has an added weight. The scenario numbers 1,2,3,4 refer to the interaction scenarios *exploration, energy, center of mass, pong game* respectively.

are higher. Using this method improves the ID resolution in all interaction scenarios and this strongly supports the usefulness top-down modulation of sensory data for enhancing data association performance(fig.4.7).

Given the above mentioned usage of top-down weighting of sensory data, we now investigate the change in tracking performance. The performance falls with the number of simulated persons as expected (fig.4.8). Nevertheless, the performance is significantly higher than when not using the a priori knowledge for upto 12 persons (Tukey-Cramer, $p < 0.05$). This speaks for the relevance of using higher level knowledge to modulate the incoming sensory data in the context of multi-person tracking in XIM.

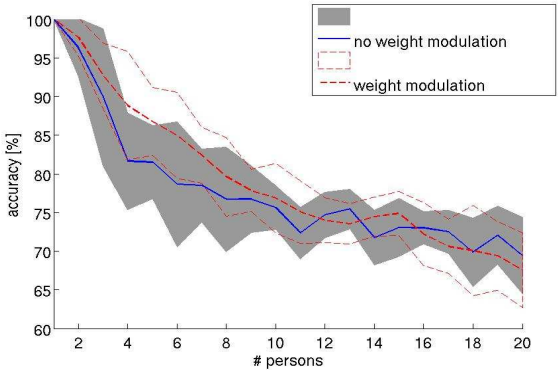

Figure 4.8: **Usage of a priori knowledge: spatiotemporal congruence of multimodal data in simulation:** The accuracy of ID resolutions in percentage is depicted as a function of the number of tracked objects in a simulation of the XIM tracking scenario. The accuracy when using the a priori knowledge to weight modulate data and when not using it is shown.

PASAR's just-in-time attention trigger allows to drive the pan-tilt cameras, which is a limited resource, to make them follow moving persons in XIM and extract hue information at the right moment (fig.4.9). The top-down attention for such deployment of movable cameras and moving lights is triggered as discussed in the section 4.3.1, using the similarity interference paradigm. Sample images from the four moving cameras for two subjects in XIM are depicted in figure 4.9. We evaluated the similarity of the computed mean hue for two different subjects. The computed hue bin means were significantly different (student's t-test, $p < 0.05$)(fig.4.10).

Although hue extraction is a simple feature extraction method, it serves as a proof of concept for motor action generation from attention. By actively collecting hue information of subjects in the space, their IDs can be corrected. Latency for the recuperation of IDs after an ID confusion, using this attentional deployment of the controllable pan-tilts are shown in figure 4.10 for two subjects acting in the space simultaneously for 10 minutes. Mean time for ID recuperations is 17 seconds after confusion.

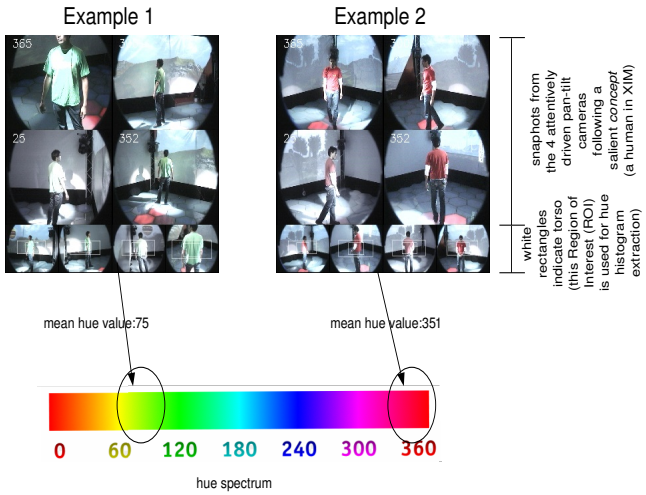

Figure 4.9: **Attention-guided feature extraction under noise and limited resources constraints:** PASAR attention system follows subjects in XIM and hue extraction from torsos. Two such attempts are shown, one for green and one red. The snapshots are from a moving camera image and the bottom indicates the images used for hue extraction. The Region-of-Interests (ROIs) of the images used to extract the hues are indicated by the white rectangular boxes in the smaller images at the bottom.

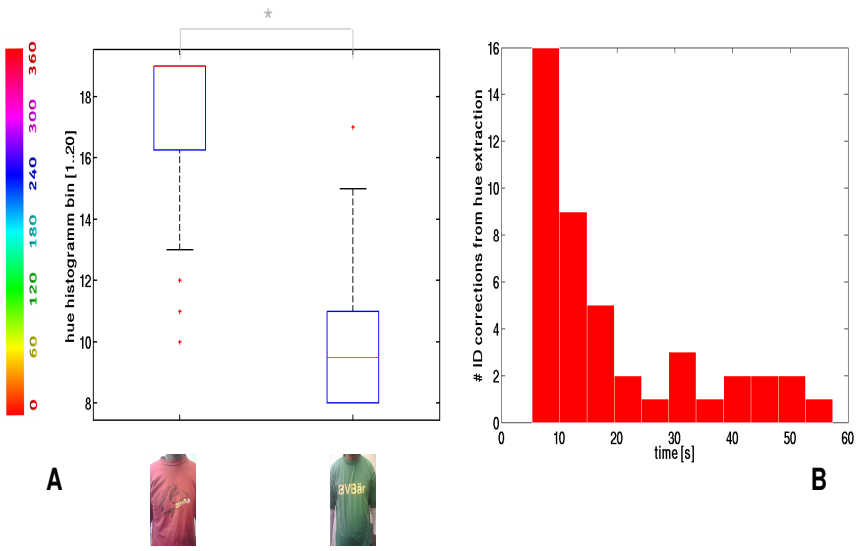

Figure 4.10: **Attention-guided feature extraction under noise and limited resources constraints: A)** Subjects with two different hues are identified as belonging to two different hue bins with a significant difference (student's t-test, $p < 0.05$). **B) Latency of recuperation:** Latency of recuperation of IDs using hue feature extraction after an ID confusion (mean 17 seconds). The data shown is extracted from two subjects acting simultaneously in XIM for 5 minutes.

4.5.2 Robot Rescue Simulation Testbed

In this second testbed the objective is to evaluate the exploitation of a world-model for the generation of actions maximizing a given utility. Also we evaluate the contributions of the different component of PASAR, prediction, attention and memory decay, to performance. See section 4.3.2 for details of the experiment. For each test case mentioned in section 4.3.2, 100 trials were performed. Each trial lasted 160 seconds. The expiry time of the normal robots was 30 seconds and of the PASAR rescue robot was 60 seconds.

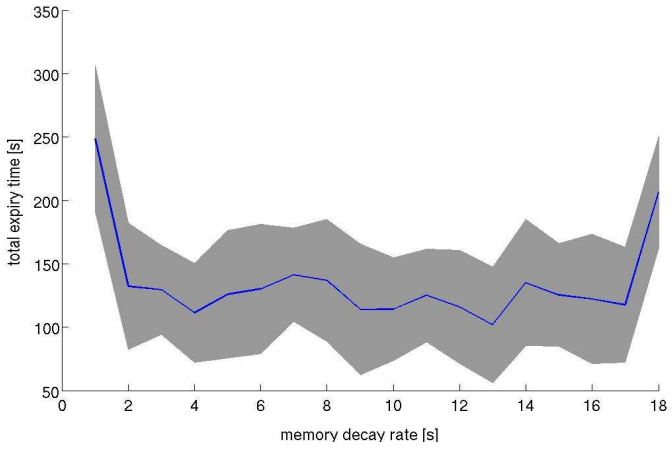

Figure 4.11: **Total expiry time of robots as a function of the memory decay:** Memory decay rate is used in seconds. Decay rate refers to the time in seconds in which the *concept* variance falls to a predefined baseline.

In order to evaluate the performance of the PASAR rescue robot, we study the total expiry time of the agents and the number of rescued agents in the limited time. In order to study the contributions of the subcomponents of PASAR, we evaluate the performance when using isolated subcomponents of PASAR to solve the same task. Figure 4.11 shows the total expiry time of agents as a function of memory decay rate. It shows

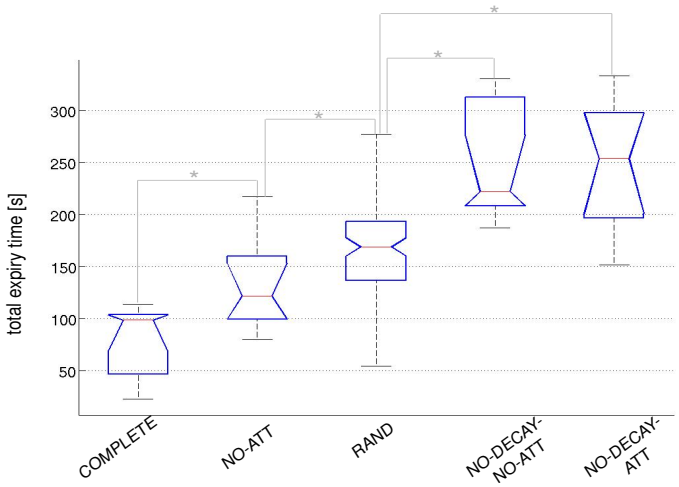

Figure 4.12: **Total expiry time for different testcases:** Performance of PASAR in different test cases. Asterisks indicate significant difference of means (Tukey-Cramer multiple comparison, $p < 0.05$). *COMPLETE* test case performs the best.

that neither a too low nor a too high memory decay rate is good for performance. In the *COMPLETE* case we achieve a mean performance of 100.6567 seconds and standard deviation 42.4679. In the *NO-ATT* case we achieve a mean performance of 131.0965 seconds and standard deviation 43.9256. In the *NO-DECAY-NO-ATT* case we achieve a mean performance of 249.5249 seconds and standard deviation 55.5471. In the test case without memory decay, but with attention (*NO-DECAY-ATT*) we achieve a mean performance of 248.0998 seconds and standard deviation 62.9844. Finally, in the random case *RAND* (i.e. without using predictions of utility) a mean performance of 145.9758 seconds and standard deviation 53.1304 is achieved.

We summarize our results as following:
1) using the predictions of the world model together with attention and a good memory decay rate performs the best (figure 4.12, *COMPLETE*)
2) Using attention is better than not using it (figure 4.12, *COMPLETE* vs.

NO-ATT)
3) Using memory decay has a significant effect on performance (*COMPLETE* and *NO-ATT* compared to *NO-DECAY-NO-ATT* and *NO-DECAY-ATT*).
4) Further, attention does not seem to help performance if there is no memory decay (*NO-DECAY-ATT* vs. *COMPLETE* and *NO-ATT*).
5) Using utility prediction does not help if no memory decay is used (*RAND* vs. *NO-DECAY-NO-ATT*).

4.6 Conclusions

We proposed and evaluated PASAR, a concise and modular framework for quantitatively assessing the integration of prediction, anticipation, sensation, attention and response. PASAR allows the evaluation of system performance in complex tasks using the whole system and also selected components of the system. We conducted experiments in simulations and complex real-world tasks to address the question of how each subcomponent of PASAR contributes to the performance of the overall system in the given task. First we demonstrated the feasibility of our model for solving complex real-world problems using the XIM setup to solve a multi-person multi-modal tracking problem. In the XIM tracking task, we demonstrated that PASAR is able to learn sensory map alignment, create and maintain a world-model under limited resources constraints when acting in an unknown environment and deploy attentional mechanisms for active information acquisition. The second testbed of rescue robot simulation demonstrated PASAR's optimal usage of the acquired world-model for multiple goal decision making and allowed to evaluate the contributions of the individual components of PASAR to the overall performance. Our results on the interplay of anticipation, perception, attention and response suggest that a complete sensori-motor system with attentional, anticipatory and predictive mechanisms perform clearly better than incomplete subsystems in complex tasks. We find evidence that the use of attentional mechanisms and prediction is only beneficial, if

there is a forgetting (memory decay) mechanism at work. Building novel bio-inspired robotic systems for real-world applications can benefit from our findings, by using prediction, anticipation, sensation attention and response in the suggested combinations. For example, the usage of memory decay together with attention and predictive mechanisms for controlling a humanoid robot in a human-robot interaction scenario would not only enable the robot to attend to the most relevant human or object at a given time, but also enable it to predict the future attentional relevance of objects and to gradually forget the past in order to manage limited memory resources. We also believe that our results suggest more specific physiological and psychophysical experiments to support the findings of interplay of the different sub-systems of cognition in biological systems. For example it would be very interesting to perform psychophysical experiments to investigate the existence of anticipatory gates (validation gates) in human/animal perception.

4.7 Discussion

Our model allows to evaluate the sub-components of an artificial cognitive system and we tested it in both simulation and real-world setups. Even though the model is inspired by the hierarchichal architecture of biological systems and has been shown to be very efficient for artificial sensori-motor systems, concrete evidence of such a framework in biological systems is yet to be found. Targeted research has to be conducted to find support for a JPDA like processing for data association in biological systems. Similar highly influential cognitive architectures that try to characterize brain function and cognition have their own particular strengths, e.g. in powerful symbol manipulation and automation mechanisms [5], extremely versatile knowledge representation schemes [65], primacy of action and perception over cognition [67], language processing [33] etc. However, unlike other cognitive architectures, PASAR provides a generic framework for integrating subcomponents of cognition and testing their interplay. PASAR thereby makes use of a so-called *forward model* by

harnessing predictions and anticipations [60]. In this context, prediction is essentially a problem of matching the current state (the current situation of each *concept* in the *world-model* at a single point in time) to future state possibilities produced by the model. Similarly, anticipation is essentially the process of expecting stimuli or events in the n-dimensional spatiotemporal vicinity of the predicted state. Very related to this discussion of predictions of future states of items in memory is the so-called human ability of *theory of mind*[90]. It is thought that something similar to such *state-matching* happens in the human mind, through the ability known as *theory of mind*, which attributes mental states (beliefs, desires, intentions, etc.) to others and uses them to predict how others will behave [90]. A very interesting research question would be to ask if the modular concept of PASAR can be used in the context of theory-of-mind to understand the interplay of attention, prediction, anticipation, memory and actions in humans.

In the next chapter we discuss a psychophysical experiment in humans to reveal the existence of JPDA-like validation gates in a visual data association task. Additionally we investigate how such validation gates change with changing cognitive load, supporting the hypothesis of top-down control of the use of limited resources.

Chapter 5

TESTING PASAR: THE BOTTOM-UP AND TOP-DOWN INFLUENCES IN HUMAN VISUAL PROCESSING

In the previous chapter we investigated the performance of PASAR on artificial systems in complex scenarios. Also, we investigated how the different subcomponents of PASAR interact with each other to achieve complex task solving behavior. PASAR thereby integrated both low and high level cognitive mechanisms like prediction, attention, sensation, attention and response in a single framework. The particular case of human visual processing requires the involvement of both low-level sensory-motor mechanisms and higher level cognitive functionalities [57]. In this chapter we investigate the existence and role of higher level cognitive mechanisms like prediction, anticipation and attention in human visual processing and how saccadic control is affected by this. We thereby use a psychophysical reverse correlation method for analyzing conscious decisions and saccadic eye movements in a human psychophysics experiment.

The question whether data association is related to attention is subject of ongoing debate. Some studies have formalized the unexpected observation (or surprise) in a Bayesian sense and linked this to attention [56]. But the link between data association and attention, and the influence of higher level mechanisms on such a system still remains unclear. Anticipation of future stimuli is a crucial component of a data association mechanism in classical dynamical systems [10]. Some support for this in human vision comes from studies that showed anticipatory eye behavior for predictable movements [23]. Furthermore, anticipation is seen as an integral part of visual cognition [104].

Psychophysicists have often used the Multiple Object Tracking (MOT) experimental paradigm to test the prediction hypothesis in vision [94, 119]. The prediction hypothesis states that momentarily disappearing objects are often perceived as persisting when they reappear with a velocity and trajectory that was consistent with what was previously viewed [61]. Many earlier studies support the prediction hypothesis in MOT [110, 109]. Nevertheless, a rigorous experimental paradigm to measure the interplay of top-down predictive processes and bottom-up sensory processes is still to be proposed. Furthermore, the role of top-down cognitive mechanisms on the generation of express saccades and saccades of longer delays are not well known. The early/express saccade window has been observed to be in the range of 80-110 ms in humans [39] and the late saccades have reaction times around 200 ms [41, 37]. Some experiments suggest a top-down influence on late saccades while the same for early saccades remains unexplored [37].

Here we hypothesize that a single generic framework, consistent with PASAR, could be at work for data association and generation of event-related saccades. Our model builds on the hypothesis of *violation of expectation* that trigger attention. The starting point for our model is that attention is object based. Even though there is some evidence for space-based attention, evidence for object based attention is overwhelming at psychophysical [34], neurophysiological [88], clinical [12] and conceptual [61] levels. We use PASAR as a model of object-based attention triggering in human visual processing. We also hypothesize the existence

of, so called, anticipatory gates in predictive dynamic scenarios and the modulation of the anticipatory gate by higher level cognitive mechanisms. Inspired by our model, we propose a variant of the MOT paradigm and a psychophysical reverse correlation method to test the model. Our results support the notion of top-down prediction of visual stimuli, revealing the existence of an anticipatory field. We show that human perception relies more on predictions when working under higher cognitive loads. Also our results show that express saccades of shortest latency (80-110ms) are independent from higher level cognitive and decision-making processes. Nevertheless, our results suggest that later saccades at around 200ms are influenced by higher-level predictions. The PASAR model reproduces the influence of higher level cognitive mechanisms on the anticipatory field in varying cognitive load conditions.

5.1 Methods

5.1.1 Model

We describe a model of data association based on the principle of anticipatory gate and violation of expectations. The model is able to integrate higher-level influences and bottom-up sensory information for performing data association. We formulate the anticipatory gate in the model and discuss how anticipations can be violated and how this can be used for data association. We hypothesize which parameters of the model should vary with the cognitive load, under limited resources constraints.

Prediction in predictable dynamic scenarios

The so-called prediction hypothesis has been discussed widely in psychophysical literature and the Multiple Object Tracking (MOT) has been used widely to test this hypothesis [94, 119, 61]. In vision research, the prediction hypothesis states that momentarily disappearing objects are often perceived as persisting when they reappear with a velocity and trajectory that was consistent with what was previously viewed, i.e. when they

reappear predictably relative to their pre-disappearance trajectories [61]. Many earlier studies support the prediction hypothesis in MOT [110]. Also we know that subjects keep information object velocity when tracking [109]. Nevertheless some studies doubt the validity of the prediction hypothesis [61]. Therefore, even though the existence of forward-models in human cognition is widely accepted, the usage of forward-models (e.g. for prediction) in human visual tasks like MOT is not beyond discussion.

In our opinion MOT is not appropriate for testing the prediction hypothesis. Occlusion experiments in MOT pose the question whether displacements effect MOT performance. We think that MOT performance cannot give a measure on the use of predictions in visual perception, as a high MOT performance can be achieved using higher-level object ID recovery mechanisms after object reappearance. E.g. as the number of tracked objects is usually fixed, the subject can use this information to probabilistically assign object IDs after reappearance. This is in accordance with a persistent object based model of attention, that allows to filter out objects when those objects are relevant to current goals [48].

In the above mentioned MOT context, the role of saccades is still largely unexplored. Express saccades refer to saccades in the time window observed earlier in humans in the 80-110 ms range after the occurrence of a perceptual event [39]. We further refer to saccades in this time interval as *early* saccades. Slower saccades with reaction times around 200 ms after the occurrence of a perceptual event have also been studied earlier [41, 37]; we refer further to these as *late* saccades. Some work suggests top-down influences on late saccades, while the same for for early saccades remains unexplored [37]. We propose a psychophysical experimental paradigm, that enables us to explicitly verify the prediction hypothesis, which is a prerequisite for our computational model for data association. We investigate the top-down (anticipatory) influence on both kinds of saccades and compare them with the conscious decisions made, with the goal of investigating the role of high-level predictions in data association.

Probabilistic data association in predictable scenarios

As discussed in section 3.3.2 to model the PASAR framework, we consider the Joint probabilistic data association (JPDA) algorithm as the model underlying human visual data association in dynamic predictable scenarios. Here we summarize shortly the JPDA algorithm to motivate its usage in this context. As discussed in section 3.3.2 JPDA enumerates all possible associations between observations and targets at each time step and computes the association probabilities β_{jk}, which is the probability that the j-th observation originated from the k-th target. Given such association probabilities, the target state is estimated by Kalman filtering [10] and this conditional expectation of the state is weighted by the association probability. Let x_t^k indicate the state of target k at time step t, ω_{jk} the association event where the observation j is associated to target k and $Y_{1:t}$ stays for all the observations from time step 1 to time step t. Using a priori knowledge about the world (e.g. state transition matrix(A), process noise (Q), measurement matrix (H), control-input model (B) and the control input-vector ($\hat{u}$) of the Kalman filter) and the current state of the *target*, a prediction is made for each *target*. At timestep t, for each *target* k, we compute the state prediction, its covariance and the measurement prediction as follows

$$\tilde{x}_k^k = A\hat{x}_{t-1}^k + B\hat{u}_{t-1}^k \tag{5.1}$$

$$\tilde{P}_t^k = A\hat{P}_{t-1}^k A^T + Q_{t-1}^k \tag{5.2}$$

$$\tilde{y}_t^k = H\tilde{x}_t^k \tag{5.3}$$

Then the state of the target can be estimated as:

$$E(x_t^k|Y_{1:t}) = \sum_{\omega} E(x_t^k|\omega, Y_{1:t})P(\omega|Y_{1:t}) \tag{5.4}$$

$$= \sum_{j} E(x_t^k|\omega_{jk}, Y_{1:t})P(\omega_{jk}|Y_{1:t}) \tag{5.5}$$

where ω_{jk} denotes the association event and observation j is associated to target k and ω_{0k} denotes the event that no observation is associated to target k. Therefore the event association probability is $\beta_{jk} =$

$P(\omega_{jk}|Y_{1:t})$. JPDA computes a anticipatory gate for each target using the Kalman innovation of new observations. It only considers observations inside the anticipatory gate for each target. The ellipsoidal anticipatory gate using the Kalman filter is discussed in section 5.1.1.

The ellipsoidal anticipatory gate hypothesis and the violation of anticipations

We consider the linear state evolution model for state dynamics of target x at time k:

$$x_k = Ax_{k-1} + Bu_{k-1} + \rho_p \tag{5.6}$$

where ρ_p is the process noise with time-invariant covariance matrix Q, B is the control-input model and u_k the control vector. The well-known linear Kalman filter prediction and estimation step is used to update the state. The ellipsoidal anticipatory gate is optimal for the above linear observation model[1] with additive noise:

$$z = Hx + \varphi \tag{5.7}$$

where φ is the zero Gaussian measurement error with $p(\varphi) = \mathcal{N}(\varphi; 0, R)$ and is independent of the state x. H is the observation model which maps the true state space into the observed space. The state probability density function is Gaussian $p(x) = \mathcal{N}(x; \hat{x}, P)$. The validity of measurement y_i is determined from its innovation with the predicted observation

$$\nu = y_i - H\hat{x} \tag{5.8}$$

with the covariance $S = R + HPH^T$. The anticipatory gate is computed by gating the Mahanalobis distance (the normalized innovation squared (NIS))

$$\nu^T S^{-1} \nu < M_d \tag{5.9}$$

[1] further we omit the time-subscripts of state space variables for the sake of clarity

M_d is the threshold for an innovation dimension d and can be computed efficiently since the NIS follows a chi-square probability density function. E.g. to compute the probability that $j\%$ of true associations are accepted, M_d is obtained from

$$\frac{j}{100} = P(\frac{d}{2}, \frac{M_d}{2}) \tag{5.10}$$

where

$$P(a, b) = \frac{1}{\Gamma(a)} \int_0^b e^{-t} t^{a-1}\, dt \tag{5.11}$$

is the incomplete gamma function [92]. The anticipatory gate (commonly known as *validation gate*) defines a region of acceptance such that $(100-j)\%$ of true measurements are rejected given that the measurements y_i are distributed according to

$$p(y) = \mathcal{N}(y; H\hat{x}, S) \tag{5.12}$$

This formulation avoids the necessity to model clutter, which is usually very hard to model, and also unlikely associations are eliminated (see figure 5.1 for an illustration). For non-linear anticipatory gates for non-Gaussian models see [9].

We hypothesize the existence of the above described ellipsoidal anticipatory gate in human visual perception, when dealing with dynamic but predictable scenarios. And we hypothesize that data association is performed using such a gate. Given this hypothesis, increasing the cognitive load in humans corresponds to increasing the process noise covariance (Q) as in equation 5.6. We propose a psychophysical experimental paradigm using a displacement detection task to test our hypothesis of the existence of anticipatory gates. Further, increasing the cognitive load should lead thereby to increasing the covariance of process noise, which should be reflected in the anticipatory gate described above. More concretely, the anticipatory gates in higher cognitive loads should have higher eccentricities along predicted movement directions (a higher process noise covariance Q has that effect). This is a reasonable effect as this

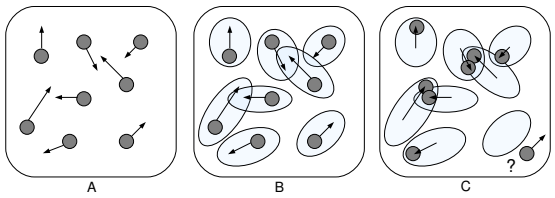

Figure 5.1: **Schema of ellipsoidal anticipatory gates:** *A:* Moving targets with predicted positions indicated by arrows. *B:* Ellipsoidal anticipatory gates for data association. *C:* Target states after one movement step. One anticipation was violated by a displacement (bottom right) and the displacement falls outside the anticipatory gate. The question mark indicates if the subjects answers ”yes” or ”no” to the question if this displacement was noticed.

would allow a limited resources system, like the human brain, to have a riskier but more efficient data association strategy when under high cognitive load.

5.1.2 Displacement detection task

The subject watches a fixed number of moving identical non-filled white circles (referred to as *targets*) on a black background (as in MOT [61]) that move on predictable linear paths at constant speed and bounce at the boundaries. This allows the subject to use linear predictions of the movements. We avoid visual habituation when performing smooth-pursuit of a single linear movement (as in [38]), by using several simultaneously moving circular items ($N = 10$). Once every $T = 3$ seconds just one of the moving objects displaces itself from the linear trajectory and then continues the linear motion at the same speed as before the displacement (see figure 5.1, C). The displacement and direction is chosen randomly around the movement direction and current target position. The subject is instructed to press a button whenever he/she perceives a displacement from the normal linear motion. Simultaneously, using infra-red

eye-tracking we also track the eye movements of the subject. We conduct three trials of 3 minutes each per subject: trial one is of low cognitive load where the subject solely performs the above psychophysics task (mentioned as the low load task). In trial 2 we increase the subject's cognitive load by instructing him/her to continuously count aloud the even numbers (in his/her mother tongue) while performing the same psychophysics task (medium load task). In trial 3 the subject is instructed to continuously count aloud the the alphabet in reverse order (also in his/her mother tongue) until the experiment stop (high load task). The low, medium and high cognitive tasks were designed to modulate the cognitive load without affecting the perceptual load [25]. Recalling less automatized chains (alphabets in reverse order) results in higher cognitive loads than more automatized chains like the numbers, while all counting is resource demanding [25].

We used the Tobii© x120 eye tracker to log eye tracking data at 120 Hz. The psychophysical experiment was developed using the OpenGL library in Linux Fedora 8, C++ environment and runs at 200Hz on average on a quadcore Intel(R) Xeon(R) CPU of 2.00GHz speed. The button press reaction of the subjects and the movements of the circular items were logged time synchronized with the eye tracking data. The screen resolution was 1400x900 and the subject sat at 60 cms from the screen, stabilized using a chin rest of 35 cms height. The movement speed of the circular targets were in between 1 and 10 $^\circ/s$. The speed of a target was altered slightly only when bouncing at the peripheries (random change of $\pm$0.001 $^\circ/s$). Subjects were 8 male university (under)graduate students between 23 and 32 years old. The total experiment consisted of 3 trials of 3 minutes each (one trial for each cognitive load). Eye calibration was performed before each trial. The radius of all circular items were identical at 0.20 $^\circ$.

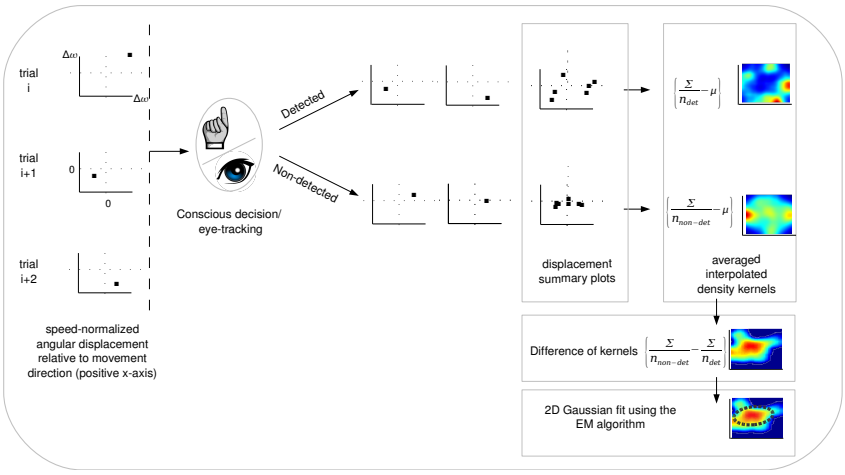

Figure 5.2: **Schematic of the psychophysical kernel computation:** All trials are sorted to detected and non-detected trials and all displacements normalized. A single kernel is computed from the density plots of the two sorted data groups (see text for more details).

5.1.3 Psychophysical reverse correlation

Psychophysical reverse correlation has been used in a number of studies to characterize human observer's strategies in visual tasks [3]. Also, many physiological studies have used reverse correlation to characterize neural responses to visual stimuli (see [114] for a review). Both in physiology and psychophysics, reverse correlation has proven to be a strong technique for seeking relationships between a high-dimensional variable (e.g. an image) and a categorical variable (two-choice decision or neural spiking) [114]. Here we tailor psychophysical reverse correlation to analyze the two-choice decision strategy and express saccades. Each stimulus is a displacement that is plotted as a point on the speed-normalized and direction-corrected coordinate system (see figure 5.2), where the positive x-axis is the linear movement direction of the circular target before and after the displacement. For each displacement the direction and length

of displacement chosen from a uniform distribution. This displacement is then normalized with respect to its speed and corrected for direction so that all displacements can be plotted on the same reference frame, where the positive x-axis denotes the movement direction of the object (see figure 5.2). We then sort the stimuli according to the 'detected' and 'non-detected' choices (analogously using early and late saccade data, see below). We then computed the average detection and non-detection matrices and used interpolation to incorporate datasets of different sizes for detection and non-detection. This yields a two-dimensional probability distribution each for detection and non-detection classes. The difference between the two probability distributions preceding non-detected choices and detected choices defines the dataset which is fitted using the Expectation Maximization algorithm to find the 2D Gaussian. The covariance ellipse of this fitted Gaussian is referred to as the psychophysical kernel hereafter (the ellipse covers 39.4 % of the total probability mass). The goodness of the Gaussian fit is estimated by multivariate normality tests using skewness and kurtosis.

We analyze the eye tracking data, to detect a possible correlation between displacements and eye behavior. Here we formalize an operational definition of *saccade* towards displacement position as follows: we compute the distance between the eye position and the displacement position at the beginning ($dist_b$) and at the end ($dist_e$) of a given time window. We define that a saccade occurred if $dist_e < \frac{dist_b}{2}$. For a time window of 110ms such saccades were observed for 90% of the displacements. Also see figure 5.4(a). We looked at two kinds of saccades and computed the psychophysical kernels for each of them separately. First we looked at the *early* saccades, that occur at around 100ms after displacement (see figure 5.4(a)). Secondly we looked at the *late* saccades at around 200ms after displacement. The early/express saccade window has been observed earlier to be 80-110 ms in humans [39] and the late saccades have reaction times round 200 ms [41, 37]. Some work suggest top-down influence on late saccades while the same for early saccades remains unexplored [37].

5.2 Results

The *eccentricity* ϵ of the psychophysical ellipse is the eccentricity of the covariance matrix of the psychophysical kernel indicated by the ellipse is computed as: $\sqrt{1-\frac{\lambda_2}{\lambda_1}}$, where λ_1 and λ_2 are the first and the second eigenvalues of the covariance matrix ($\epsilon = 0$ is circle, $\epsilon = 1$ is 1, the higher the ϵ, the higher the eccentricity of an ellipse). The orientation γ of the psychophysical ellipse is given by the covariance matrix of the kernel; readable from the orientation of the eigenvector corresponding to the largest eigenvalue of the covariance matrix. (we have -90° for vertically up through 0 ° for movement direction, to +90° vertically down). We computed the mean kernels for all subjects as shown in figure 5.3.

The mean areas of the psychophysical kernel ellipses of the subjects in the low(l), medium(m) and high(h) cognitive load trials do not change relevantly (1-way ANOVA, p = $0.39, 0.39, 0.39$ for the null hypothesis that the area remains the same for decision, early saccade and late saccade kernels respectively). Also, the mean shift of the psychophysical kernel ellipse does not change relevantly (1-way ANOVA, p = $0.95, 0.95, 0.95$ for the null hypothesis that the shift remains the same for decision, early saccade and late saccade kernels respectively). Further, the mean of the psychophysical kernel ellipse orientation also does not change relevantly (1-way ANOVA, p = 0.39, 0.99, 0.39 for the null hypothesis that the shift remains the same for decision, early saccade and late saccade kernels respectively). The only parameter of the ellipse that changes over the different cognitive loads is the eccentricity (1-way ANOVA, p = 0.0005, 0.95, 0.0005 for the null hypothesis that the shift remains the same for decision, early saccade and late saccade kernels respectively). As the p-values indicate, the eccentricity mean changes relevantly only for the late saccade and the conscious decision. This indicates that cognitive load has an effect on both the decision making process and the late saccades, but not on the early saccades. To further analyze this, we also analyzed the intra-subject change in eccentricities and orientations of the psychophysical kernels. The results are shown in figure 5.4(b) and figure 5.4(c).

The results indicate that the eccentricity of the ellipse increases along

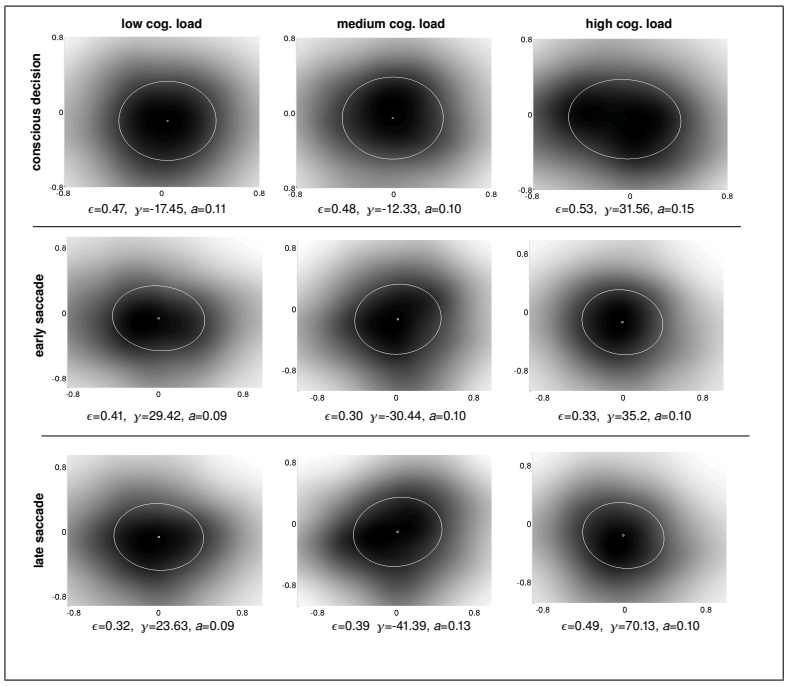

Figure 5.3: **Psychophysical kernels** for all subjects for conscious decision, early and late saccades and in different cognitive loads (low, medium and high). The area (a), eccentricity (ϵ) and the orientation (γ) of the kernel ellipses are indicated.

the movement direction with cognitive load for decisions and late saccades, but not for the early saccade. To see the statistical relevance of this change, we perform the signtest for the above as shown in table 5.1. The results suggest that the effect of the change of the cognitive load is reflected solely in the elongation of the psychophysical ellipse eccentricity. The eccentricity increases along the movement direction reflecting the existence of a riskier but more efficient data association mechanism at work, as predicted by the model in section 5.1.1. It is trivial to compute the psychophysical kernel ellipses for the different conditions using linear motion equations, and as the speed of the movement of the targets are

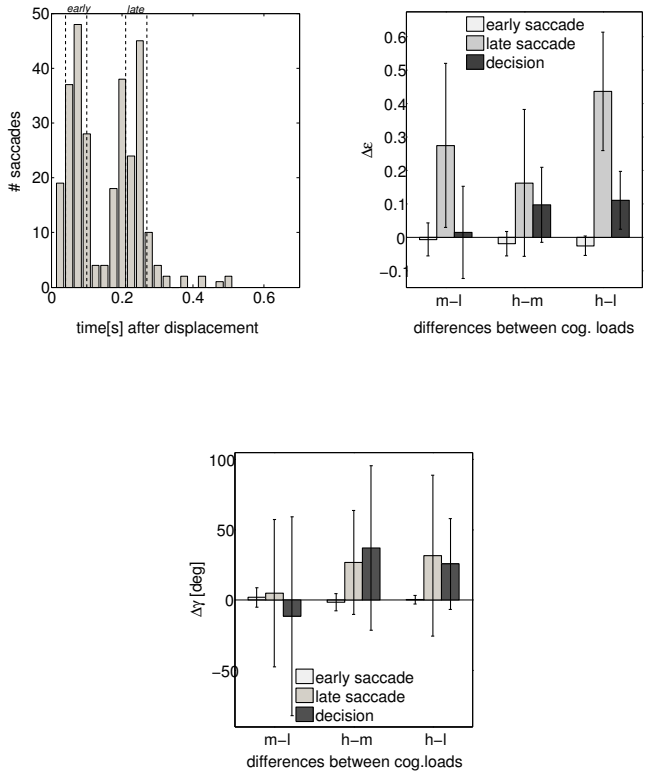

Figure 5.4: **a)** Saccade histograms with early and late saccade intervals indicated. **b)** Change in intra-subject eccentricities. **c)** Change in intra-subject orientations.

known. The process noise covariance matrix Q as in equation 5.1.1 can simply be adapted to obtain the observed eccentricity of the psychophysical kernel ellipses for the different cognitive loads.

Table 5.1: **p-values** of the two-sided sign test for the eccentricity(ϵ) and orientation(γ) differences of the psychophysical kernel ellipses at individual subject level between low(*l*), medium(*m*) and high(*h*) load experiments. The kernels computed by the subjects' decisions, the express saccades and the *late* saccades are separately analyzed. The bold values indicate small values of p ($<= 0.05$), where the null hypothesis of 0 median is rejected.

	decision			*express*			*late*		
	m-l	*h-m*	*h-l*	*m-l*	*h-m*	*h-l*	*m-l*	*h-m*	*h-l*
ϵ	0.726	0.289	**0.007**	1.0	0.697	0.218	0.218	0.687	**0.031**
γ	0.726	0.070	0.0703	1.0	1.0	0.687	1.0	0.218	0.687

5.3 Conclusions

In this chapter we investigated the existence of an anticipatory/validation gate, and the influence of high-level cognitive loads on saccade generation and decision making processes on (visual) data association tasks using the PASAR framework. The probabilistic computational framework of PASAR hypothesizes that anticipation of future stimuli is measurable and that data association in visual processing can be explained using a paradigm of violation of anticipations. We investigated the mechanisms that underlie top-down decision making and saccade generation in the context of visual data association in a psychophysical task. We have shown that the top-down influences on conscious decision making and early/late saccades are measurable by means of the formulation of a psychophysical kernel. The proposed experimental paradigm (a modified version of Multiple Object Tracking (MOT)) serves exactly the purpose of computing the psychophysical kernels constructed on the basis of predictability. The conventional MOT paradigm was insufficient to reveal the existence and the properties of an anticipatory field. The possibility to

quantify anticipation as psychophysical kernels has enabled us to measure the anticipation of future stimuli.

The psychophysical data has evidenced the existence of a modulation of the anticipatory gates. This modulation was observed only for late saccades and the conscious decisions, but not for the early saccades. This supports the idea of a different process driving the early/express saccades, independently from high-level neuronal processes. At the same time, our results support the idea that late saccades have top-down influences as they follow the trend of the psychophysical kernel of conscious decision in low, medium and high cognitive load tasks.

The existence of such modulated elliptical anticipatory gates gives support to our integrated data association framework, and thus validating the use of PASAR for explaining human visual processing at different levels of the sensory-decision making hierarchy, and modeling the interplay of attention, decision, cognitive load, anticipation and the generation of saccades.

We believe that this novel psychophysical paradigm to measure anticipation and the interplay of the above mentioned systems is extremely valuable to approach deficits in the human visual processing such as unilateral neglect patients or patients with other attentional deficits. The computed psychophysical kernel could possibly then be used for diagnosis of attentional deficits, and to further understand the mechanisms in place for an eventual rehabilitation. Also, data association in humans is usually multi-modal, and it needs to be investigated how the psychophysical kernel generalizes when anticipations are violated across modalities. Hence we aim at extending our psychophysical kernel paradigm to include 3D sound spatialization.

Chapter 6

CONCLUSIONS

In this dissertation, we have addressed the issue of modeling the integration of forward model mechanisms like prediction and anticipation with attention and motor response in artificial and biological cognitive systems. We posed the question of what the minimal subcomponents of cognition contribute to the performance of the cognitive system. We addressed this question in experiments with biological systems and in artificial cognitive systems. Our phylogenic model-based approach allowed us to refine our initial minimal model in a stepwise fashion. Our initial model is based on the first version of the DAC architecture [113]. Other recent variants of the DAC architecture also contain explicit forward-model mechanisms for integrating behavioral and perceptual learning [35]. Nevertheless, the other recent variants of DAC do not provide a framework to integrate attentional mechanisms with forward model mechanisms and therefore do not allow the investigation of the specific contributions of the subcomponents of cognition to the overall task solving performance.

In this thesis, we first presented a mapless navigational model based on ant navigation strategies, that included different aspects of insect-navigation like chemical search, path integration and landmark navigation and was inspired by earlier insect navigational studies suggesting that insects make use of vector-like memory representations to achieve robust navigation [29, 124, 123]. This initial model, based on the first version of the Dis-

tributed Adaptive Control framework [113, 111], did not possess any forward model mechanisms like prediction, anticipation or attention, but despite these limitations was capable of mapless landmark navigation using chemo-visual sensors. The model was implemented and tested on a ground robot in a chemo-foraging task [74]. Unlike navigational models based on place/map like representations, our model used solely heading direction accumulation and proprioceptive information in combination with landmark recognition. This approach proposed a solution to autonomous landmark navigation without having the need to learn place representations, based on which the *SyntheticAnt* robot was able to learn a graph structure using low memory usage.

Nevertheless, the feasibility of this initial model was challenged by dynamic landmark scenarios. We showed that forward model mechanisms like prediction of future positions of landmarks were necessary to explain the behavior of real ants when navigating in dynamic scenarios. Thus, we enhanced our model with an expectation reinforcement mechanism and transient memory based on insect studies to allow the artificial forager to navigate in unknown dynamic environments [122]. The proposed navigational strategy enabled the navigator to learn the reliability in the landmarks by using expectation reinforcement. We also proposed a version of Lévy walk, which supported the idea of expectation reinforcement, by enabling the navigator to trace back to known terrain whenever expectations were violated. We tested our navigational model on the simulated *SyntheticAnt*, and compared its behavior to its biological counterpart. The striking behavioral similarity of our model to the real ant support the principle of our model. In fact, our model formulated navigation as a dynamic memory reconsolidation process, which made use of an expectation reinforcement mechanism. By modeling ant navigation and then directly comparing the results of our navigational model to real ant navigational behavior, we could better understand the capabilities and limits of a non-forward model. In summary, we saw the necessity of forward models to capture the ant behavior in dynamic scenarios [73]. Also, our approach proposes a viable and biologically plausible alternative to the solution of the SLAM problem [99]. The main differences to

the conventional solutions are the reformulation of mapping as recalling a graph-like structure and the reinterpretation of localization as relative distances and directions to known landmarks.

Subsequently we moved on to propose the PASAR framework that enabled us to integrate and quantify the minimal ingredients (including forward models) of cognition such as prediction, anticipation, sensation, attention and motor response needed for task solving in dynamic, partially known environments under limited resources constraints. PASAR allowed us to pose specific questions about the role and contributions of each of its subcomponents. The interplay of these cognitive mechanisms were analyzed in a complex robotic task in the mixed reality environment of XIM. In the XIM tracking task, we demonstrated that PASAR was able to learn sensory map alignment, create and maintain a world-model under limited resources constraints when acting in an unknown environment and deploy attentional mechanisms for active information acquisition [70, 72]. The second testbed, the rescue robot simulation, demonstrated PASAR's optimality in the usage of the acquired world-model for multiple goal decision making and allowed to evaluate the contributions of the individual components of PASAR to the overall performance [71]. Our results in the XIM and robot simulation testbeds demonstrate the feasibility of the PASAR framework for use in artificial cognitive systems. Furthermore, our results on the interplay of anticipation, perception, attention and response suggest that a complete sensori-motor system with attentional, anticipatory and predictive mechanisms perform clearly better than incomplete subsystems in complex tasks. Besides that, our results also suggest that the use of attentional mechanisms and prediction is only beneficial, if there is a forgetting (memory decay) mechanism at work. Our findings can serve designing novel artificial cognitive systems by using prediction, anticipation, sensation attention and response in constructive interplay.

Our results with PASAR in artificial cognitive systems postulated a number of testable predictions on the interplay of the different sub-systems of cognition in biological systems. To address this we designed a human psychophysical experiment and a reverse correlation paradigm to study the feasibility of PASAR in human visual processing and investigated the

influence of high-level cognitive loads on saccade generation and decision making processes in a visual displacement detection task. The data association mechanism of PASAR hypothesizes that anticipation of future stimuli is measurable and that data association in visual processing could be explained using a paradigm of violation of anticipations. The psychophysical task showed that the top-down influences on conscious decision making and early/late saccades are measurable by means of the formulation of a psychophysical kernel. Our results suggested the existence of an anticipatory gate in human visual processing, and that this gate is modulated by top-down influence. This modulation was stronger when acting under higher cognitive load, suggesting that the brain traded off sensory data processing for alloting computational resources to the extra cognitive task by relying more on predictions for decision making and for triggering late saccades.

In summary, we identified prediction, anticipation, sensation, attention and motor response as minimal components of cognitive systems, and analyzed their interplay in artificial and biological cognitive systems. Predictive and anticipatory mechanisms are increasingly thought to play an important role in motor control, goal oriented behavior and cognition in biological systems [128]. Biological cognitive systems are thought to use *forward models* to achieve this by predicting the sensory consequences of actions to ensure robust adaptive behavior [60]. Our findings of forward models in insect cognition is supported by a wide range of recent insect studies (see [120] for a review). In mammalian neuroscience, there is increasing interest in interpreting the function of various brain areas in terms of forward models (e.g. the cerebellum [76] or the substantia nigra of the midbrain[78]). Besides that, several authors have suggested the relevance of forward modeling in understanding the brain circuitry that underlies cognition [27, 11, 31]. There is support, on the one hand, for the existence of a forward model mechanism to modulate bottom-up sensory information in order to fit expectations based on past events, and on the other hand, for its close relationship to attentional mechanisms [60, 57, 101]. The notion of *top-down* and *bottom-up* information flows, commonly used in attention literature [57], is of particular

interest to our model as it makes use of top-down modulation of anticipations and bottom-up sensory input. In the context of this dissertation we addressed the issue of integrating attention mechanisms with prediction, anticipation, sensation and motor response in a single framework. We thereby took a phylogenic approach and modeled a cognitive system, starting with a simple model and then incorporating forward models and attention mechanisms. We then tested our model in complex real-world and simulated robotic tasks and in human visual processing.

The so-called prediction hypothesis in human visual processing has been discussed in many earlier studies [94, 119, 61]. Some studies support the prediction hypothesis in MOT [110, 119, 61], but also some studies doubt the validity of the same [61]. Here we not only provide a signature of an anticipatory gate (which makes use of predictions) in human visual processing, but also model the same using the PASAR data association mechanism. Our findings support the prediction hypothesis (and the related anticipatory mechanism) and shows that humans harness more the available anticipations about future stimuli with increasing cognitive load.

It is our strong belief that the proposed PASAR framework will contribute to the design of novel control architectures of artificial robotic systems. For this reason, in future work, we plan to test PASAR on the state-of-the-art humanoid robotic platform iCub[2]. A humanoid robot platform offers a plethora of possibilities to test a framework like PASAR in real-world interactions with humans, which involves, prediction, anticipation, attention, sensation and motor response. Also, we plan to evaluate the PASAR framework more elaborately in biological systems using brain imaging techniques to uncover the existence of the neural correlates of the hypothesized anticipatory gates.

[2]http://www.robotcub.org/

Chapter 7

APPENDIX

7.1 MCMC Implementation for JPDA Event Probability Computation

The problem is reformulated as a bipartite graph as discussed in previous work [71]. Consider the bipartite graph $G = (U, V, E)$, where U is a vertex set of predicted observations, V is the vertex set of observations and E is mapping predicted observations (or in other words a *concept*) to an observation. We thereby only consider feasible mappings, i.e. the ones that respect the validation gate criteria for the JPDA. The algorithm starts with one such feasible mapping and then a Markov chain is generated. The polynomial time complexity with respect to the number of *concepts* allows MCMC to be used for computing β_{jk} in real-time. For details of the MCMC approximation of β_{jk}, its convergence and stability see [83] and [71].

7.2 Sensory MAP Alignment Learning in the XIM Mixed-Reality Space

Neural plasticity guarantees shaping and maintaining mutual spatial alignment across different sensory representations.The PASAR adaptive layer employs a learning mechanism so that purely reactive responses are progressively replaced by learned responses. PASAR is transparent to the specific learning mechanism itself, and we have demonstrated the capability of PASAR using two different learning paradigms, asymmetric Hebbian learning and Levenberg-Marquardt. In the first testbed, PASAR makes use of asymmetric Hebbian learning to learn one sensory representation by using another one as the reference. The sensory modality which delivers reliable data is used as the reference to learn the space representation of another modality. The Hebbian learning rule mediates the learning to correct the synaptic weights of a neural network connecting the neural representation of one modality to the other. Once the Hebbian learning converges on a low resolution neural representation, a cubic interpolation is applied to get high resolution mapping of space of the learned representation. The transparence of the PASAR adaptive layer to the specific learning algorithm is demonstrated by implementing a Levenberg-Marquardt algorithm to learn the extrinsic parameters of active sensory devices.

We take a close look at how sensory map learning in XIM is achieved online during human interaction in the space. Firstly, we use the PASAR adaptive layer to learn the sensory map of the overhead camera using the floor map as the reference. The overhead infrared camera, placed in an arbitrary position, has intrinsic perspective and distortive errors. Based on the superior colliculus sensory map alignment [102, 58], this can be implemented using a Hebbian learning rule in the PASAR adaptive layer (see also section 3.3.4). The tactile floor, which delivers reliable but low resolution position data, is used as the reference. The Hebbian learning rule mediates the learning to correct the synaptic weights of a neural network connecting the overhead camera neural group with the floor group (figure 7.1). The procedure for learning the camera sensory map consists

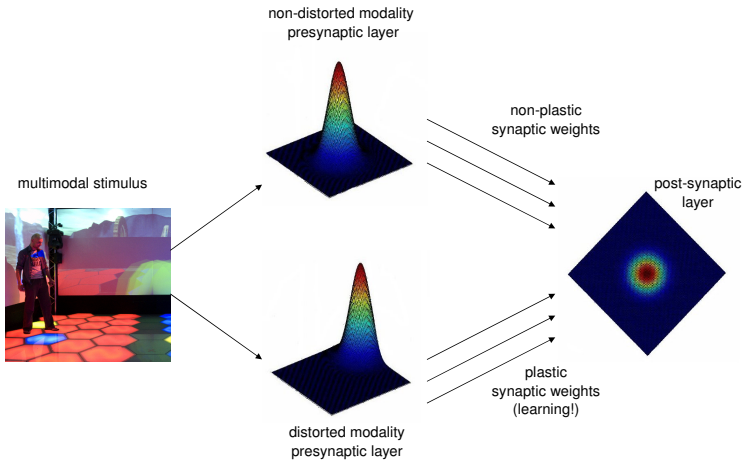

Figure 7.1: **Learning Sensory Maps:** Using the PASAR adaptive layer, the space representation errors of one sensory modality are corrected using a different modality stimulus.

of a person walking freely in XIM while the tactile floor and the overhead infrared camera tracking data are used by the PASAR adaptive layer. This basically learns the synaptic weight of a neural network connecting a 72 by 72 linear threshold cell group to another 72 by 72 linear threshold cell group by means of Hebbian plasticity. The details of the usage of the DAC adaptive layer for Hebbian learning can be consulted in [35]. After the Hebbian learning stabilizes, a cubic interpolation is used to regain the high resolution mapping of the overhead camera. After the Hebbian learning has converged, a cubic interpolation is applied to regain the high resolution of the camera space representation. This online mechanism of PASAR allows to learn the space representation of a sensor placed arbitrarily in space.

Secondly, we use the same PASAR adaptive layer for online learning of the extrinsic parameters of the four controllable color cameras placed in arbitrary positions in XIM (figure 4) by means of the Levenberg Mar-

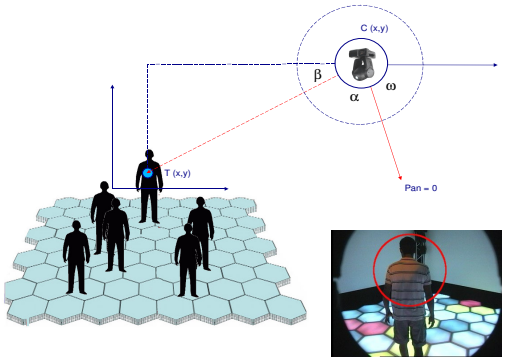

Figure 7.2: **Online learning of the extrinsic parameters of movable cameras:** Using the PASAR adaptive layer, the controllable color cameras extrinsic parameters are learned using tracking information of a person walking in XIM as the reference. $C(x, y)$ is the camera position and the angels α, β and ω are used for the yaw computation. The controllable cameras scan the space and upon human torso detection (snapshot on the right bottom) the extrinsic parameter approximation is iteratively corrected.

quardt error minimizing algorithm [69]. The extrinsic parameters of these four cameras (position in 3D space, yaw and pitch) are learned iteratively: the pan-tilt cameras scan the XIM space for human torsos. When a human torso is detected in the camera image, the tracked position of the person is used as the reference to correct the extrinsic parameter estimation of the pan-tilt camera.

This online learning of the camera extrinsic parameters can be practically carried out by placing the pan-tilt cameras in arbitrary positions and a single person walking in the space. We consider the error minimization for the camera x-y position and yaw. Let ω be the yaw of the pan-tilt camera, (t_x, t_y) the position of the tracked human in XIM and (c_x, c_y) the pan-tilt camera position. The angles α and β are indicated in figure 7.2. Using simple trigonometry we compute α:

$$\beta = arctan(\frac{c_y - t_y}{c_x - t_x}) \tag{7.1}$$

$$\alpha = 180 - \beta - \omega \tag{7.2}$$

$$\alpha = f(t_x, t_y) = 180 - arctan(\frac{c_y - t_y}{c_x - t_x}) - \omega \tag{7.3}$$

While scanning the XIM space, the pan-tilt camera detects humans and stores the tracked position of the human (t_x, t_y) and the yaw α. For a set of corresponding measurements $\hat{t}_i$ and $\hat{\alpha}_i$ the cost function

$$C(\vec{p}) = \sum_{i=1}^{n} [\alpha_i - f(\hat{t}_i|\vec{p})]^2 \tag{7.4}$$

has to be minimized by optimizing the parameter vector:

$$\vec{p} = (c_x, c_y, \omega)^T$$

The online estimation of pitch is carried out analogously [54].

7.3 Multi-robot Testbed Equations

In the following we elaborate on how the general PASAR equations 12, 13 and 14 are applied to the multi-robot testbed. Let us assume that the motor action consists simply of choosing a point (x, y) in space distance, both x and $y \in 1..20$. The best action is then chosen as a point (x, y) the world-model, to which then PASAR moves. As in the general equation 15, here are interested in computing the best point on the (x, y) plane. Therefore we are interested in the probability:

$$P(XY|F_s^t(\Theta_s^{t-1})A^t(s))$$

F is a time decay function that depends on time t, since the time of a previous stimulus associated to this *concept*. With a_i we denote the attentional weight for *concept* i. For n *concepts* we formalize the above probability as:

$$P(XY|y_1, ...y_n t_1, ...t_n x_1, ...x_n a_1, .., a_n) \tag{7.5}$$

First we consider the conditional probability in equation7.5 as if there were only one *concept* i and without attentional inputs a_i. Assuming conditional independence for X and Y, we do the following decomposition:

$$P(XY|y_i t_i x_i) = P(X|y_i t_i x_i)P(Y|y_i t_i x_i)P(t_i y_i x_i)$$

The probability distributions $P(X|y_i t_i x_i)$ and $P(Y|y_i t_i x_i)$ are Gaussian distributions as shown in the following equations.

$$P(X|y_i t_i x_i) = \mathcal{N}(x_i, \frac{t_i}{c_1}) \tag{7.6}$$

$$P(Y|y_i t_i x_i) = \mathcal{N}(y_i, \frac{t_i}{c_2}) \tag{7.7}$$

Where the Gaussian distributions are centered on x_i and y_i at which the *concept* i is located. The standard deviation is a function of time t_i at which this *concept* was last perceived. This allows PASAR to gradually loose certainty (time decay) of what it had seen in the past, as past information is always prone to change in a dynamic world.

And we assume the uniform distribution $\mathcal{U}$ for the joint probability $P(t_i y_i x_i)$ as we do not have any prior information about possible correlations between those random variables.

$$P(t_i y_i x_i) = \mathcal{U} \tag{7.8}$$

where c_1 and c_2 are pre-defined constants.

Now to consider the utilities of all the *concepts* for the computation of the total utility as shown in equation 14, in which we bring back the attentional components a_i and consider the following conditional probability distribution:

$$P(XY|y_1, ...y_n t_1, ...t_n x_1, ...x_n a_1, .., a_n) = \tag{7.9}$$

$$\sum_i \frac{a_i}{a_{tot}} P(X|y_i t_i x_i)P(Y|y_i t_i x_i)P(t_i y_i x_i) \tag{7.10}$$

where a_{tot} is the sum of all attentional components a_i, which are the attentional saliencies for individual *concepts* depending on their detected remaining charge.

This means that the attentional components a_i weight the shares of the individual *concept*s to form the joint conditional probability distribution. In other words, attention modulates the world model, which is expressed as a probability distribution that changes in each step with the sensory input.

This formulation allows to test the individual components of PASAR, such as prediction, attention and time decay of memory. For instance to test the contribution of attention on performance, we run trials where the attention of a *concept* is inversely proportional to the perceived power of the robot and also trials where attention is the same for all robots.

7.4 Multi-Person Tracking Experiment in XIM

In this case, the world-model, containing high-dimensional information about the humans interacting freely in the space, is to be constructed and maintained for tracking purposes using the available sensors. For this PASAR makes use of the contextual layer to fuse and associate the multimodal sensory data. Tactile floor tiles and overhead infrared cameras are the sensors used for this. A *concept* here is a single human in XIM. We use a 8-dimensional space for the *concepts* containing the x-y positions, x-y velocities, x-y accelerations, hue of the outfit and weight. To test the precision of the world-model during interactions involving different difficulty levels of tracking, a number of experiments are performed. ID maintenence is analyzed for four different interaction scenarios: *exploration, energy, center of mass, pong game*. Different interaction scenarios are considered to analyze the performance in varying tracking conditions. The four interaction scenarios are different from each other in how humans move in XIM. In the exploration scenario humans move randomly exploring the space. In the center-of-mass scenario they form a highly cluttered tracking scenario. In the energy scenario, high speed move-

ments are produced by running around in the space. Pong involves team cooperation, where people coordinate their movement to achieve a team performance as discussed in [55]. We further consider the use of a priori information for improving the performance of PASAR. The idea of using this is to be able to modulate the association probabilities of sensory data to persons using a priori information about the world. PASAR computed the association probabilities of sensory data to *concepts* in the world-model using the JPDA algorithm and updates the *concept* states as discussed in chapter 3, section 3.3.2 and particularly in equation 3.10. We make use of this here by adding the heuristic that spatio-temporal proximity of multimodal sensory data has to be weighted more. In other words, sensory data congruent to sensory data of another modality is weighted higher. Here the camera data that is proximal to floor data in space and time is weighted more, i.e. the association probabilities of such data *concepts* are higher.

7.5 Bottom-up and Top-Down Attention for Action Generation in XIM

In this case, the recruitment of active sensors under limited resources constraints (e.g. 10 people in the space where only 4 controllable color cameras are available) to acquire features of the tracked humans is tested. The extracted features of the tracked humans are highly useful for ID maintenence in cluttered situations. Controllable color cameras and moving lights are allocated using the above discussed PASAR *attentional spotlight* mechanism to extract hues of the humans. We use a just-in-need feature extraction mechanism, which is very useful for autonomous systems with limited resources like the XIM. This becomes highly relevant for ID correction in XIM, where there are usually more than four subjects interacting in the space when there are only four controllable color cameras for hue feature extraction. Nevertheless, PASAR allows to drive the pan-tilt cameras to make them follow moving persons in XIM and extract hue information at the right moment (guaranteeing line of sight). Stan-

dard image processing techniques are applied to extract the hue of the subject torso despite distracting background noise such as other subjects, virtual world projection screens, floor illumination etc. At the same time, the moving lights are used to shine white light on the subject to aid hue extraction. From the movable camera images, hue histograms are computed for predefined hue bins (we used bin size 18, giving 20 bins for hue values range from 0 to 360). The top-down attention for such deployment of movable cameras and moving lights is triggered as discussed in the methods section using the similarity interference paradigm. Although hue extraction is a simple feature extraction method, it serves as a proof of concept for motor action generation from attention. By actively collecting hue information of subjects in the space, their IDs can be corrected.

Bibliography

[1] *http://opencv.willowgarage.com/wiki/*.

[2] *www.bayesian-programming.org*.

[3] A J Ahumada. Perceptual classification images from vernier acuity masked by noise. *Perception*, 26(18), 1996.

[4] A Akesson and R Wehner. Visual navigation in desert ants cataglyphis fortis: are snapshots coupled to a celestial system of reference? *The Journal of experimental biology*, 205(Pt 14):1971–1978, Jul 2002.

[5] J R Anderson. Act: A simple theory of complex cognition. *American Psychologist 51*, pages 355–365, 1996.

[6] H Andreasson, A Treptow, and T Duckett. Localization for mobile robots using panoramic vision, local features and particle filter. *Robotics and Automation, 2005. ICRA 2005. Proceedings of the 2005 IEEE International Conference on*, pages 3348–3353, April 2005.

[7] A Arleo and W Gerstner. Spatial cognition and neuro-mimetic navigation: a model of hippocampal place cell activity. *Biological Cybernetics*, 83(3):287–299, 2000.

[8] A Baddeley. Working memory. *Science*, page 556:559, 1992.

[9] T Bailey, B Upcroft, and H Durrant-Whyte. Validation gating for non-linear non-gaussian target tracking. IEEE Conference on Information Fusion, 2006.

[10] Yaakov Bar-Shalom and Thomas E. Fortmann. *Tracking and data association*. Boston Academic Press, 1988.

[11] L Barsalou. Perceptual symbol systems. *Behavioral Brain Sciences 22*, page 577:609, 1999.

[12] M Behrmann and S P Tipper. Object-centered not scene-based visual neglect. *Journal of experimental psychology Human perception and performance*, 22(5):1261–1278, 1996.

[13] R Benenson, S Petti, T Fraichard, and M Parent. Towards urban driverless vehicles. *International Journal of Vehicle Autonomous Systems*, 6(1/2):4–23, 2006.

[14] O Berger. Statistical decision theory and bayesian analysis. *Springer Series in Statistics*, 1980.

[15] S Bermudez, P Pyk, and P Verschure. A fly-locust based neuronal control system applied to an unmanned aerial vehicle: the invertebrate neuronal principles for course stabilization, altitude control and collision avoidance. *The International Journal of Robotics Research*, 26, 2007.

[16] U Bernardet, S Bermudez, and P Verschure. A model for the neuronal substrate of dead reckoning and memory in arthropods: a comparative computational and behavioral study. *Theory in Biosciences*, 127:163 – 175, 2008.

[17] U Bernardet, M Blanchard, and P Verschure. Iqr: A distributed system for real-time real-world neuronal simulation. *Neurocomputing*, 44-46:1043–1048, 2002.

[18] Ulysses Bernardet and Paul F. M. J. Verschure. *The eXperience Induction Machine: A New Paradigm for Mixed Reality Interaction Design and Psychological Experimentation*. Springer, 2009.

[19] M Botvinick and Z Rosen. Anticipation of cognitive demand during decision-making. *Psychological Research*, pages 1–8, 2008.

[20] R Brooks. A robust layered control system for a mobile robot. *IEEE Journal of Robotics and Automation*, 2:14–23, 1986.

[21] R Brooks. Intelligence without representation. *Artif. Intell*, pages 139–159, 1991.

[22] M A Brown and P E Sharp. Simulation of spatial learning in the morris water maze by a neural network model of the hippocampal formation and nucleus accumbens. *Hippocampus*, 5(3):171–188, 1995.

[23] M R Burke and G R Barnes. Anticipatory eye movements evoked after active following versus passive observation of a predictable motion stimulus. *Brain research*, 1245:74–81, December 2008.

[24] J M Camhi and A Levy. Organization of a complex movement: fixed and variable components of the cockroach escape behavior. *Journal of Comparative Physiology*, 1988.

[25] V Camos and P Barrouillet. Adult counting is resource demanding. *British journal of psychology London England 1953*, 95(Pt 1):19–30, 2004.

[26] D A Chernyak and L W Stark. Top-down guided eye movements. *IEEE transactions on systems, man, and cybernetics.Part B, Cybernetics : a publication of the IEEE Systems, Man, and Cybernetics Society*, pages 514–522, 2001.

[27] A Clark and R Grush. Towards a cognitive robotics. *Adapt. Behav. 7*, page 5:16, 1999.

[28] T S Collett. Insect navigation: visual panoramas and the sky compass. *Current biology : CB*, 18(22):R1058–61, Nov 25 2008.

[29] T S Collett and M Collett. Memory use in insect visual navigation. *Nature reviews.Neuroscience*, 3(7):542–552, Jul 2002.

[30] J Collins and J Uhlmann. Efficient gating in data association with multivariate gaussian distributed states. *Aerospace and Electronic Systems, IEEE Transactions on*, pages 909–916, 1992.

[31] H Crüse. The evolution of cognition - a hypothesis. *Cognit. Sci. 27*, page 135:155, 2003.

[32] Y Demiris and B Khadhouri. Hierarchical attentive multiple models for execution and recognition (hammer). *Robotics and Autonomous Systems, 54*, page 361:369, 2006.

[33] P F Dominey and J D Boucher. Learning to talk about events from narrated video in the construction grammar framework. *Artificial Intelligence, 167*, 2005.

[34] J Driver and G Baylis. Visual attention and objects: evidence for hierarchical coding of location. *Journal of experimental psychology Human perception and performance*, 19(3):451–470, 1993.

[35] Armin Duff and Paul F.M.J. Verschure. Unifying perceptual and behavioral learning with a correlative subspace learning rule. *Neurocomputing*, 73:1818:1830, 2010.

[36] R Dunbar and S Susanne. Understanding primate brain evolution. *Philosophical Transactions of the Royal Society B: Biological Sciences*, 362(1480):649–658, April 2007.

[37] J Edelman, A KristjÃ¡nsson, and K Nakayama. The influence of object-relative visuomotor set on express saccades. *Journal of Vision*, 7(6):12, 2007.

[38] T Eggert, J Ladda, and A Straube. Inferring the future target trajectory from visual context: is visual background structure used for anticipatory smooth pursuit? *Experimental brain research*, 196(2):205–215, 2009.

[39] B Fischer and E Rampsberger. Human express saccades: Extremely short reation times to goal directed eye movements. *Experimental Brain Research*, 57:191–195, 1984.

[40] J G Fleischer and J L Krichmar. Sensory integration and remapping in a model of the medial temporal lobe during maze navigation by a brain-based device. *Journal of integrative neuroscience*, pages 403–431, 2007.

[41] W Fletcher and J Sharpe. Saccadic eye movement dysfunction in alzheimer's disease. *Annals of Neurology*, 20:464–471, 1986.

[42] Matthias O. Franz and Hanspeter A. Mallot. Biomimetic robot navigation. *Robotics and autonomous Systems*, 30:133–153, 2000.

[43] Mariana Gil, Rodrigo J De Marco, and Randolf Menzel. Learning reward expectations in honeybees. *Learning & Memory (Cold Spring Harbor, N.Y.)*, 14(7):491–496, July 2007.

[44] Mariana Gil, Randolf Menzel, and Rodrigo J. De Marco. Does an insect's unconditioned response to sucrose reveal expectations of reward? *PLoS ONE*, 3(7):e2810, 07 2008.

[45] C Giovannangeli and P Gaussier. Autonomous vision-based navigation: Goal-oriented action planning by transient states prediction, cognitive map building, and sensory-motor learning. *Intelligent Robots and Systems, 2008. IROS 2008. IEEE/RSJ International Conference on*, pages 676–683, Sept. 2008.

[46] C Giovannangeli, Ph Gaussier, and J P Banquet. Robustness of visual place cells in dynamic indoor and outdoor environment. *International Journal of Advanced Robotic Systems*, 3(2):115–124, jun 2006.

[47] J I Gold and M N Shadlen. Representation of a perceptual decision in developing oculomotor commands. *Nature*, pages 390–394, 2000.

[48] A S Greenberg and L Gmeindl. Strategic control of attention to objects and locations. *J. Neurosci.*, 28(3):564–565, 2008.

[49] R J Greenspan and B van Swinderen. Cognitive consonance: Complex brain functions in the fruit fly and its relatives. *Trends in Neurosciences 27*, page 707:711, 2004.

[50] A Guanella and P Verschure. Prediction of the position of an animal based on populations of grid and place cells: a comparative simulation study. *Journal of Integrative Neuroscience*, 6:433 – 446, 2007.

[51] M E Hasselmo and M P Brandon. Linking cellular mechanisms to behavior: entorhinal persistent spiking and membrane potential oscillations may underlie path integration, grid cell firing, and episodic memory. *Neural plasticity*, 2008:658323, 2008.

[52] H R Heekeren, S Marrett, and L G Ungerleider. The neural systems that mediate human perceptual decision making. *Nature Reviews Neuroscience*, pages 467–479, 2008.

[53] M Heisenberg. What do mushroom bodies do for the insect brain? *Learn. Mem. 5*, page 1:10, 1998.

[54] Henning Herbers. Active vision in interactive spaces. *Master's thesis, Technical University of Munich*, 2008.

[55] M Inderbitzin, S Wierenga, A Väljamäe, U Bernardet, and P Verschure. Social cooperation and competition in the mixed reality space experience induction machine. *Virtual Reality*, pages 153–158, 2009.

[56] L Itti and P Baldi. Bayesian surprise attracts human attention. In *Neural Information Processing Systems (NIPS)*, 2005.

[57] L Itti and C Koch. Feature combination strategies for saliency-based visual attention systems. *Journal of Electronic Imaging*, 2001.

[58] M F Jay and D L Sparks. Sensorimotor integration in the primate superior colliculus. i. motor convergence. *Journal of neurophysiology*, pages 22–34, 1987.

[59] R E Kalman. A new approach to linear filtering and prediction problems. *Transactions of the ASME–Journal of Basic Engineering 82 (Series D)*, pages 35–45, 1960.

[60] M Kawato. Internal models for motor control and trajectory planning. *Current Opinion in Neurobiology 9 (6)*, 1999.

[61] B Keane and Z Pylyshyn. Is motion extrapolation employed in multiple object tracking? tracking as a low-level, non-predictive function. *Cognitive Psychology*, 52(4):346 – 368, 2006.

[62] E I Knudsen. Instructed learning in the auditory localization pathway of the barn owl. *Nature*, pages 322–328, 2002.

[63] P König and N Krüger. Symbols as self-emergent entities in an optimization process of feature extraction and predictions. *Biological Cybernetics*, pages 325–334, 2006.

[64] J L Kubie and A A Fenton. Heading-vector navigation based on head-direction cells and path integration. *Hippocampus*, Dec 12 2008.

[65] J E Laird, A Newell, and P S Rosenbloom. Soar: an architecture for general intelligence, artificial intelligence 33 1. pages 1–64, 1987.

[66] P Langley, D Choi, and S Rogers. Acquisition of hierarchical reactive skills in a unified cognitive architecture. *Cognitive Systems Research, 10*, pages 316–332, 2009.

[67] P Langley, K B McKusick, and J A Allen. A design for the icarus architecture. *SIGART Bulletin 2*, pages 104–109, 1991.

[68] P C Mahalanobis. On the generalised distance in statistics. *Proceedings National Institute of Science, India 2 (1)*, pages 49–55, 1936.

[69] Donald W Marquardt. An algorithm for least-squares estimation of nonlinear parameters. *SIAM Journal on Applied Mathematics*, 11(2):431–441, 1963.

[70] Z Mathews, S Bermúdez, and P Verschure. A novel brain-based approach for multi-modal multi-target tracking in a mixed reality space. *Intuition Workshop and Conference on Virtual Reality and Virtual Environments*, 2007.

[71] Z Mathews, S Bermúdez, and P Verschure. Intelligent motor decision: From selective attention to a bayesian world model. *IEEE Intelligent Systems Conference,*, 2008.

[72] Z Mathews, S Bermúdez, and P Verschure. *Series Ed.: Kacprzyk, Janusz, Studies in Computational Intelligence, Springer Verlag, (in press)*, 2010.

[73] Z Mathews, S Bermúdez, and P Verschure. An insect-based method for learning landmark reliability using expectation reinforcement in dynamic environments. *Robotics and Automation (ICRA), IEEE/RSJ International Conference on*, 2010.

[74] Z Mathews, M Lechón, J M Blanco, A Dhir, A Duff, S Bermúdez, and P Verschure. Insect-like mapless navigation based on head direction cells and contextual learning using chemo-visual sensors. *Intelligent Robots and Systems (IROS), IEEE/RSJ International Conference on*, 2009.

[75] B L McNaughton, F P Battaglia, O Jensen, E I Moser, and M B Moser. Path integration and the neural basis of the 'cognitive map'. *Nature reviews.Neuroscience*, 7(8):663–678, Aug 2006.

[76] R C Miall, M Malkmus, and EM Roberston. Sensory prediction as a role for the cerebellum. *Behav. Brain Sc. 19*, page 466:467, 1996.

[77] R U Muller, M Stead, and J Pach. The hippocampus as a cognitive graph. *The Journal of general physiology*, 107(6):663–694, Jun 1996.

[78] G K Murray, P R Corlett, L Clark, M Pessiglione, A D Blackwell, G Honey, P B Jones, E T Bullmore, T W Robbins, and P C Fletcher. Substantia nigra/ventral tegmental reward prediction error disruption in psychosis. *Molecular psychiatry*, 13(3):239–276, 2008.

[79] Karim Nader and Oliver Hardt. A single standard for memory: the case for reconsolidation. *Nature Reviews Neuroscience*, 10(3):224–234, mar 2009.

[80] J S Nairne. Remembering over the short-term: the case against the standard model. *Annual Review of Psychology 53*, pages 53–81, 2002.

[81] A Newell. Unified theories of cognition. *Harvard University Press*, 1994.

[82] H Nienborg and B G Cumming. Decision-related activity in sensory neurons reflects more than a neuron's causal effect. *Nature*, pages 89–92, 2009.

[83] S Oh and S Sastry. A polynomial-time approximation algorithm for joint probabilistic data association. *American Control Conference*, pages 1283–1288, 2005.

[84] J O'Keefe and J Dostrovsky. The hippocampus as a spatial map. preliminary evidence from unit activity in the freely-moving rat. *Brain research*, 34(1):171–175, Nov 1971.

[85] J O'Keefe and L Nadel. *The Hippocampus as a Cognitive Map*. Oxford University Press, USA, 1978-12-07 1978.

[86] John O'Keefe. *The hippocampal cognitive map and navigational strategies*. Oxford University Press, USA, 1991.

[87] B A Olshausen, C H Anderson, and D C V Essen. A neurobiological model of visual attention and invariant pattern recognition based on dynamic routing of information. *The Journal of neuroscience : the official journal of the Society for Neuroscience 13 (11)*, pages 4700–4719, 1993.

[88] C R Olson. Object-based vision and attention in primates. *Current Opinion in Neurobiology*, 11(2):171–179, 2001.

[89] M A Pinsk, G Doniger, and S Kastner. Push-pull mechanism of selective attention in human extrastriate cortex. *Journal of Neurophysiology 92*, pages 622–629, 2004.

[90] D G Premack and G Woodruff. Does the chimpanzee have a theory of mind? *Behavioral and Brain Sciences, 1,*, pages 515–526, 1978.

[91] T J Prescott, P Redgrave, and K Gurney. Layered control architectures in robots and vertebrates. *Adaptive Behavior, 7*, pages 99–127, 1999.

[92] William H Press, Saul A Teukolsky, William T Vetterling, and Brian P Flannery. *Numerical recipes in C (2nd ed.): the art of scientific computing*. Cambridge University Press, New York, NY, USA, 1992.

[93] Pawel Pyk, Sergi Bermúdez i Badia, Ulysses Bernardet, Philipp Knüsel, Mikael Carlsson, Jing Gu, Eric Chanie, Bill S. Hansson, Tim C. Pearce, and Paul F. M. J. Verschure. An artificial moth: Chemical source localization using a robot based neuronal model of moth optomotor anemotactic search. *Autonomous Robots*, 20(3):197–213, 2006.

[94] Z Pylyshyn and R W Storm. Tracking multiple independent targets: Evidence for a parallel tracking mechanism. *Spatial Vision*, 3:179 – 197, 1988.

[95] P Rakic. Specification of cerebral cortical areas. *Science 241 (4862)*, page 170:176, 1988.

[96] Andrew M. Reynolds, Alan D. Smith, Don R. Reynolds, Norman L. Carreck, and Juliet L. Osborne. Honeybees perform optimal scale-free searching flights when attempting to locate a food source. *Journal of Experimental Biology*, 210(21):3763–3770, nov 2007.

[97] E Royer, J Bom, M Dhome, B Thuilot, M Lhuillier, and F Marmoiton. Outdoor autonomous navigation using monocular vision. *Intelligent Robots and Systems, 2005. (IROS 2005). 2005 IEEE/RSJ International Conference on*, pages 1253–1258, Aug. 2005.

[98] Aung Si, Mandyam V Srinivasan, and Shaowu Zhang. Honeybee navigation: properties of the visually driven 'odometer'. *The Journal of Experimental Biology*, 206(Pt 8):1265–1273, 2003.

[99] R C Smith and P Cheeseman. On the representation and estimation of spatial uncertainty. *The International Journal of Robotics Research*, 5(4):56:68, 1986.

[100] R W Stackman and J S Taube. Firing properties of rat lateral mammillary single units: head direction, head pitch, and angular head velocity. *The Journal of neuroscience : the official journal of the Society for Neuroscience*, 18(21):9020–9037, Nov 1 1998.

[101] B E Stein. The development of a dialogue between cortex and midbrain to integrate multisensory information. *Experimental Brain Research 166*, pages 305–315, 2005.

[102] B E Stein and M A Meredith. The merging of the senses. *The MIT Press Cambridge, Massachusetts, London, England,*, 1993.

[103] D W Stephens, J S Brown, and R C Ydenberg. *Foraging:Behavior and Ecology*. Chicago: University of Chicago Press, 2007.

[104] Christopher Summerfield and Tobias Egner. Expectation (and attention) in visual cognition. *Trends in Cognitive Sciences*, 13(9):403–409, September 2009.

[105] E C Tolman. Cognitive maps in rats and men. *Psychological review*, 55(4):189–208, July 1948.

[106] R Toro, M Perron, B Pike, L Richer, S Veillette, Z Pausova, and T Paus. Brain size and folding of the human cerebral cortex. *Cerebral cortex 18 (10)*, page 2352:7, 2008.

[107] D S Touretzky and A D Redish. Theory of rodent navigation based on interacting representations of space. *Hippocampus*, 6(3):247–270, 1996.

[108] S Treue. Neural correlates of attention in primate visual cortex. *Trends in neurosciences 24 (5)*, pages 295–300, 2001.

[109] S Tripathy and B Barrett. Severe loss of positional information when detecting deviations in multiple trajectories. *Journal of Vision*, 4(12):1020–1043.

[110] P Verghese and S McKee. Predicting future motion. *Journal of Vision*, 2(5):413–423, 2002.

[111] P Verschure and P Althaus. A real-world rational agent: unifying old and new ai. *Cognitive Science A Multidisciplinary Journal*, 27(4):561–590, 2003.

[112] P Verschure and P Althaus. A real-world rational agent: Unifying old and new ai. *Cognitive Science*, 27:561–590, 2003.

[113] P Verschure, T Voegtlin, and R J Douglas. Environmentally mediated synergy between perception and behaviour in mobile robots. *Nature*, 425(6958):620–624, Oct 9 2003.

[114] Jonathan D Victor. Analyzing receptive fields, classification images and functional images: challenges with opportunities for synergy. *Nature Neuroscience*, 8(12):1651–1656, 2005.

[115] P Viola and M Jones. Rapid object detection using a boosted cascade of simple features. *Computer Vision and Pattern Recognition, 2001. CVPR 2001. Proceedings of the 2001 IEEE Computer Society Conference on (Vol.1)*, pages 511–518, 2001.

[116] G M Viswanathan, Sergey V. Buldyrev, Shlomo Havlin, M. G. E. da Luz, E. P. Raposo, and H. Eugene Stanley. Optimizing the success of random searches. *Nature*, 401(6756):911–914, oct 1999.

[117] K. von Frisch. Decoding the language of the bee. *Science (New York, N.Y.)*, 185(4152):663–668, Aug 23 1974.

[118] E von Holst and H Mittlestaedt. Das reafferenzprinzip. *Die Naturwissenschaften*, 37:464:476, 1950.

[119] E Vul, C Frank, , J B Tenenbaum, and G Alvarez. Explaining human multiple object tracking as resource-constrined approximate inference in a dynamic probabilistic model. In *Neural Information Processing Systems (NIPS)*, 2009.

[120] B Webb. Neural mechanisms for prediction: do insects have forward models? *Trends in Neurosciences 27*, page 278:282, 2004.

[121] R Wehner. Matched filters: neural models of the externalworld. *J. Comp. Physiol. A, Sens. Neural. Behav. Physiol. 161*, page 511:531, 1987.

[122] R Wehner. Desert ant navigation: how miniature brains solve complex tasks. *Journal of comparative physiology.A, Neuroethology, sensory, neural, and behavioral physiology*, 189(8):579–588, Aug 2003.

[123] R Wehner, M Boyer, F Loertscher, S Sommer, and U Menzi. Ant navigation: one-way routes rather than maps. *Current biology : CB*, 16(1):75–79, Jan 10 2006.

[124] R Wehner, B Michel, and P Antonsen. Visual navigation in insects: coupling of egocentric and geocentric information. *The Journal of experimental biology*, 199(Pt 1):129–140, 1996.

[125] M Witkowski and D Randell. A model of modes of attention and inattention for artificial perception. *Bioinspiration and biomimetics*, 2(3):S94–S115, Sep 2007.

[126] I B Witten, E I Knudsen, and H Sompolinsky. A hebbian learning rule mediates asymmetric plasticity in aligning sensory representations. *Journal of neurophysiology 100 (2)*, pages 1067–1079, 2008.

[127] H Wolf and R Wehner. Pinpointing food sources: olfactory and anemotactic orientation in desert ants, cataglyphis fortis. *J Exp Biol*, 203(5):857–868, 2000.

[128] D M Wolpert and Z Ghahramani. Computational principles of movement neuroscience. *Nature Neuroscience 3*, page 1212:1217, 2000.

[129] S Wood. Representation and purposeful autonomous agents. *Robotics and Autonomous Systems, Knowledge Engineering and Ontologies for Autonomous Systems, AAAI Spring Symposium 49 (1-2)*, pages 79 – 90, 2004.

[130] R H Wurtz, M A Sommer, and J Cavanaugh. Drivers from the deep: the contribution of collicular input to thalamocortical processing. *Progress in brain research*, 149:207–225, 2005.

[131] Reto Wyss and Paul F. M. J. Verschure. Bounded invariance and the formation of place fields. *Advances in Neural Information Processing Systems NIPS*, 2003.